CHARACTERIZATION OF LOCAL MASS TRANSFER RATE DOWNSTREAM OF AN ORIFICE

CHARACTERIZATION OF LOCAL MASS TRANSFER RATE DOWNSTREAM OF AN ORIFICE

By

DONGDONG WANG, B.Sc.

A Thesis

Submitted to the School of Graduate Studies

in Partial Fulfillment of the Requirements

for the Degree

Master of Applied Science

McMaster University

Hamilton, Ontario, Canada

MASTER OF APPLIED SCIENCE (2011) (Mechanical Engineering)	McMaster University Hamilton, Ontario, Canada

TITLE	Characterization of local mass transfer rate downstream of an orifice
AUTHOR	Dongdong Wang,
SUPERVISOR	Dr. Chan Y. Ching, Professor Department of Mechanical Engineering
NUMBER OF PAGES	xvi, 143

ABSTRACT

Flow accelerated corrosion(FAC) results in wall thinning of pipes, tubes or vessels from exposure to flow due to corrosion. If FAC is not detected, it can lead to sudden failure of piping components. Orifices are used in piping systems to monitor and control the flow. Flow separation and reattachment downstream of an orifice can enhance the mass transfer of the pipe wall. In this thesis, the effect of Reynolds numbers and surface roughness on the mass transfer rate downstream of an orifice was investigated. A dissolving wall method was used to measure the wall mass transfer. The test sections were cast from gypsum with water as the working fluid. Multiple destructive tests were performed for different test times in a 2.5 cm diameter flow loop, and the wear topology measured by a laser scanner to obtain the progression of wear with time over the pipe surface. None-destructive tests were performed in a 20 cm diameter flow loop using test section with an inner gypsum lining, and measured online at selected locations using an ultrasonic method. Experiments were performed at Reynolds numbers of 80000, 140000 and 200000 in the 2.5 cm diameter flow loop, and at 180,000 in the 20 cm diameter flow loop with an orifice to pipe diameter ratio of 0.5. The results show that different surface roughness patterns are developed at different Reynolds numbers from the initially smooth surfaces. The different surface roughness patterns have a significantly different effect on the mass transfer rate downstream of an orifice. A larger population of scallops developed from the smooth pipe surface, as the Reynolds number was increased, which enhanced the mass transfer rate. The mass transfer rate in the 20 cm diameter test section was much smaller than in the 2.5 cm diameter test section at a similar Reynolds number. The pattern

of the roughness in the 20 cm diameter test section was formed as isolated roughness which is similar to the roughness pattern in 2.5 cm diameter test section at much lower Reynolds number.

ACKNOWLEDGEMENTS

The author would like to acknowledge his gratitude to his supervisor Dr. Chan Y. Ching for his supervision, guidance, motivation and support throughout the course of this research. The author would like to give special thanks to Dr. Daniel Ewing for his support and critical advice throughout this research. The author also appreciates Dr. Jim Cotton's advice during this research. The author is grateful to Yossef Ziada's time for his help on developing part of the Matlab code for the ultrasonic measurements.

The technicians in the Mechanical Engineering department shop, Joe Verhaeghe, J. P. Talon, Ron Lodewyks, Jim McLaren and Mark Mackenzie provided valuable help at many points during this project.

The author would like to express his gratitude to all his friends and colleagues in the Thermal Management Research Laboratory for their continuous support throughout the course of his graduate program. The author also would like to express his sincere gratitude to his parents, who always encouraged and supported him in all his difficulties. The support from his wife, Linyin Guo is priceless to the author and without her support it would be impossible to accomplish many achievements.

TABLE OF CONTENTS

LIST OF TABLES

LIST OF FIGURES

NOMENCLATURE

Symbols

$\dot{m}$	Mass flow rate of water (Kg/s)
Δ	Difference
A	Cross-sectional area, surface area (m^2)
C	Concentration(Kg/m^3)
c	Wave speed(m/s)
d	Pipe diameter downstream of orifice or expansion(m)
D	Pipe diameter upstream of orifice or expansion(m)
D_{diff}	Diffusivity of gypsum(m^2/s)
F	Faraday constant (s A/mol)
I_L	Limiting current (amp)
L	Length (m)
m	Mass removed from the test section(kg)
n_e	valence charge of ion species
Nu	Nusselt number
p	Pitch between different scallops(roughness)
Pr	Prandtl number
r	Radius (m)
Re	Reynolds number
Sc	Schmidt number
Sh	Sherwood number
t	Time(s)
u_o	Average flow velocity (m/s)
v	Volume (m^3)
V	Velocity(m/s)
V	voltage

Subscripts

b	Bulk
c	Corrosion
d	Diffusivity
diff	Diffusivity
fd	Fully developed
i	Ideal
max	Maximum
o	Orifice
r	Rough
s	Smooth
t	total

w	Wall

Chapter 1 INTRODUCTION

Flow accelerated corrosion (FAC) is a wall thinning phenomena of pipes, tubes or vessels from exposure to flow due to corrosion. Unexpected degradation of components due to FAC can cause rupture of piping components in power plants with release of high amounts of energy, which can cause severe plant damage. FAC is a major safety issue in power generation plants, and has been studied for over 3 decades. The major factors that influence FAC are well recognized. FAC is basically a two-step process, which includes (i) the chemical reaction at the surface, which depends on the chemical composition of the solution at the surface, such as Fe^{2+}, OH^- ions for steel pipes, and (ii) molecular diffusion across the diffusion boundary layer ε, which strongly depends on the hydrodynamic conditions.. A number of correlations for the pipe wall thinning rates of piping components are available; however, there are very few systematic investigations for the wall mass transfer rates are under controlled conditions.

A number of accidents in nuclear and fossil power generation plants have been attributed to FAC. There have been several fatal accidents, including those at Surry (1986), Pleasant Prairie (1996), Mihama (2004) and Latan (2007). The accident in Pleasant Prairie was caused by the fracture of a feedwater pipe between the isolation valve and economizer inlet. The location of the accident in Mihama was at the feedwater piping between low pressure heaters and deaerator, while that in Latan was at the superheater attemperation line from the discharge of boiler feed pump. There have been a number of accidents due to FAC under two phase flow conditions (1). The most common failure locations are where there are large changes in the flow, such as at sudden expansions or contractions, bends and T joints.

Geometrical changes in pipe lines are common in power generation plant. These changes give rise to variation in hydrodynamic conditions, which can enhance the local mass transfer rate. There have been several studies of FAC in bends, sudden expansions, orifices, nozzles and T-joints (2) (3) (4) (5)(6) (7) (8)(9). Orifices are commonly used in piping systems in piping systems of power plants for measuring and restricting the flow rate. Pipe ruptures downstream of orifices have been reported at several nuclear power plants. A serious pipeline explosion occurred in a 10 percent feed line immediately downstream of an orifice on February 9, 2006, in the Kakrapar Atomic Power Station unit-2 after only ten years of service (10). The flow dynamics downstream of an orifice is complex, with flow separation at the sharp edge lip of the orifice, leading to the development of vortices that can shed downstream.

A number of correlations for the maximum mass transfer rate downstream of an orifice or sudden expansion have been proposed, however, they have been developed using experiments performed on smooth pipes (4) (6). Large discrepancies have been reported between predicted and measured mass transfer values downstream of an orifice. For example, Poulson (11) provides the discrepancy for the maximum mass transfer downstream of an orifice in Table 1.1. As seen, the ratio of the measured and predicted values can be up to about a factor of 20.

Table 1.1 Enhancement factor of mass transfer rate downstream of an orifice

Material	Environment	Re	Predicted enhancement	Measured enhancement
Copper	0.1 N HCl +2 g/l Fe^{3+}, at 50 ℃		4.6	5.4
Carbon steel	0.1 N HCl +2 g/l Fe^{3+}, at 50 ℃		4.6	103
Carbon steel	4M NH_4 NO_3 at 90 ℃		5.1	54
Carbon steel	0.1 N HCl + 1M NaCl at 50 ℃	2.7×10^4	4.6	12
		1.3×10^4	5.2	4
		7×10^3	6	1.3
Carbon steel	AGR Boiler Water pH 9.8 Temperature 155 ℃		3.2	19.4

Scallops are commonly observed on the surface of failed pipes. Due to FAC, they are mostly developed in the flow reattachment or vortex region. A typical picture of the failed pipe surface is shown in Figure 1.1.The surface roughness due to these scallops can have a significant effect on FAC. Roughness effects on mass transfer rate have been studied using defined V-shaped roughness , or rib-like roughness patterns (12)(13)(14). However, the roughness that develops naturally due to the flow in piping components due to the flow over time can be different from that studied using a defined roughness in terms of shape and spacing, which are important parameters in mass transfer rate.

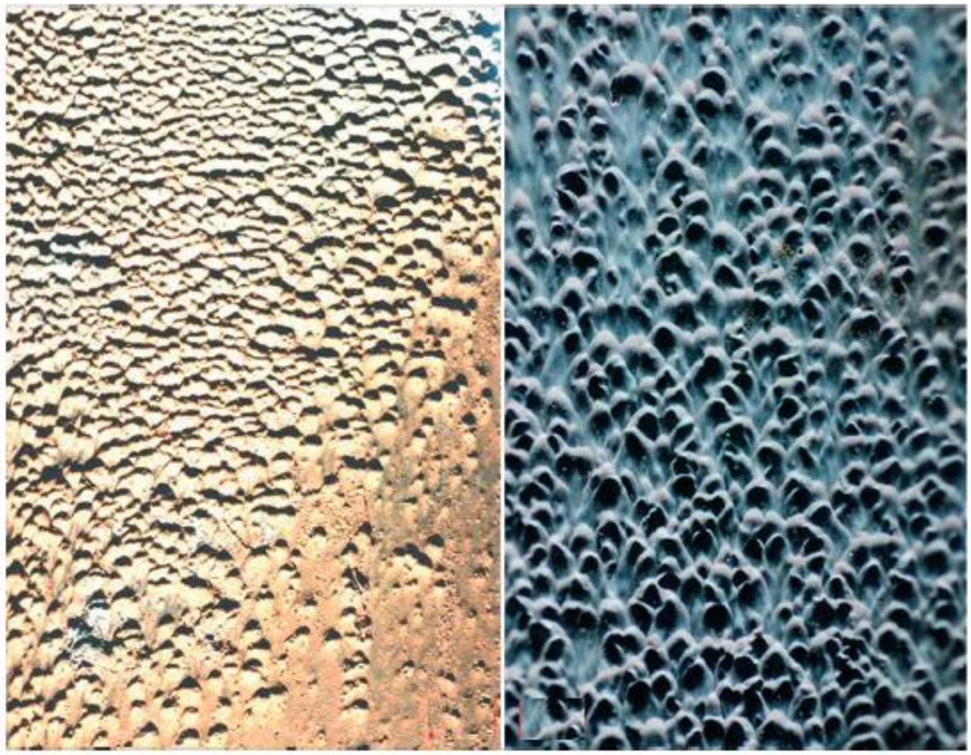

(a) (b)

Figure 1.1 Surface apparatus of the failed pipe(1)

The objective of the present work is to investigate the mass transfer rate downstream of an orifice. In particular, the effect of the Reynolds number and the evolving roughness effects on the mass transfer rate downstream of an orifice were investigated. A series of mass transfer tests downstream of an orifice were performed in a 2.5 cm and a 20 cm diameter flow loop at different Reynolds numbers. A dissolving wall method was used for the mass transfer tests, and the test sections were cast out of hydrocal with an initially smooth wall surface. Non-dimensionalized parameters Re, Sc and Sc are commonly used to represent the material and fluid properties in mass transfer. In addition, Wall dissolving method with gypsum at high Reynolds number produces the similar surface roughness patterns as the surface roughness on the worn pipes in industry as demonstrated in Chapter 4. Therefore, gypsum is used for testing to predict the mass transfer rate of the steel pipe in power plants.

Destructive tests are performed in the 2.5 cm diameter flow loop, where the test section is cut in half after a given run time. The worn surface topology is obtained by a laser scan of the surface, and the mass transfer rates obtained from the progression of wear with time. In the 20 cm diameter flow loop, non-destructive tests are performed. Ultrasonic measurements for the pipe wall thickness are taken for calculating local mass transfer rate. At the completion of the test, the surface topology is mapped using a laser scanning. The effect of roughness on mass transfer rate downstream of the orifice at different Reynolds numbers is determined.

This thesis is divided into five chapters. Chapter 2 provides background on the mass transfer rate on downstream of an orifice and the roughness effect on mass transfer rate. Chapter 3 outlines the experimental set up and methodology used for the experiments both in the 2.5 cm and 20 cm diameter test facilities. The results of the experimental findings are presented and discussed in Chapter 4. Previous model predictions are compared with current the experimental results. Chapter 5 summarizes the work and provides recommendations for future work.

Chapter 2 LITERATURE REVIEW

Flow-accelerated corrosion (FAC) has been studied over the last 2 to 3 decades because of its importance in power generation plants. When carbon steel piping is exposed to water, Fe_3O_4 develops on the surface, and dissolves into water as Fe^{2+} ions. FAC is basically a two-step process, which includes (i) the chemical reaction at the surface, which depends on the chemical composition of the solution at the surface, such as Fe^{2+}, OH^- ions for steel pipes, and (ii) molecular diffusion across the diffusion boundary layer ε, which strongly depends on the hydrodynamic conditions. The transport by molecular diffusion can change significantly under different flow conditions (15). The schematic of the FAC process is demonstrated in Figure 2.1 (1). As shown, the chemical reaction on the carbon steel surface is

$$\mathrm{Fe} + 2\mathrm{H_2O} \rightarrow \mathrm{Fe^{2+}} + 2\mathrm{OH^-} + 2\mathrm{H_2} \qquad 2.1$$

and then the ions diffuse through the boundary layer. The dissolution rate of a solid in an aqueous solution is controlled either by the chemical reaction or by the molecular diffusion.

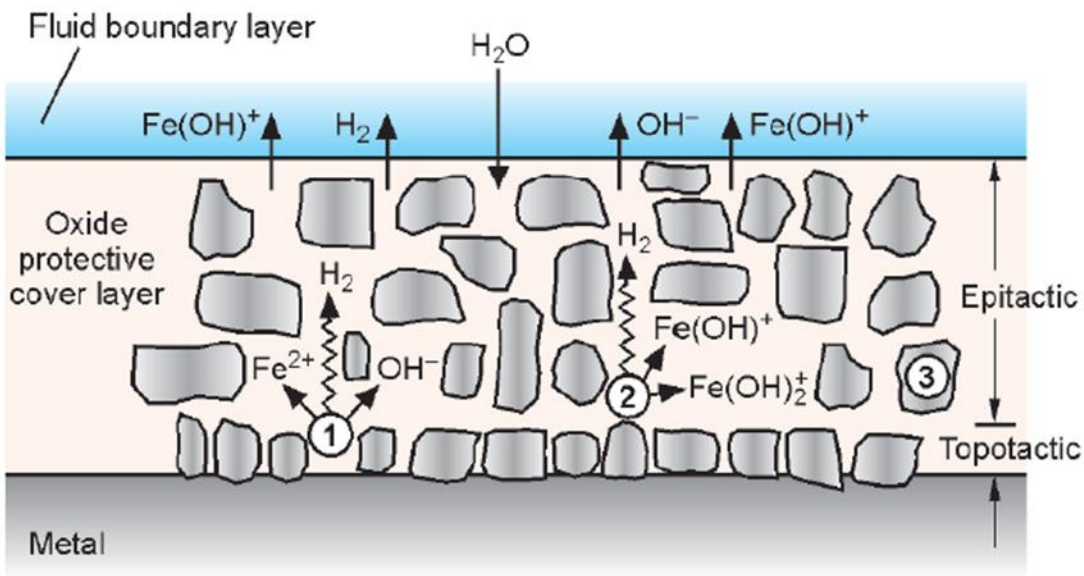

Figure 2.1 Schematic of flow accelerated corrosion (FAC)

In both cases, mass flux resulting from the dissolution of the surface, must equal to the mass flux transport through the diffusion layer. Therefore, both processes affect the mass transfer rate simultaneously. The overall mass transfer rate is controlled by the lower value. If the thickness of the diffusion boundary layer ε is extremely small, diffusion becomes really efficient, so that the overall mass transfer rate become surface reaction controlled, and vice versa.

A number of different techniques have been developed to measure mass transfer in piping components. The most widely used are: (i) the analogy with heat transfer, (ii) the limiting current density electrochemical technique (LCDT) and (iii) the dissolving wall method. The governing transport equations for heat and mass transfer are identical, with the driving potentials being the temperature gradient, and species concentration gradient for heat and mass transfer (16). Thus, mass transfer can be inferred from heat transfer studies which are simpler to perform. For example, Krall and Sparrow (4) performed heat transfer experiments downstream of an orifice to mimic the mass transfer rate for that flow geometry. The drawback of using this technique is that the Prandtl numbers in most heat transfer experiments are usually less than 10, which are much lower than the Schmidt numbers relevant to mass transfer in carbon steel pipes which are on the order of 1500.

The limiting current diffusion technique has been widely used in mass transfer experiments (5) (6) (12)(17)(18)(9). This technique is well understood, and explained in detail in many books (19) (20) (21), so a detailed explanation is not addressed here in this thesis. A typical experimental setup is shown in Figure 2.2. By measuring the current through the local cathode I_L, which is conducted by the ion in the flow, the local mass transfer coefficient at that cathode can be calculated as:

$$k_d = \frac{I_L}{n_e F A C_b} \tag{2.2}$$

where I_L is the limiting current, n_e is valence charge of ion species, F is Faraday constant, A is surface area of studied electrode (cathode), and C_b is bulk concentration of reacting species. There are many advantages of this technique; especially the surface topology does not change noticeably during the tests. Therefore, tests can be performed on smooth surfaces or using predetermined roughness with different roughness geometry, size and spacing. However, it does have some drawbacks, such as the location of a large number of

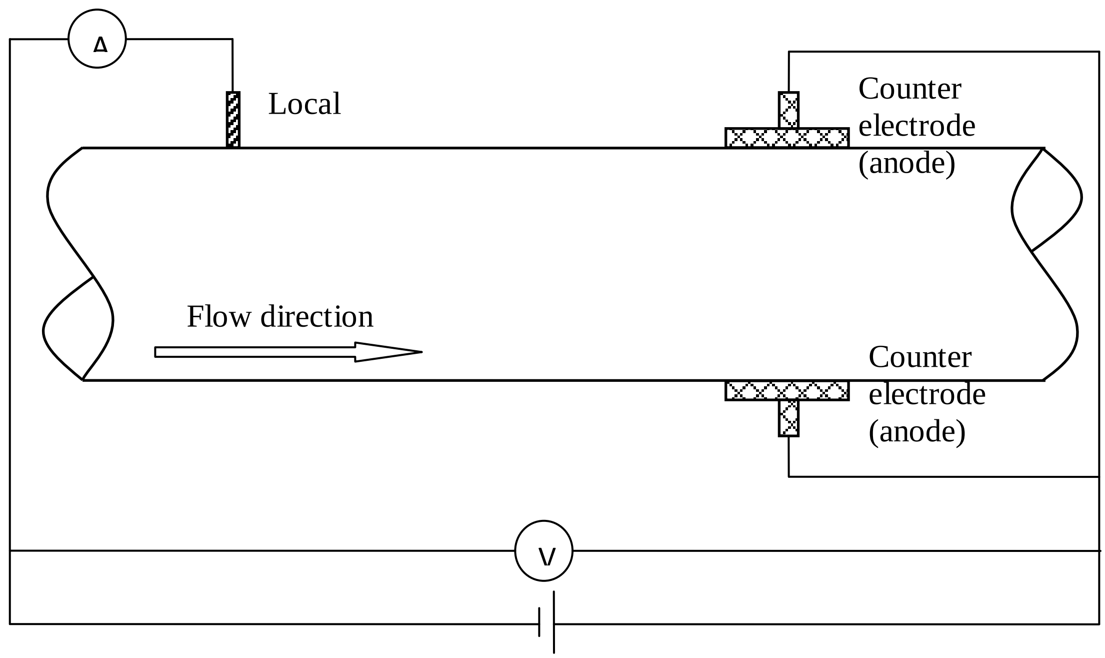

Figure 2.2 Schematic diagram of LCDT for measuring the local mass transfer rate at the Cathode

local cathodes in the bulk cathode, the suitable positioning of the anode to ensure uniform current distribution, and avoiding the disturbance of the flow by the presence of the electrodes is difficult. The electrodes are used for the measurement of the diffusion current at their locations(9).

In the dissolving wall method, test samples are made of or coated with a material that is soluble in the test solution. The mass transfer rate is directly inferred from the change in wall thickness of the test samples. Copper tubes were used to perform dissolving wall tests with oxygenated acidified NaCl solutions by Poulson (9). One of the most common materials for this method is gypsum in water (22). The advantage of this technique is that the surface roughness develops naturally due to the flow in contrast to the other techniques. In the dissolving wall technique, mass transfer can occur by both erosion and dissolution, and hence it is important to ensure that there is no erosion. The present tests used the dissolving wall method with test section cast from gypsum. It has many advantages in that it can be cast into complex shapes, and naturally developed scallops or roughness are formed during the tests which are more relevant to industrial piping systems (9) (23) (24). Plaster of paris has been extensively used in previous mass transfer studies (24) (25). For example, Allen investigated the development of scallops from beds of hardened Plaster of Paris (calcium sulphate) exposed to turbulent streams of water (26). It was found that for a given initial roughness, the population of scallops increased with Reynolds number, while the sizes of the scallops decrease(27). Wilkin performed a series of tests on strait pipes with gypsum(24). Only a few scallops were observe at Re 87000, while the population and the size of scallops observed at Re 63500 are much large.

The dissolution of plaster in water is a dissolution controlled mass transfer phenomena (28) driven process by the concentration difference between the saturated gypsum solution on the surface and the bulk concentration, given by

$$R = h(C_w - C_b) \qquad 2.3$$

where R is the mass transfer rate, h is mass transfer coefficient, C_w is solubility(wall concentration) of gypsum in water and C_b is bulk concentration of gypsum in the flow. If the mass transfer is surface diffusion controlled, the overall mass transfer rate is strongly affected by diffusion rate, which can be accelerated by the flow (1).

The mass transfer downstream of an orifice or sudden expansion is often reported as an enhancement ratio relative to the corresponding fully developed pipe flow, which are extensively studied (17) (29) (30). Berger and Hau (17) developed a correlation for the mass transfer rate in fully developed pipe flows. They employed the LCDT to study the mass transfer rate in smooth nickel pipes with e/D < 0.000018. Over a Reynolds number in the range $8 \times 10^3 < Re < 2 \times 10^5$ and Schmidt numbers in the range 1000 and 6000 the correlation for Sh was presented as

$$Sh_{pipe} = 0.0165\, Re^{0.86} Sc^{0.33} \qquad 2.4$$

Another popular correlation for fully developed pipe flow was developed by Chilton and Colburn (31) with heat transfer analogy as

$$Sh_{pipe} = 0.023\, Re^{0.8} Sc^{0.33} \qquad 2.5$$

The coefficient of Chilton and Colburn is greater than it is of Burger and Hau, while the Reynolds number exponent is slightly lower, and the exponent of Schmidt numbers are the same.

In general, wall roughness can have a significant effect on mass transfer. The mass transfer on roughened surfaces in fully developed pipe flow has been studied by different researchers (12)(13)(14) . The surface roughness has a great impact on the flow by breaking up the thin viscous sublayer, and increasing the wall friction (32). The mass transfer enhancement factor due to a V-shaped grooved roughness on fully developed pipes over a wide range of Re range was as high as 4(13).

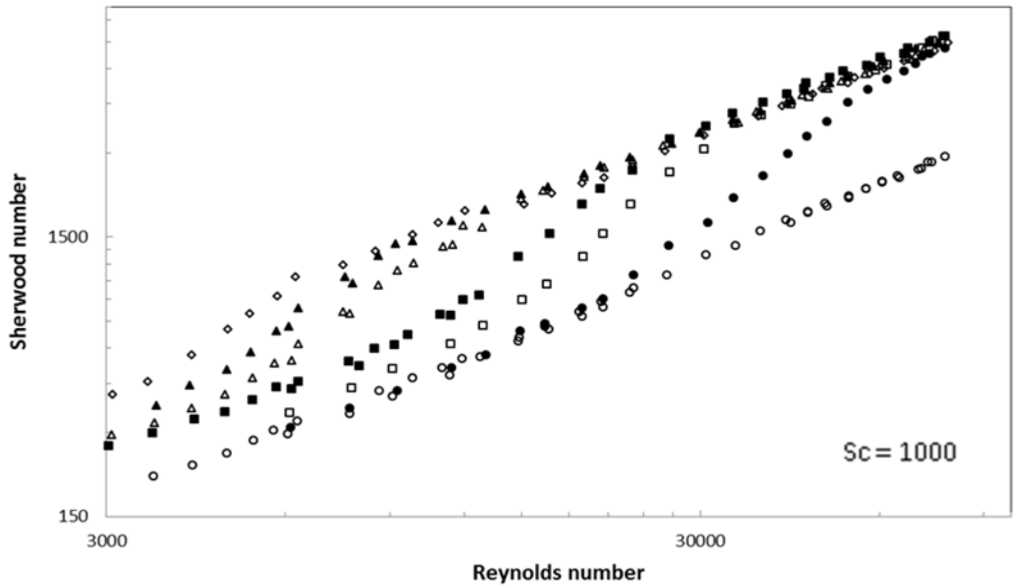

Figure 2.3 Dimensionless mass transfer coefficients from Dawson et al.(12) ○smooth ● e 0.056 mm, p/e 4.5 □ e 0.1 mm, p/e 4 ■ e 0.13 mm, p/e 4 Δ e 0.2 mm , p/e 4 ▲ e 0.28, p/e 4 ◊ e 0.35 mm, p/e 4

Dawson et al. (12) performed a series of mass transfer experiments with LCDT on ducts made of nickel plate with different V-shaped groove roughness. The V-shaped grooves ran across the flow direction and a series of test were done with geometrically similar V-shape rough surfaces and pitch/height ratio, but with different sizes. Another series of tests were done on the roughness of modified V-shapes and different pitch/height ratio. The Sherwood numbers at different Reynolds numbers on multiple surface roughness at Schmidt number 1000 are shown in Figure 2.3, in which e is defined as the roughness height, and p is the pitch between v-shaped grooves. There is an enhancement of the mass transfer with the surface roughness. The Sherwood numbers over the entire Reynolds number range on smooth surface and fully roughness formed lower and upper bounds for Sherwood numbers on different surface roughness. The fully rough data was obtained on a

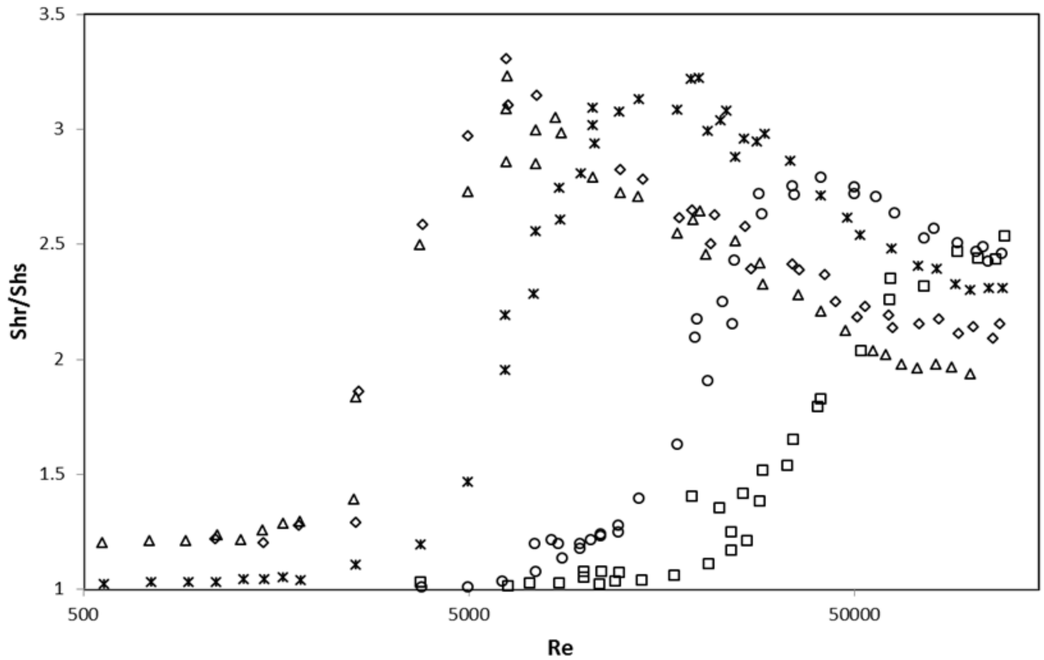

Figure 2.4 Sherwood number ration vs. Reynolds number, surface Δ e = 1.5 mm , p/e = 5;◊ e = 1 mm , p/e = 5, * e = 0.5 mm , p/e = 5; ○ e = 0.173 mm , p/e = 7; □ e = 0.076 mm , p/e = 8

surface with roughness height 13.6 mm and roughness pitch 50 mm apart. For a given roughness, as Reynolds number increases, the Sherwood number increases from a smooth wall value to fully rough wall value. For a higher surface roughness, the mass transfer is enhanced at lower Reynolds numbers.

Zhao and Trass (13) performed tests with similar V-shape groove surface roughness as Dawson and Trass(12), but in circular nickel test sections. The experiments suggested that the mass transfer rate on the fully rough pipes at Re ≥ 60000 is

$$Sh_{pipe} = 0.03\, Re^{0.79} Sc^{0.45} \qquad 2.6$$

The coefficient of this equation (0.03) is higher than that in the correlation of Krall and Sparrow (4), and Tagg et al.(6) for smooth pipe mass transfer, while the exponents of Reynolds numbers are similar, and the exponents of Sc is higher than it is for smooth pipe mass transfer. The ratio of the mass transfer rate for different roughened surfaces and smooth surfaces (Sh_r/Sh_s) at different Reynolds numbers were quantified as shown in Figure 2.4 for at Sc = 4720.

Mass transfer is enhanced at piping locations where there are large flow changes, which includes bends, fabrication discontinuities, valves, and orifices. Large changes in the flow and turbulence can change the mass transfer rate. The turbulent flow structure in the separated and reattached regions downstream of an orifice is complex and the details of the mass transfer mechanism are not clearly understood at present. There are large discrepancies in the correlations for the location and value of maximum mass transfer rate downstream of an orifice, nozzle or sudden expansion. A number of studies of FAC in these flow geometries have been performed (2)(3). The mass transfer downstream of an orifice has been studied extensively (4)(5)(6)(7) , including the effect of orifice to pipe diameter ratio, Reynolds number and Schmidt number. However, most experiments have been performed using smooth surfaces.

The FAC mechanism downstream of an orifice and sudden expansion are similar, both of which have flow separation and flow reattachment. A vena contracta is produced downstream of an orifice, with the area typically about 60% of the orifice area. Therefore, the maximum mass transfer rate is greater downstream of an orifice than it is downstream of a sudden expansion at the same Re_o and Re_d (18), where Re_o is the orifice Reynolds number and Re_d is the upstream pipe Reynolds number before the sudden expansion defined as

$$Re_o = \frac{u_o D}{\nu} \qquad 2.7$$

and

$$Re_d = \frac{u_d d}{\nu} \qquad 2.8$$

where u_o is average velocity across the orifice plate, u_d is the average velocity across the upstream pipe before the sudden expansion, D is the diameter of the orifice, d is the diameter of the upstream pipe, and ν is the kinematic viscosity of the fluid

Krall & Sparrow (4) investigated the heat transfer in the separated, reattached, and redevelopment regions downstream of an orifice in a circular tube. The experiments were performed at a pipe Reynolds number range from 10000 to 131000, with Prandtl number in the range 3 to 6 using stainless-steel tubing of relative wall roughness (e/D) 0.0024. The Nusselt number was found to scale with the 2/3 exponent of the Reynolds number and the maximum in the Nusselt number was correlated as

$$(Nu)_{max} = 0.398\, {Re_o}^{2/3} \qquad 2.9$$

where Nu is Nusselt number. The dependence on Prandtl number was not included in this correlation. The maximum heat transfer was found to occur in the range 1.25 to 2.5 pipe diameters downstream of an orifice.

Tagg et al. (6) did a series of tests to study heat and mass transfer downstream of abrupt nozzle expansions in turbulent flow using the limiting diffusion current technique (LDCT). The experiments were performed using a nickel tube polished with progressively finer grades of emery paper, but the roughness was not quantified. The Reynolds number

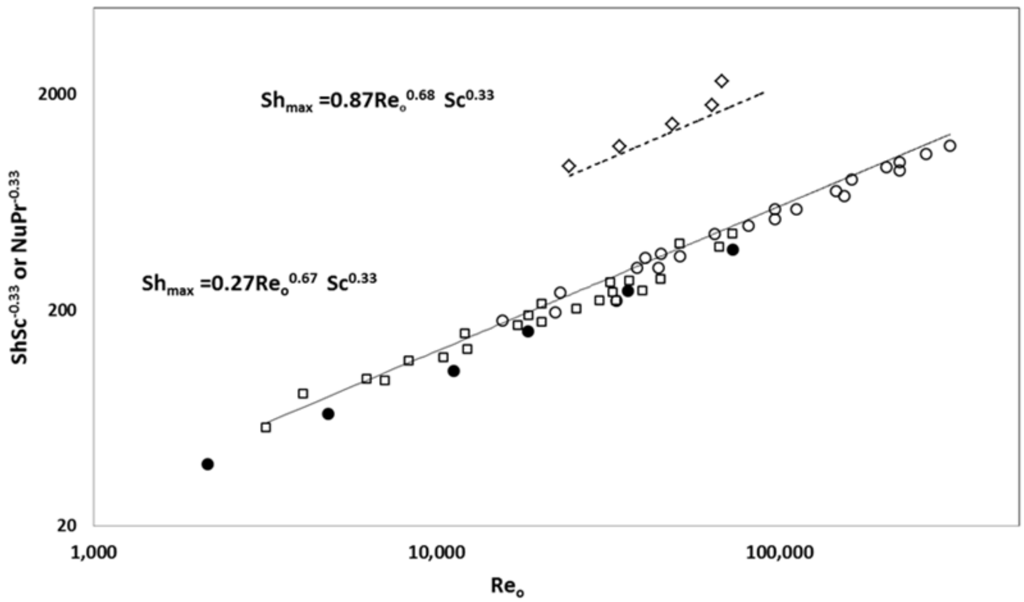

Figure 2.5 Maximum Sh for □ Wragg et al.(1979), ○ Krall and Sparrow(1966), ◊ Rizk, Thompson and Dawson(1996)● Poulson and Russell (1986)

based on the downstream duct diameter varied from 1900 to 23000, and the Schmidt number is 1450. The maximum mass transfer location moved downstream with Reynolds numbers for the same expansion ratio. Sh, as a commonly used nondimensionalized form of mass transfer coefficient, is defined as

$$Sh_{max} = \frac{hL}{D} \qquad 2.10$$

where h is the mass transfer coefficient m/s, D is mass diffusivity, and L is characteristic length. They developed a correlation for the maximum mass transfer rate as

$$Sh_{max} = 0.27\ Re_N^{0.67} Sc^{0.33} \qquad 2.11$$

where Re_N is the nozzle Reynolds number, and Sc is Schmidt number. This correlation is in agreement with the correlation of Krall and Sparrow(4) as seen in Figure 2.5, whose coefficients and exponents of Reynolds numbers and Schmidt or Prandtl numbers are identical.

Table 2.1 Comparison of measured and predicted peak Sh following the orifice

Orifice Reynolds number	measured Sh	Predicted Sh (9)	% discrepancy
793151	326	362	15
36145	561	617	12
18503	882	1077	11
11188	1352	1500	22
4819	2084	2334	10
2151	3232	3717	11

Poulson (9) performed a series of mass transfer measurements downstream of an orifice using dissolution of copper tubes in 0.1N HCl containing 2g/l ferric ion. The results for the max Sh by Poulson and the predicted values from the correlations by Krall, Sparrow and Tagg et al. are listed in Table 2.1. The data of Poulson is within 22% of the predicted values (9). In the experiments of Poulson(18), the pipe surface roughness initiated and developed naturally from the flow. However, scallops were only observed on specimens tested at the higher Reynolds numbers, and were observed only at the maximum mass transfer region. The surface roughness was not quantified in this paper. The maximum Sherwood numbers downstream of an orifice obtained by Poulson are plotted in Figure 2.5 with the others. The data is consistent with the data of Krall & Sparrow(4), and Tagg et al.(6). The effect of roughness is not observed in this experiment, which may be because of much less developed roughness during the experiments.

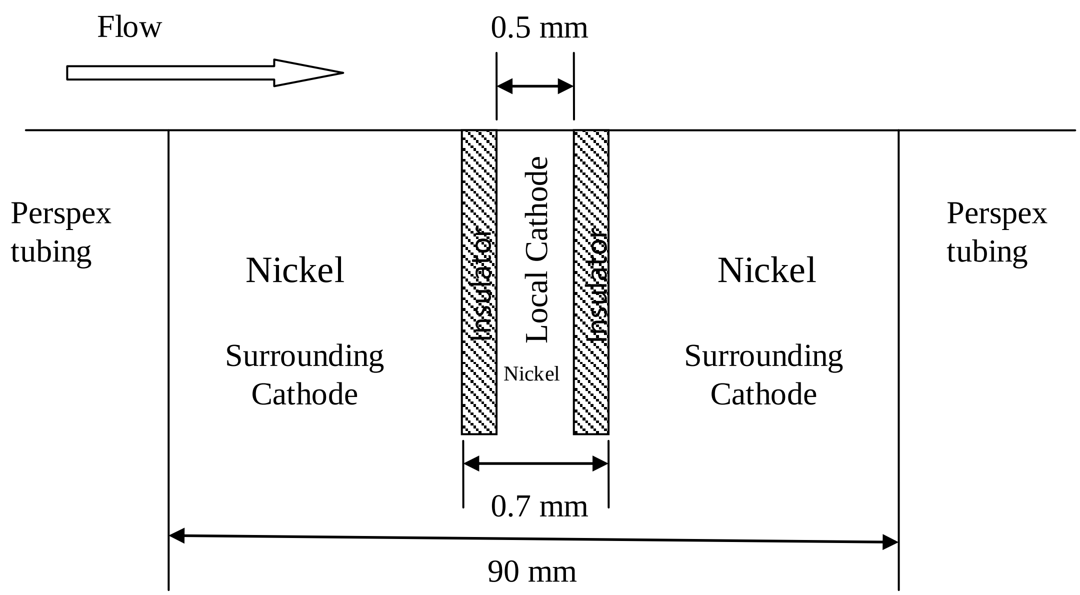

Figure 2.6 A schematic diagram of a local cathode used for mass transfer measurement by LCDT(7)

Ota(8) did a comprehensive review on the maximum heat transfer coefficient on a wide variety of flow configurations, including orifice induced separations, downward surface steps, and blunt bodies. A correlation for Sh was proposed as

$$Sh_{max} = 0.192 Re^{0.665} Sc^{1/3} \qquad 2.12$$

that is valid in the range $8x10^3 \leq Re \leq 2x10^6$; $0.7 \leq Pr \leq 9$ or $0.6 \leq Sc \leq 2500$. To cover all the flow configurations, the characteristic length, l, was based on the distance from separation point to the reattachment point. For orifice or sudden expansion, Re is the Reynolds number at the cross-section of the flow separation in equation 1.11, and the free stream velocity outside the boundary layer at the step is used to estimate Re in the case of the flow over the downward step. As a more general correlation for various shape, the characteristic lengths in the correlations of Ota are defined differently, and the coefficient of 0.192 in equation 2.11 is lower than the coefficient 0.27 in equation 2.10.

Rizk et al. (7) employed LCDT to conduct mass transfer tests downstream of a sudden expansion in smooth Perspex tubing with a different electrode design from the experiments performed by Tagg et al.(6). The cathodes used by Rizk et al.(7) were made of a 0.5 mm diameter nickel wire inserted into a 90 mm OD cathode, which was assembled to the tube as shown in Figure 2.6. While, Tagg et al. (6), however, used 1mm nickel wires inserted to the tube directly. The peak mass transfer rate over $49600 \leq Re_d \leq 97700$ for Schmidt number 1640 was given by

$$Sh_{max} = 0.87\, Re_d^{0.68} Sc^{0.33} \qquad 2.13$$

where Re_d is the Reynolds number based on the cross-section of the sudden expansion. The peaks mass transfer rates were located between 1.5 and 2.5 diameters downstream of the sudden expansion. The coefficient of the above correlation shows a significant discrepancy from others, by a factor of 3, even though the exponents of Re and Sc are identical. The data is shown in Figure 2.5. Rizk (7) believed that the different electrode design and their geometrical arrangement caused the difference.

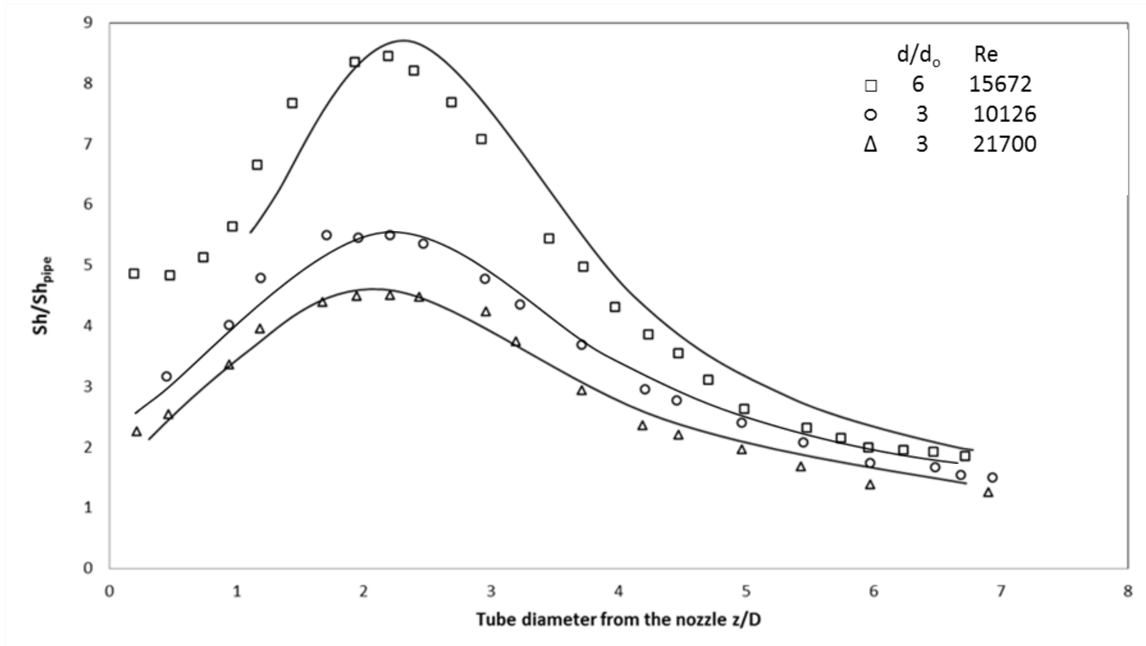

Figure 2.7 mass transfer profiles downstream of — Coney's correlation □, ○, Δ Tagg et al. data(33)

Coney (33) presented correlations for the mass transfer rate profiles instead of only the maximum values. It was suggested that an orifice and nozzle have similar effect on mass transfer rate and locations of maximum mass transfer. Based on the data of Krall and Sparrow (4) and Tagg et al. (6), Coney developed the following correlation

$$\frac{Sh_x}{Sh_{fd}} = 1 + A_x[1 + B_x\left(\frac{{Re_o}^{0.66}Sc^{0.33}}{Sh_{fd}} - 21\right)] \qquad 2.14$$

where Sh_x is the local Sherwood numbers, x is the downstream location from the orifice or sudden expansion, and Sh_{fd} is fully developed pipe Sherwood number calculated by equation 2.4. The coefficients A_x and B_x at different downstream locations (x) are shown in the following table

Table 2.2 values of constant in Coney's equation for mass transfer profiles of orifices (33) KS data Valid: $2 \leq d/d_o \leq 4$, $10^4 \leq Re \leq 1.3x10^5$; $3 \leq Pr \leq 6$, TPW data Valid: $2 \leq d/d_o \leq 6$, $8x10^3 \leq Re \leq 2.2x10^4$; Sc = 1450

Distance from orifice in tube diameter (x)	A		B	
	KS	TPW	KS	TPW
0.5	2.72	2.12	0.057	0.073
1	3.67	3	0.051	0.049
1.5	4.52	3.75	0.059	0.062
2	4.7	4.2	0.066	0.072
2.5	4.5	4.17	0.068	0.079
3	4	3.74	0.067	0.078
3.5	3.15	2.92	0.065	0.073
4	2.45	2.25	0.064	0.069
4.5	1.72	1.62	0.063	0.064
5	1.45	1.27	0.062	0.063
5.5	1.22	0.98	0.069	0.062
6	1	0.77	0.058	0.062
6.5	0.88	0.6	0.056	0.062
7	0.67	0.45	0.055	0.062

Coney's correlation is based on data either at low Reynolds numbers, high Schmidt number $8x10^3 \leq Re \leq 2.2x10^4$; Sc = 1450 or high Reynolds numbers and low Prandtl numbers $10^4 \leq Re \leq 1.3x10^5$; $3 \leq Pr \leq 6$. The mass transfer profiles from the correlations of Coney are presented in Figure 2.7, along with the data of Tagg et al.. It is shown that the correlation, in general, has good agreement with the experimental data. However, it has better match for $d/d_o = 3$ rather than 6.

Up to now, there have been very few studies on the mass transfer downstream of an orifice on naturally developed roughened surfaces, especially at high Reynolds number. The surface roughness enhancement factor developed for fully developed pipe flow may not be applicable for reattaching flow such as those downstream of an orifice or sudden expansion.

In summary, the data for mass transfer downstream of a sudden expansion or orifice show significant discrepancy between different researchers. The surface roughness is believed to be an important factor in the mass transfer, which is not fully understood. A series of mass transfer experiments using a dissolving wall technique at different Reynolds numbers are performed to study the roughness effect on mass transfer rate downstream of an orifice. Tests are performed in two different diameter pipes with the same orifice/pipe ratio.

Chapter 3 EXPERIMENTAL FACILITIES

Experiments were performed to examine the Reynolds number and roughness effect on the mass transfer rate downstream of an orifice. The experiments were performed in a 2.5 cm diameter test facility at Reynolds number of Re_o = 80000, 140000, and 200000, and in a 20 cm diameter test facility at Re_o = 180000. Tests were performed using test section cast from gypsum in the small bore loop and a test section that had a gypsum inner liner in the large bore loop. For all tests, the orifice to pipe diameter ratio (d_o/D) was kept at 0.5. In the small bore loop, for each Reynolds number, a series of tests were performed using different test samples for different test times. After each test time, the test sections are sectioned, and the wear surface topologies mapped using a laser scanning technique. The surface roughness was analyzed from the scanned images. The large bore test was performed at Re = 180000 to compare with the test in the 2.5 cm diameter test facility. In this experiment, the wear was measured at fixed axial locations using ultrasonic measurements. The test section was cut into half at the end of the test and the surface was laser scanned to determine the surface topology. The two test facilities and the experimental methodology are described in this chapter. The data reduction techniques for the mass transfer coefficients are also presented.

3.1. 2.5 CM DIAMETER BORE EXPERIMENTS

3.1.1. 2.5 cm diameter bore test facility

The 2.5 cm diameter test facility is shown schematically in figure 1.1. Water is circulated using a centrifugal pump capable of generating a flow rate up to 2 Liters/sec. The facility is operated as a closed loop using a 100 liter capacity plastic tank reservoir. A cooling coil is placed in the tank to maintain the temperature constant during the test times. A conductivity probe is also located in the tank to monitor the dissolution of the gypsum from the test section into the recirculating water. The flow rate through the test section was adjusted through a bypass valve. There is a 1.5 meter long, 2.5 cm ID (inside diameter) acrylic tube attached horizontally upstream of the test section to allow the flow to be fully developed(34), which is longer than the 56 tube diameters recommended in BS 1042(35) for orifices. An ASME standard orifice with orifice diameter do = 1.25 cm was placed upstream of the gypsum test section. A schematic diagram of the installation of the orifice is shown in Figure 3.1 b. A 0.375 meter acrylic tube aligned with the gypsum test section was attached downstream of the test section. The flow discharged into the tank and the

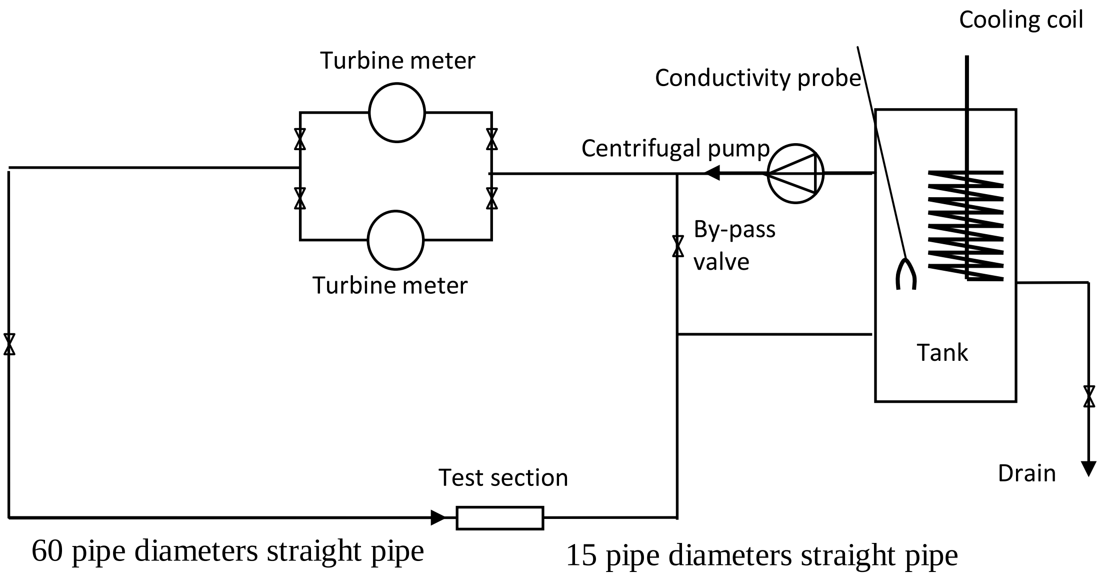

(a)

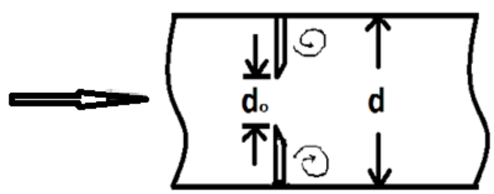

(b)

Figure 3.1 (a) Schematic of the 2.5 cm bore test facility (b) Schematic of an orifice

water temperature was maintained at 25 ±0.5 ℃ using a dedicated chiller to circulate chilled water through the cooling coil. After each test, the water was fully drained from the system to ensure all tests had the same initial condition.

One of two turbine meters placed in parallel with different ranges was used to measure the volume flow rate. The conductivity probe has a built in temperature probe, which was used to monitor the water temperature during the test. The conductivity and temperature data were recorded online to a dedicated computer. A bypass loop was used to bring the flow condition to steady state before the flow is passed through the test section.

3.1.2. 2.5 cm diameter bore experiment methodology

The mass transfer rate at a given Reynolds number was obtained by running tests for different test times. A different test section was used for each time. The test sections were fabricated in a well-controlled manner to ensure consistency of the test samples. The test sections were cast in a mold as shown in Figure 3.2. The mold was assembled from 5 PVC plates with grooves that were machined to high precision. The mold was assembled together by a set of flat head screws. The core for the pipe is made of four segments to form a tube of outside diameter 2.5 cm as shown in Figure 3.2 b. The 4-piece design of the core allowed the mold to be released without damage to the casting. The core was wrapped by a Latex balloon to minimize any effects of the seams and prevent the liquid hydrocal mixture from leaking into the core during the casting process. The four-piece core was 3D printed using a rapid prototype machine. The two smaller keyways of the core were aligned along the top and bottom to minimize their effect on the casting. The diameter difference over the core is 25 $\pm$ 0.1 mm. The cores are oriented identically during each casting with a position lock, so that the initial test sections are identical to minimize any initial discrepancies in the cast sections. A stainless steel rod is press fit to the core to prevent the core from collapsing during the casting. A picture of the prepared mold ready for casting is shown in Figure 3.3.

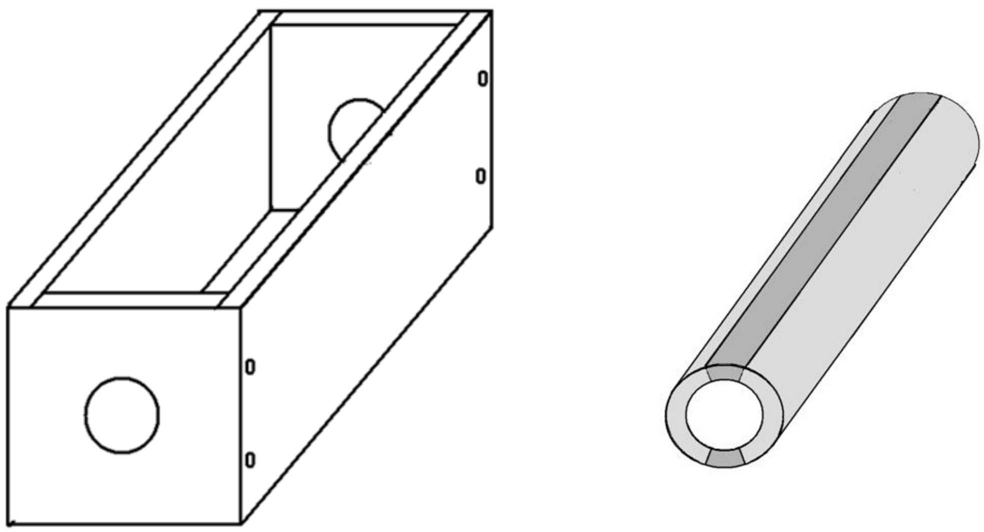

(a) (b)

Figure 3.2 Schematic of casting mold for 2.5 cm diameter bore test sections

The hydrocal mixture was prepared by first dissolving citric acid into deionized water in a clean beaker before the Hydrocal was added to extend the reaction time between Hydrocal with water from about 5 minutes to 25 minutes. The reaction between water and hydrocal is given by

$$CaSO_4 * 1/2\, H_2O + \frac{3}{2} H_2O \Rightarrow CaSO_4 . 2H_2O \qquad 3.1$$

The mass ratio between hydrocal and water for a complete reaction is 141:15 respectively. However, the ratio of Hydrocal, water and citric acid used was 175:65:1 respectively, where excess water is used to ensure a complete reaction with Hydrocal (36). The mixture is stirred for 2 two minutes, and then placed in a vacuum chamber for 4

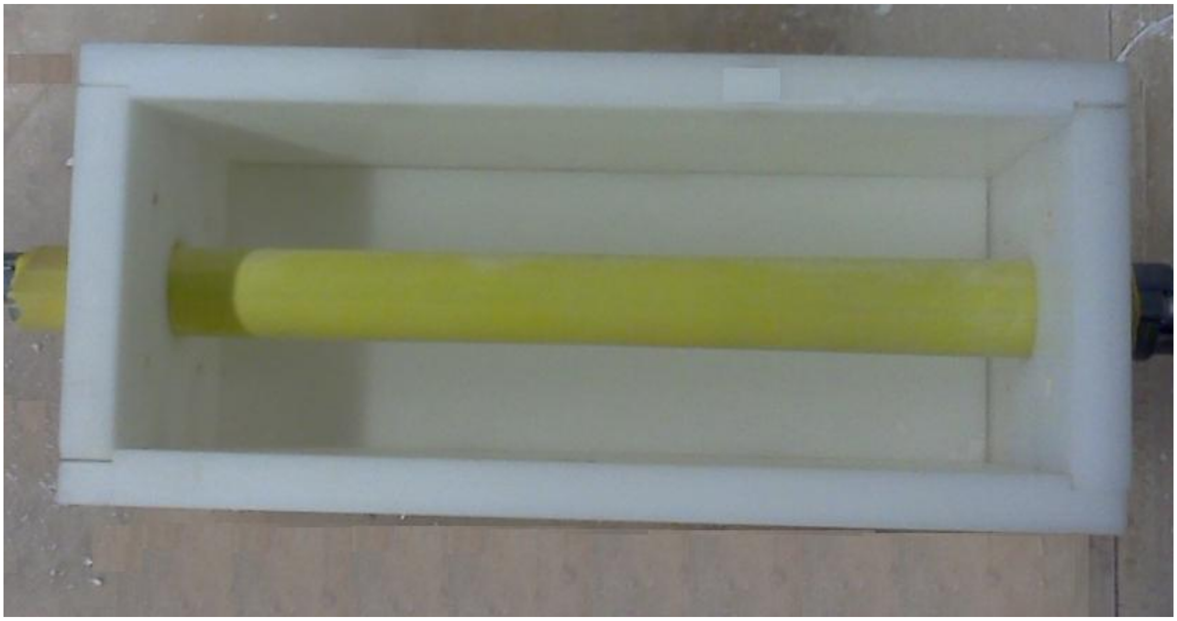

Figure 3.3 Mold of 2.5 cm diameter bore test sample

(a) (b)

Figure 3.4 Image of 2.5 cm diameter bore test section minutes to allow any trapped air bubbles during the mixing process to escape. The mixture is slowly poured into the prepared sample mold as shown (Figure 3.3).

The test section is allowed to cure for about 30 minutes, and the four-piece core was then removed from the mold. After a further two hours, the mold was disassembled and the test section allowed to dry. The test section had outer dimension of 23 x 8.5 x 8.1 cm with a 2.5 cm hollow cylinder along the centerline. The section was allowed to dry under ambient conditions, and the weight was monitored till it reached a steady value, which typically took about 10 days.

The average radius of the unworn test samples was 12.83 mm, which was slightly larger than the ideal pipe radius by 0.56 mm. The manufactured test sections were consistent. Two scanned images of unworn samples were compared, and the root mean square of local deviation between those two unworn samples was 0.084mm or 0.33% of the pipe diameter.

Tests were performed for different times for each Reynolds number. Before each test, the reservoir was filled up to 50 liters. The temperature of the water was controlled to 25 ± 0.5 °C during each test. The temperature and conductivity measurement were taken every minute, and stored to a computer for further analysis. The maximum experimental time for each Reynolds number was determined so that the maximum pipe radius change is within 10% of their initial values. Therefore, the maximum run time for Re_o of 80000, 140000, and 200000 are 75 min, 60 min and 45 min respectively. After completion of a test, the worn sample was replaced by a new sample for another experimental time. At the end of each test, the test section was removed and allowed to dry for about a week under

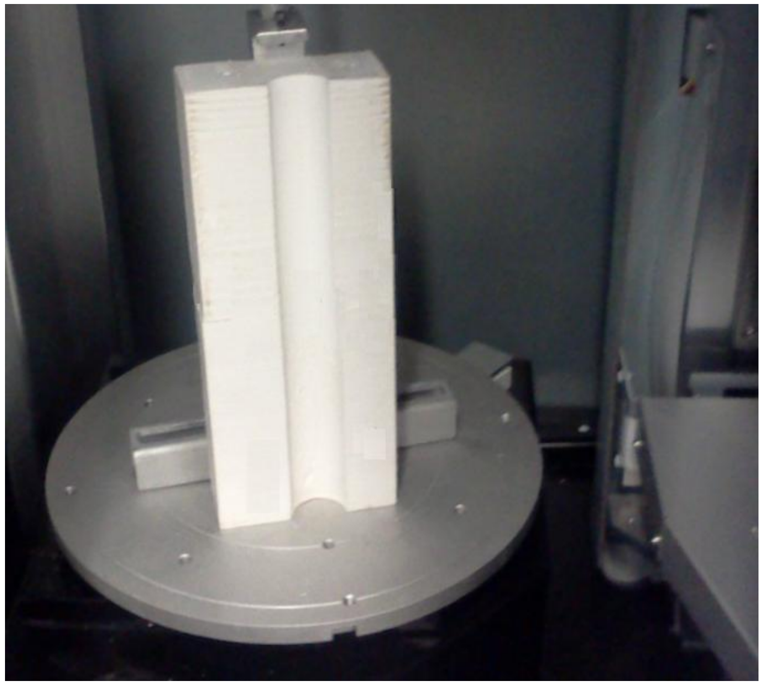

Figure 3.5 Sample set up in scanner

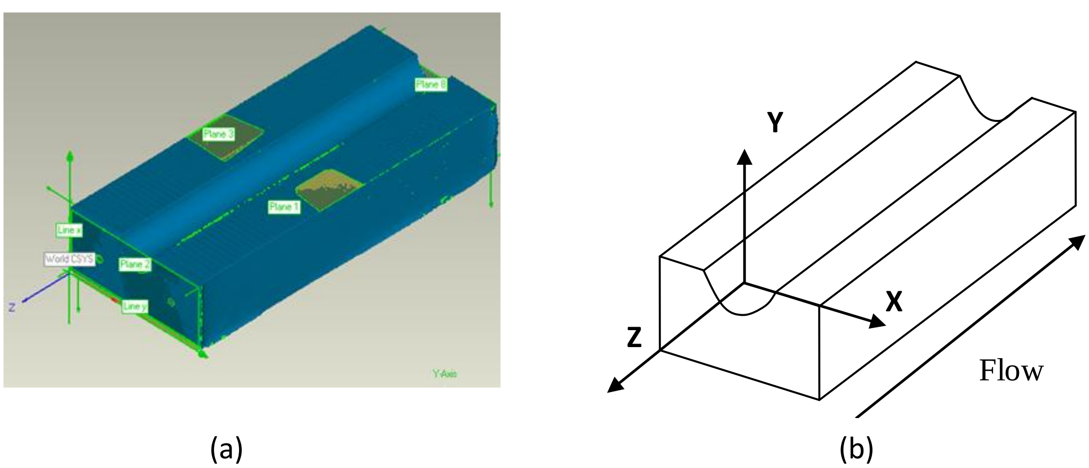

Figure 3.6 Scanned image and schematic of the test section

ambient conditions. Then each test section was sectioned into halves with a 0.7 mm thick band saw. Each piece was scanned using a three-dimensional (3D) Roland laser scanner LPX-600® to obtain the worn surface topology. The scanner uses a noncontacting laser method to scan the surface by emitting a spot beam onto the surface and detects reflected light from surface with sensors. The scan object is rotated simultaneously while the laser beam is traversed from bottom to top(37). The sample was fixed on the rotating plate by a fixture as shown in Figure 3.5. The samples were scanned by planes from 5 different angles to capture the entire pipe side walls and the flat surfaces of the cast block. The scanning pitch was 0.2 to 254 mm in width direction, and 0.2 to 406.4 mm in height direction with a repeated accuracy of ± 0.05 mm.

The scan point cloud data set is imported by Geomagic Qualify®, which is a 3D inspection software, as shown in Figure 3.6. The test section is aligned to a common coordinate system by aligning the whole cut section based on a best fit to the 3 flat side walls. The z axis is defined as the intersection between the bottom and side surface of the image, where the direction of z is opposite to the flow direction. Similarly, y is defined as the intersection of the bottom surface and the front surface, and the origin and x axis are then fixed. By aligning all the test samples to a common coordinate system, the wear progression with time can be determined by comparing the worn surfaces. The origin of the coordinate system was then shifted from the corner of the casting as defined to the center of the cylindrical worn surface, and the point cloud data are transferred to cylindrical coordinates with z as the longitudinal axis. The local radius at the different run

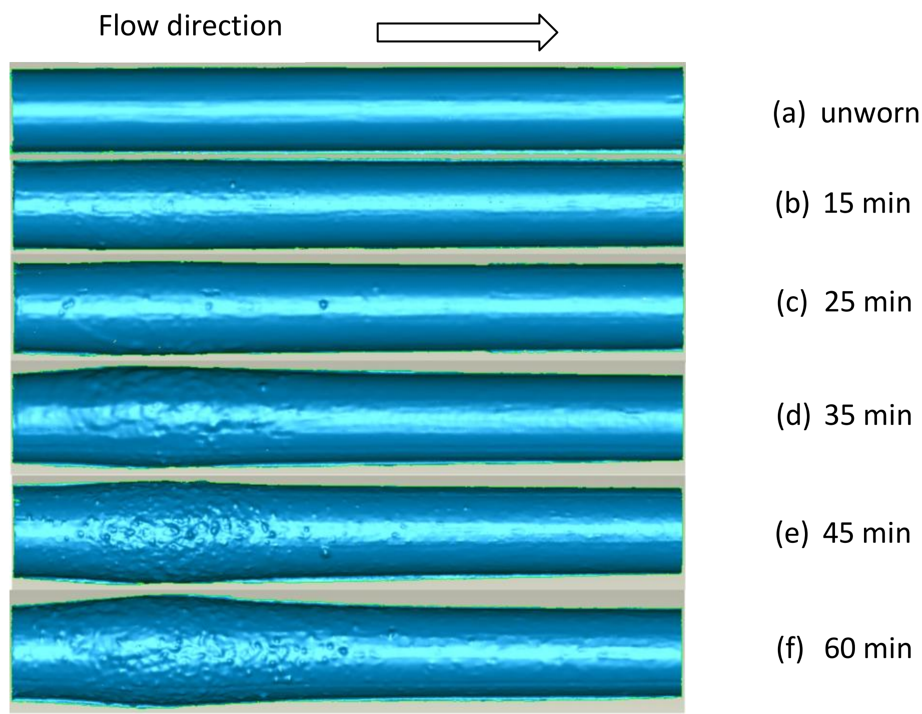

Figure 3.7 Images of downstream pipe sections at Re_o = 140000, Sc = 1280 at 25 ℃

times are compared to determine the mass transfer rate, which is discussed in detail later on. All data points other than the pipe surfaces are eliminated after this alignment procedure for further data processing. Images of the scanned surface at run times of 15, 25, 35, 45 and 60 min at Reynolds number of 140000 is shown in Figure 3.7. The images clearly show the progression of wear with time, and the maximum wear location occurs at about 1.6 to 2 pipe diameters downstream of the orifice.

3.1.3. Data reduction

The mass transfer rate is obtained from the point cloud data of the different test samples using a custom written code in MATLAB. The flow diagram of the code is shown in Figure 3.8. Firstly, the point cloud data are transferred from a Cartesian coordinate system to a cylindrical coordinate system. The data were gridded to the same grid in both longitudinal and circumferential directions for all the test cases so that they can be compared directly. The grid dimensions in the present experiment were 0.36 mm in the z direction and 1.5° in θ direction that is equivalent to an arc length of 0.36 mm for r = 12.7 mm. A schematic diagram of the grid is shown in Figure 3.9 a. The value of the local radius at each grid point was taken as the average of all radii that fall into the corresponding cell area. Generally, the scanned image cloud covered the entire scanned surface. The local radiuses at any grid with no data were obtained by interpolation of the surrounding data. After the initial alignment based on the sidewalls, the alignment of the pipe surface is refined using the condition of symmetric wear in the azimuthal direction. This is to take into consideration any initial minor casting misalignments of the sidewalls. The wear profiles along the downstream direction, which should be concentric, provide an indication of how well the alignment is based on the first alignment.

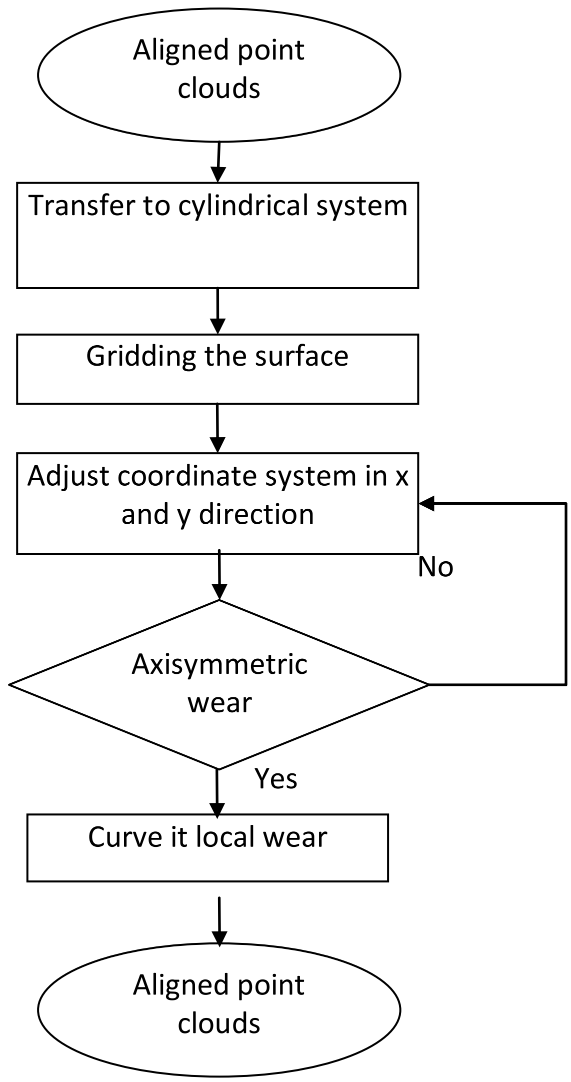

Figure 3.8 Flow diagram of MATLAB analysis

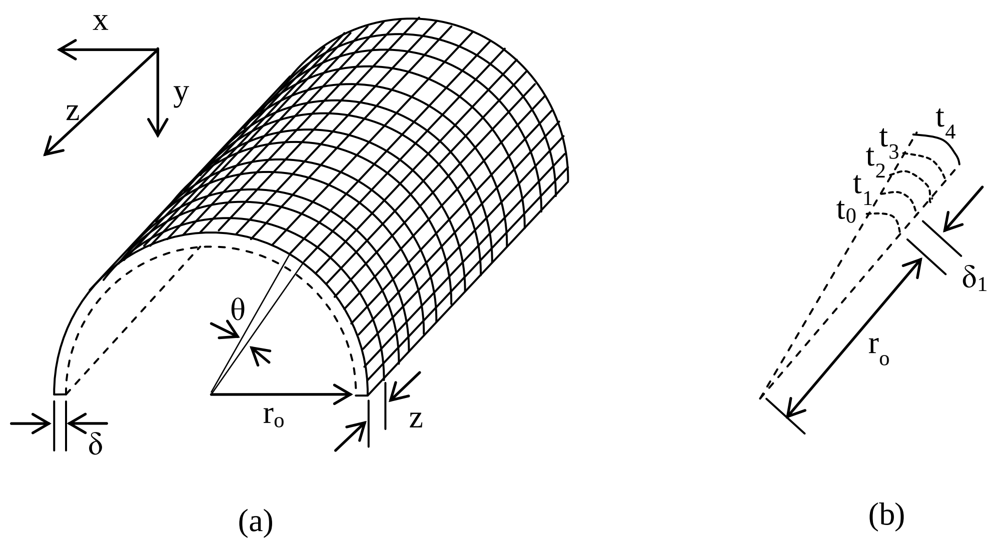

Figure 3.9 Schematic diagram of (a) the grids (b) wear progression with time

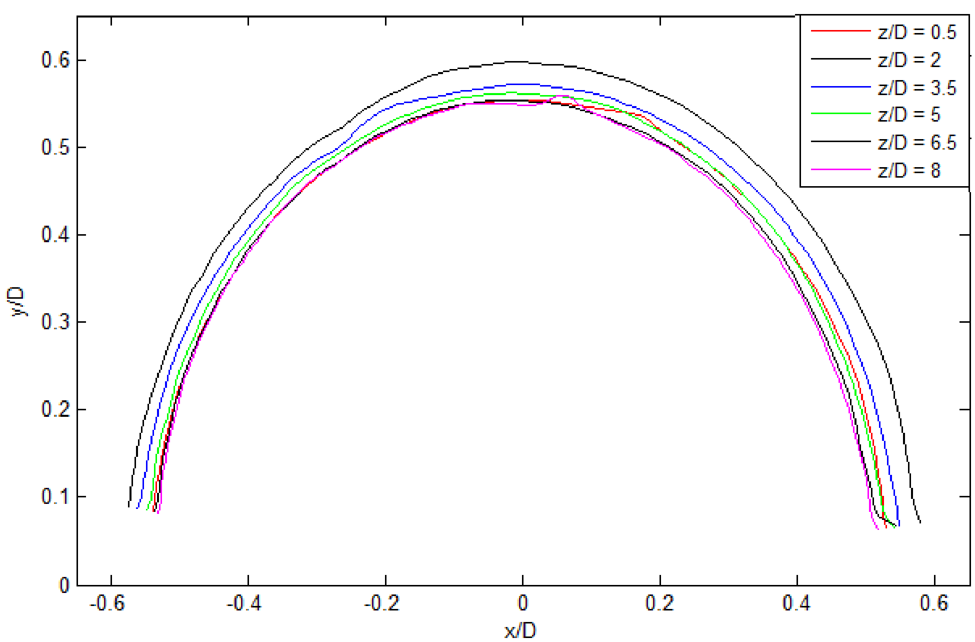

Figure 3.10 Cross-sectional worn profiles at different axial locations for Re_o = 140000 at 25 min

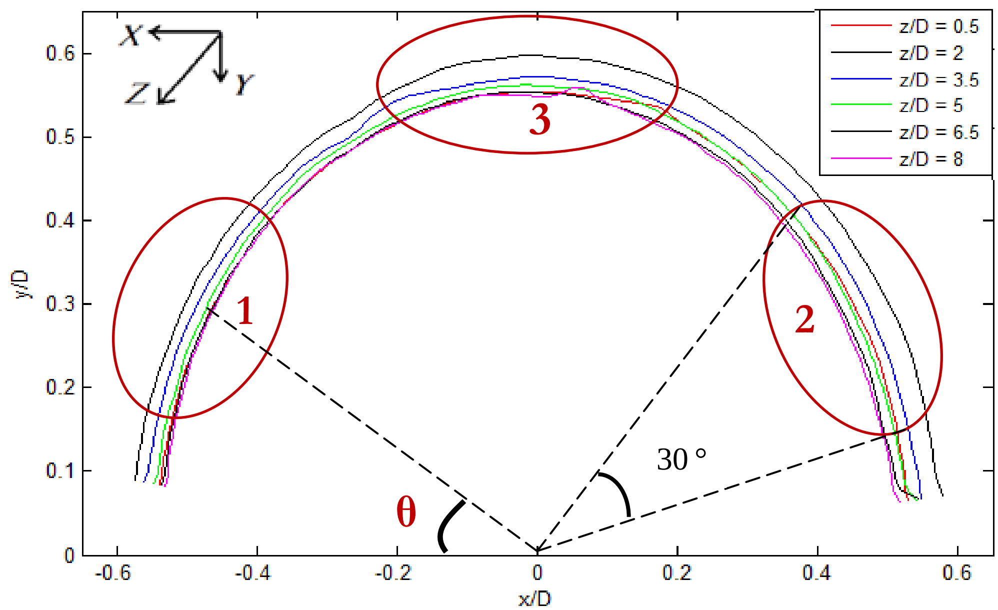

Figure 3.11 Cross sectional profiles before realignment for sample at Re_o140000 at 25 min

The cross sectional profiles along the axial direction after the first alignment for Re_o = 14000 and time = 25 minutes are shown in Figure 3.11. The profiles are not concentric in this instance which indicates the surface is misaligned with respect to the coordinate system. A systematic coordinate realignment procedure is developed to quantify and correct the misaligned coordinate system. The coordinate system is shifted and rotated in both x and y axes till the average radius in regions 1, 2, 3 shown in Figure 3.11 are equal over the entire length of the test section. Region 1 covers the area from 15 °to 45 °, Region 2 from 75 °to 105 °, and region 3 from 135 °to 165 °.

The initial alignment is refined using the methodology described here. Initially, the difference in the averaged radius in region 1 and region 2 is computed along the axial direction and the shift in the x-direction at each axial location is computed as

$$d_x = \frac{(r_1 - r_2)}{\cos\theta} \qquad 3.2$$

where r_1 is the averaged radius over region 1, and r_2 is the averaged radius over region 2. The value of d_x indicate how far the center of the semi-circle is off from the initially defined center in the x direction.

The values of d_x are plotted against the non-dimensionalized distance z/D downstream of the orifice as shown in Figure 3.12 (a). A least square straight line is fit to the data to obtain the shift and rotation necessary to re-align the coordinate system. The shift and rotation are applied so that both the slope and the level of the best fit line become zero.

The procedure is repeated for the y direction. The data are re-gridded to the same dimensions as before, and d_y at each z/D is calculated by taking the difference of the averaged radius in region 3 and the averaged radius in region 1 and 2 as

$$d_y = \frac{r_3 - (r_1 + r_2)/2}{\sin\theta} \qquad 3.3$$

Here, r_1 is the averaged radius over region 1, r_2 is the averaged radius over region 2, and r_3 is the averaged radius over region 3. The rest of the realignment procedure in the y direction is identical to that in the x direction.

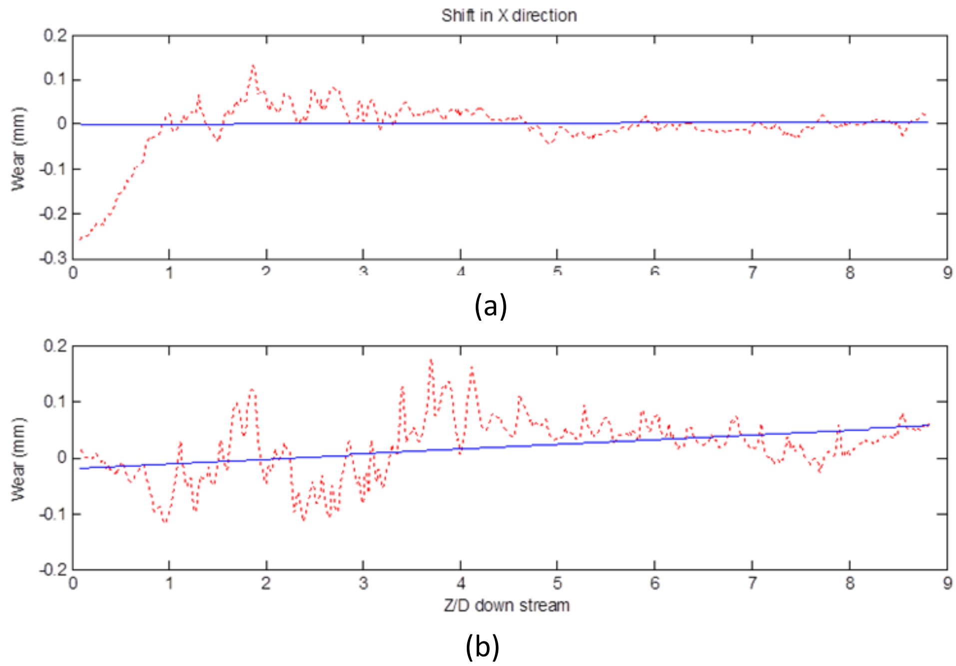

Figure 3.12 Fine alignment of each image coordinate system in (a) x direction (b) y direction

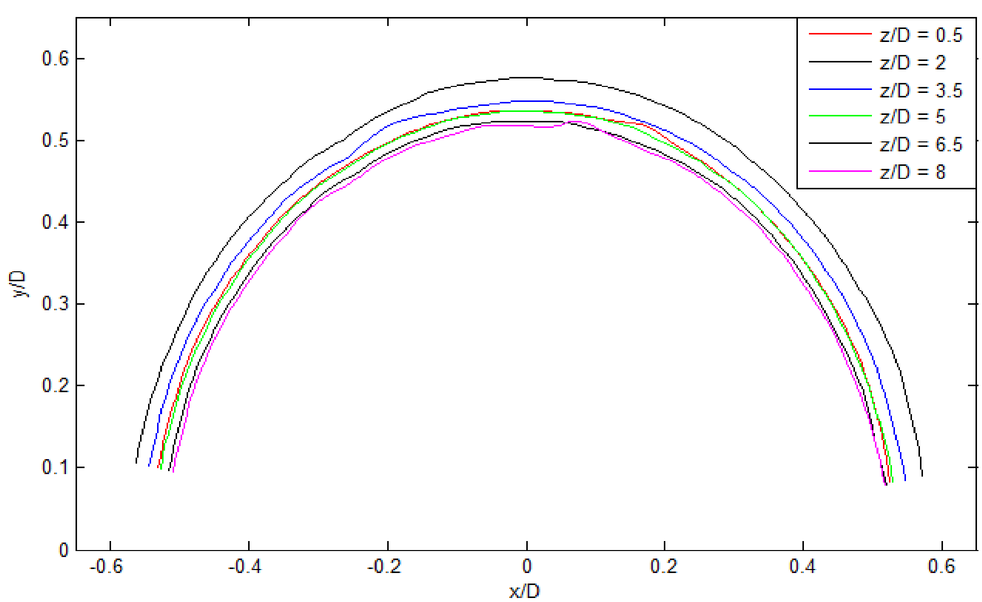

Figure 3.13 Wear profiles after realignment for Re_o = 140000 and time = 25 min

The realignment procedure was iterated until the slope of the best fit line was less than 0.00001 radian, and the intersection of the line with y axis was less than 0.001 mm. After the coordinate realignment in both x and y directions, the surface is re-gridded so that it is identical for all test sections. The detailed code is attached in Appendix A.

The balance between the total mass removed estimated from the scanned images and from the conductivity measurements are checked to ensure the accuracy of the methodology. A typical mass balance for the tests at Re_o=80000, Re_o=140000 and Re_o=200000 are shown in Figure 3.14. The mass removed from the scanned images was obtained by volume integration of the local wear over the whole worn surface as

$$m = \rho \iint (r_i - r_o)dA \qquad 3.4$$

where r_i is the local radius, r_o is the ideal radius of the unworn test section. The total mass removed measured from the conductivity meter was calculated directly from the calibration relating the amount of gypsum in solution to the conductivity. The calibration was performed by filling a beaker with 1 liter water at a temperature 25 ℃. A small amount of fine hydrocal powder is added to the solution and stirred to ensure a complete reaction. After a period of 5 minutes, the conductivity reading is taken. This is the repeated with an additional amount of hydrocal. The calibration data is plotted in Figure 3.15, and the slope of the best fit line to the data is 0.0011 (g/l)/(us/cm).

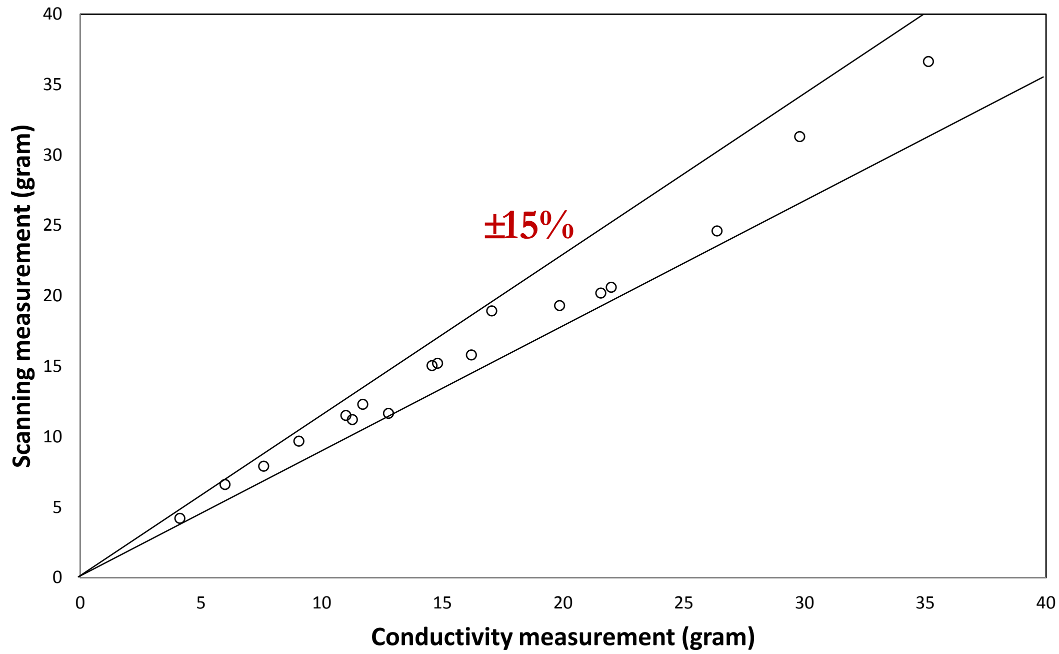

Figure 3.14 Mass balance between the measurement from the conductivity meter and integration of the scanned images

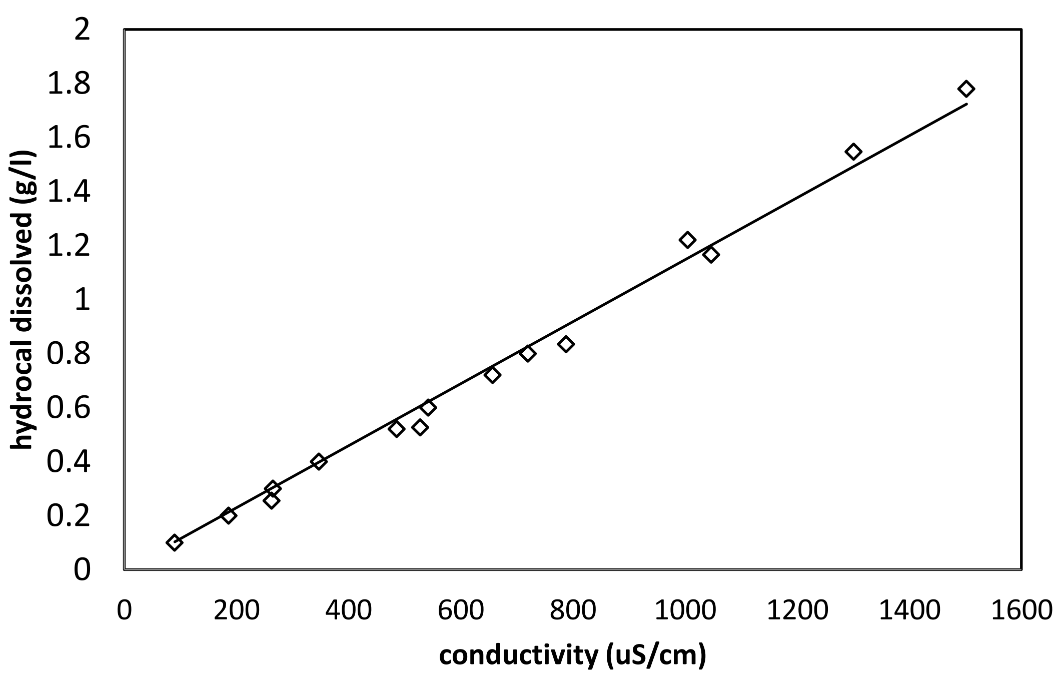

Figure 3.15 Calibration curve for the conductivity meter for hydrocal in water at 25 ℃

The total mass of gypsum that was dissolved in the tank is then given by

$$m_{cond} = 0.0011x * v_{tank} \qquad 3.5$$

where x is the conductivity reading from the conductivity probe, v_{tank} is the volume of the reservoir and all the piping in the facility, and m_{cond} is the total mass removed from the test section. The discrepancy between the mass balances from the two methods was within ±15% for all the cases providing confidence in the measurements. Any test section where the mass difference exceeded ±15%, is not considered, and the measurement repeated.

The local mass transfer rate was calculated at each grid point from the change in local radius with time. The local mass transfer rate was averaged over the circumferential direction at each axial location to obtain the axial variation of the mass transfer coefficient. The mass removed at each cell was calculated as

$$m = \rho v \qquad 3.6$$

where m is the mass removed at a grid cell from an ideal unworn pipe, ρ is gypsum density 1581 kg/m^3, v is the cell volume removed from ideal unworn pipe that is given by

$$v = z\theta r\delta(1 + \frac{\delta}{2r_o}) \qquad 3.7$$

where z is the cell length in the flow direction, θ is angular span of each cell, r_o is initial radius, and δ is the cell depth in the radial direction as illustrated in Figure 3.9. The nominal area of each cell is

$$A = z\theta(r_o + \frac{\delta}{2}) \qquad 3.8$$

By combining the above 3 equations, the mass removed per unit area is

$$\frac{\partial m}{\partial A} = \rho\delta \qquad 3.9$$

where A is the nominal cell area perpendicular to the radial direction. The mass transfer rate is

$$\frac{\partial m}{\partial A \partial t} = \rho \frac{\partial \delta}{\partial t} \qquad 3.10$$

The mass transfer coefficient h_m is defined through

$$\frac{\partial m}{\partial A \partial t} = h_m(t)\Delta C(t) \qquad 3.11$$

and

$$\Delta C(t) = C_w - C_b(t) \qquad 3.12$$

where C_w is the wall concentration of gypsum (2.4 g/l), and C_b is the bulk concentration. The bulk concentration increase while running the tests, since the loop is operated as a closed loop. The typical variation of ΔC with test time is shown in Figure 3.16.

The mass transfer coefficient is obtained by combining the 上方 three equations as

$$h_m(t) = \frac{\rho\frac{\partial \delta}{\partial t}}{\Delta C(t)} \qquad 3.13$$

Then local Sherwood number is given by (38)

$$Sh = \frac{h_m D}{D_{diff}} \qquad 3.14$$

where D is the diameter of the pipe, and D_{diff} is the diffusivity of gypsum (6.5×10^{-10} m^2/s)(38).

The local wear (δ) is calculated by taking the difference between the local radius of the worn surface from the unworn ideal radius. The term $\frac{\partial \delta}{\partial t}$ in equation 3.13 can be calculated by finite difference. The experiments are performed for five different times for

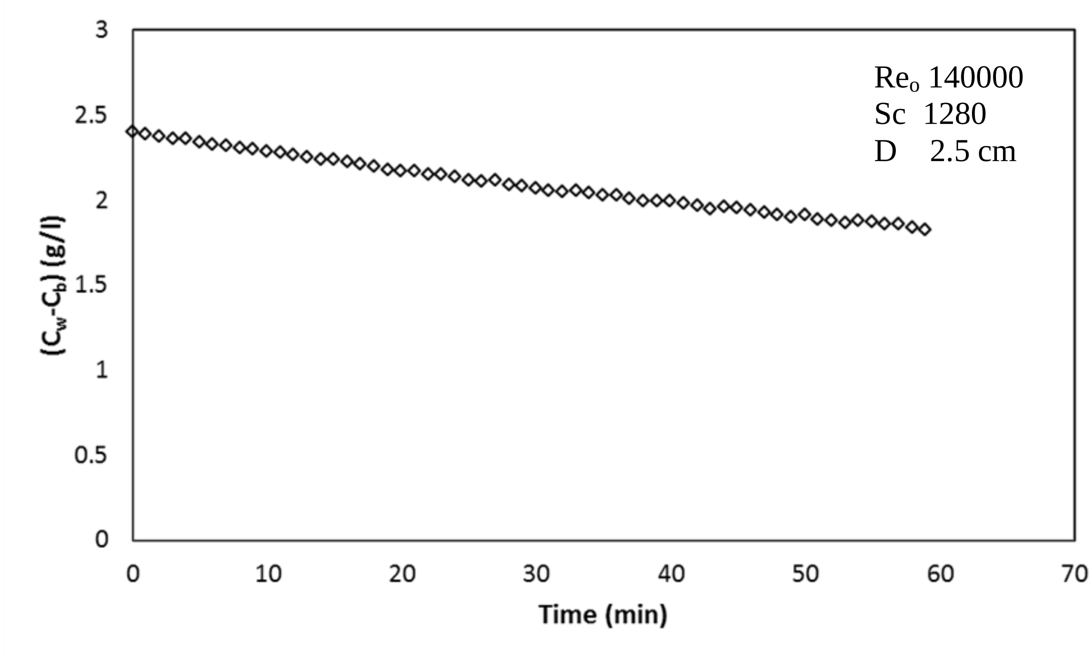

Figure 3.16 Concentration difference (C_w-C_b) with time at Re_o =140000

each Reynolds number. Since the ΔC changes with time over each test, this must be accounted for when computing the mass transfer rates. This is done by defining a modified time as

$$\tilde{t} = \frac{1}{\Delta C_0} \int_0^t \Delta C(s) ds \quad 3.15$$

to take into account the change of ΔC with time. Here, the original time axis is changed to reflect how the mass transfer driving potential ΔC(t) changes with time. The mass transfer coefficient (h_m) is calculated from

$$\frac{d\tilde{t}}{dt} = \frac{1}{\Delta C_0} \Delta C(t) \quad 3.16$$

$$\frac{\partial\delta}{\partial t} = \frac{d\delta}{d\tilde{t}}\frac{d\tilde{t}}{dt} \tag{3.17}$$

Combination of the above two equations gives

$$\frac{d\delta}{dt} = \frac{d\delta}{d\tilde{t}}\frac{\Delta C(t)}{\Delta C_0} \tag{3.18}$$

Multiplying both side by the gypsum density gives

$$\rho\frac{d\delta}{dt} = \rho\frac{d\delta}{d\tilde{t}}\frac{\Delta C(t)}{\Delta C_0} \tag{3.19}$$

Thereafter, equation 1.11 can be re-arranged as

$$h_m(t) = \frac{\rho\frac{\partial\delta}{\partial\tilde{t}}}{\Delta C_0} \tag{3.20}$$

where $\Delta C(t)$ is the concentration difference between C_w and C_b at a given time t, and ΔC_o is the concentration difference at the beginning of the test.

Once the modified time is calculated, the local wear (δ) at a given axial location averaged over the circumferential direction is plotted against the modified time for all the test times for a given Reynolds number. The slope of the linear fit line represents the mass transfer rate at that axial location. Representative plots at 6 evenly spaced z/D locations at Re_o = 80000, 140000 and 200000 are shown in Figure 3.17, Figure 3.18 and Figure 3.19. The data at zero modified time represent data from two unworn samples. The linear fit indicates the mass transfer rate remains relatively constant over the test times.

The measurement errors are considered in the present experiment. Generally, the uncertainty is a combination of the fixed error and the random error of the result and result (39) In the present experiment, the majority of the error source is the measurement error of

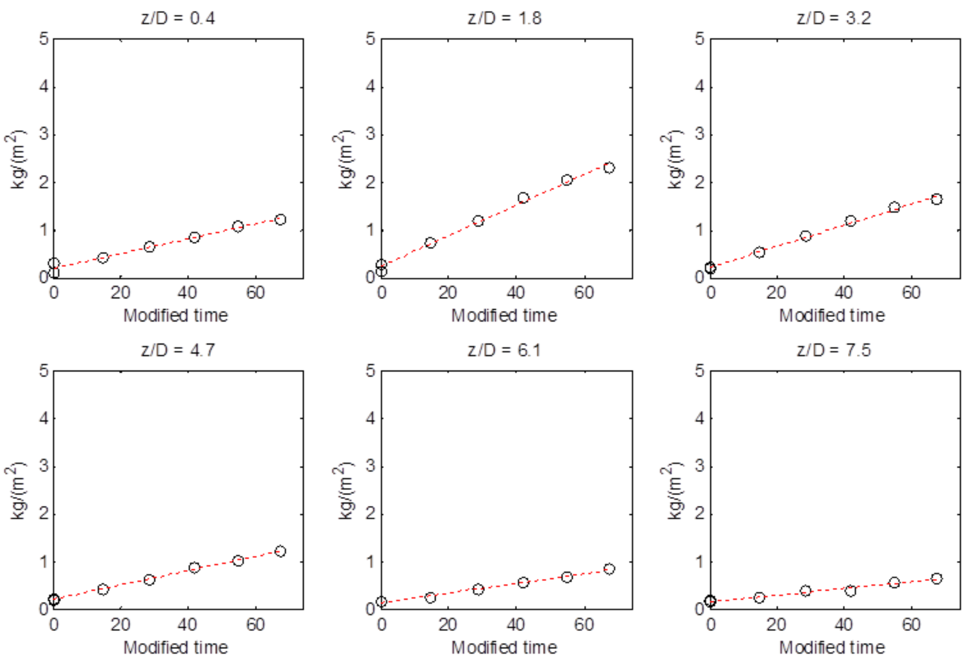

Figure 3.17 Variation of averaged mass transfer removal at different axial location with modified time at Re_o 80000

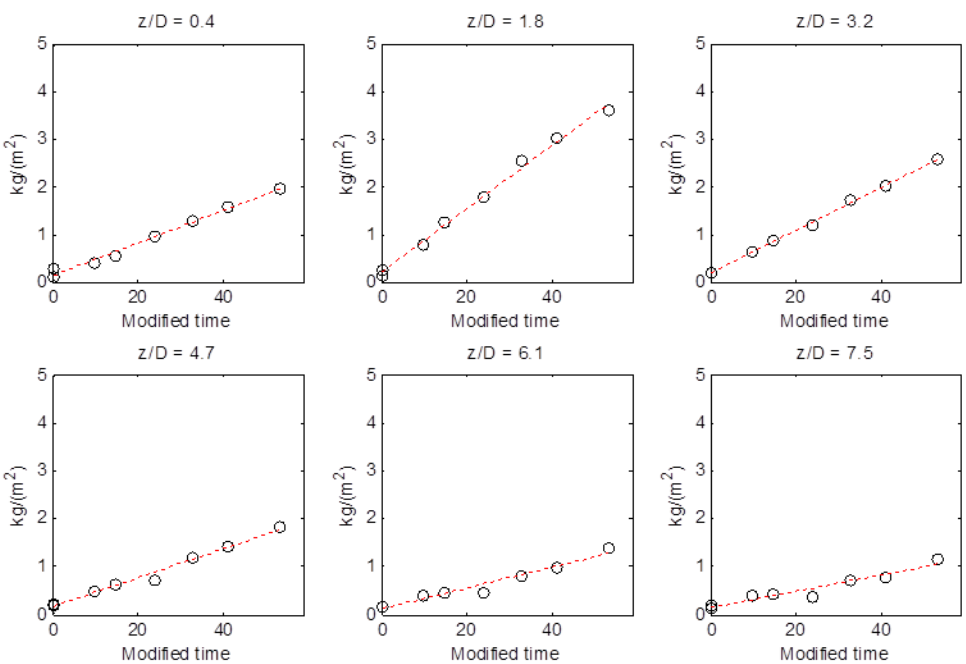

Figure 3.18 Variation of averaged mass transfer removal at different axial location with modified time at Re_o 140000

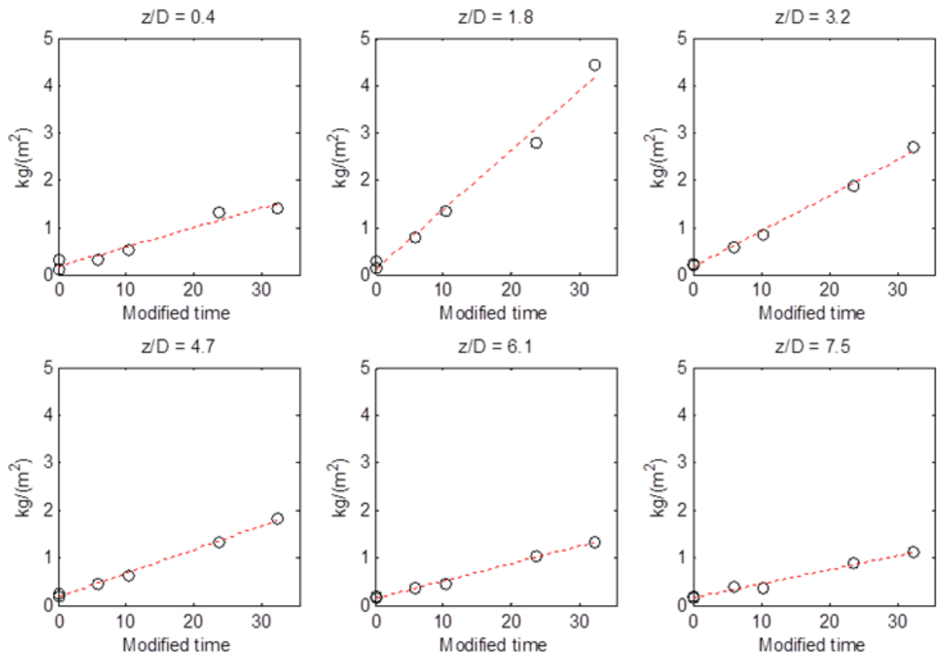

Figure 3.19 Variation of averaged mass transfer removal at different axial location with modified time at Re_o 200000

the laser scanner. The repeat accuracy of the scanner is ±0.05 mm(37). The uncertainties in calculated slope are given(40),

$$Slope_{error} = S * \sqrt{\frac{n}{(n\sum x_i{}^2)-(\sum x_i)^2}} \qquad 3.21$$

and

$$S = \sqrt{\frac{\sum(y_i - ax_i - b)^2}{n-2}} \qquad 3.22$$

where, x_i and y_i present the locations of a set of n experimental data points, a is the slope of the best fit line, and b is the intercept of the best fit line. For the mass transfer rate at each Reynolds number, experiments are performed for 5 different times. The local maximum uncertainty of the maximum mass transfer rate downstream of the orifice among these three different Reynolds numbers is 22.8%.

3.2. EROSION MASS TRANSFER TEST

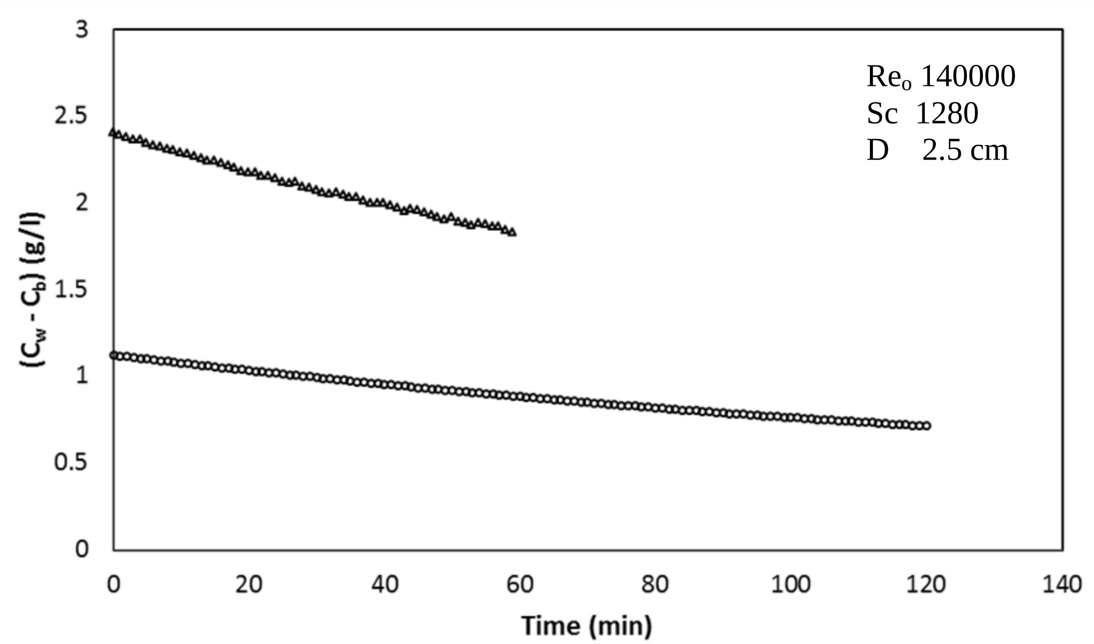

Figure 3.20 Variation of C_w-C_b at Re$_o$ 140000 with initial bulk concentration of Δ 0 g/l and ○1.28 g/l

FAC refers to the mass transfer mechanism where the wall material dissolves into a flowing fluid, while erosion is a mechanical wear process. For measurements using a dissolving wall method, it is always important to determine if erosion contributes to the mass removal. Tests were performed in the 2.5 cm diameter bore test facility to evaluate any erosion effects by running tests at the same Reynolds number with an initial bulk concentration of 1.28 g/l. Assume that both erosion and corrosion mechanism are involved in the mass removal process. The Sherwood numbers of these different cases can be compared to determine any erosion effects, as indicated in the following equation,

$$\frac{\partial m_t}{\partial A \partial t} = \frac{\partial m_e}{\partial A \partial t} + h(C_w - C_b) \qquad 3.23$$

where m_t is the total wall mass removed, m_e is the wall mass removed due to erosion. The mass transfer rate due to corrosion changes with flow condition, and the concentration difference between wall and bulk. While the mass transfer rate due to erosion changes only with the flow condition. The tests were performed at two different initial bulk concentration (C_b). m_t can be obtained from the scanned image, C_w is a constant, and C_b can be read from the conductivity meter. Thereafter, mathematically, there are two unknowns m_e and h with two sets of equations. So m_e and h and be solved with two series of the tests.

The erosion tests were performed at Re_o 140,000. The initial bulk concentration was increased by dissolving gypsum powder into the water in the reservoir and running the loop without the test section till the concentration of the gypsum reached 1.28 g/l. During this process, hydrocal, $CaSO_4 \cdot 1/2H_2O$, firstly reacts with water to form gypsum $CaSO_4 \cdot 2H_2O$, and then gypsum particles are dissolved into water to become ions. The system was stirred thoroughly to enhance the dissolving process. Tests were then performed for different times with this initial bulk concentration. The variation of the concentration difference between the wall and bulk values with time is plotted in Figure 3.20.

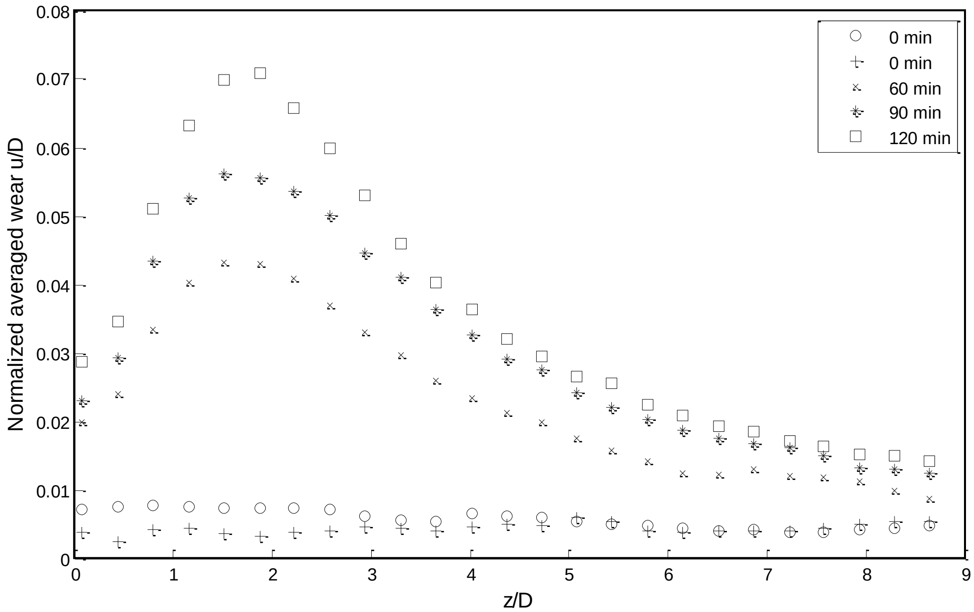

Figure 3.21 Axial distribution of circumferentially averaged wear profiles

The wear profiles from the tests with the initial bulk concentration of 1.28g/l for the three different times and the two unworn cases are presented in Figure 3.21. The Sherwood number profiles for the tests with initial bulk concentration of 0 g/l and 1.28 g/l are shown in Figure 3.22. The discrepancy between the two maximum Sherwood numbers profiles is 14.6%. As demonstrated previously, the uncertainty of our Sherwood number is 22.8%. Therefore, we can conclude that the values with the initial concentration of 1.28g/l are less which indicates that erosion is not present in these tests. This is consistent with the tests performed by Wilkin [39] using a similar wall dissolution technique. Wilkin performed tests using hydrocal sections that were exposed to $CaSO_4$-saturated water at a flow rate of 0.9 L/s in a 2.5 cm diameter pipe. No mass transfer was observed after running the test for 8 hours, which demonstrated that the hydrodynamics of the surrounding fluid alone could not result in any mass transfer at the surface.

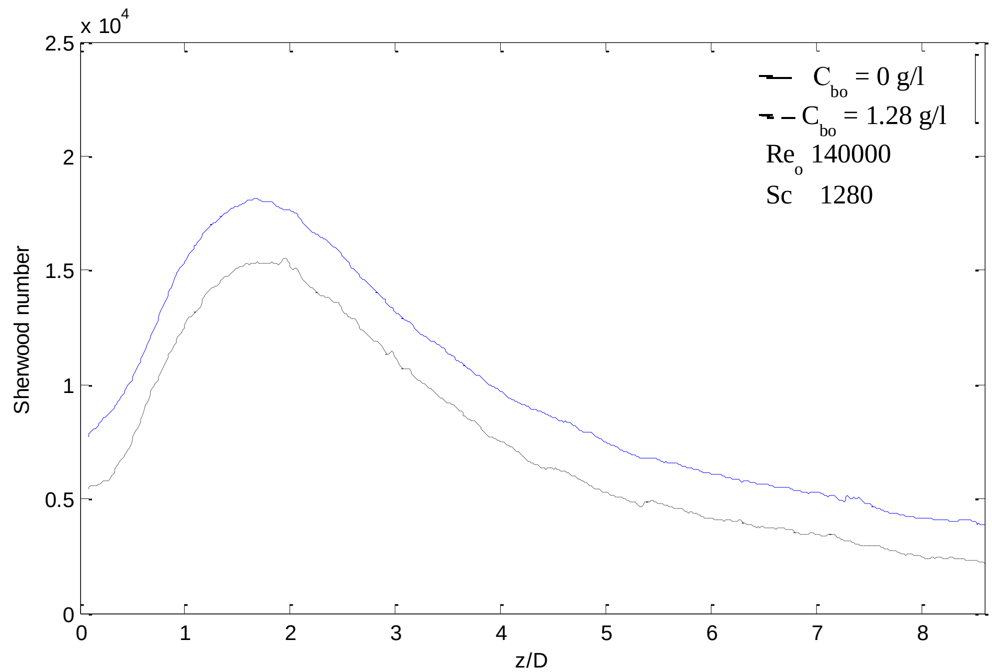

Figure 3.22 Profiles of Sh number downstream of orifice for different initial bulk concentration

3.3. 20 CM DIAMETER BORE TEST FACILITY

A schematic of the 20 cm bore test facility is shown in Figure 3.23. Water is circulated using a centrifugal pump, which has a variable speed controller. There is a 1.5 m^3 capacity stainless steel tank located on the end of the main riser pipe of the facility. A transparent tube is connected to the tank as a water level indicator. A heat exchanger is installed in the tank to maintain a constant water temperature during the tests and a conductivity probe is used to monitor the level of dissolved gypsum in the solution. The flow rate is adjusted through the pump speed controller. There is a 0.2 m diameter, 8 meter long acrylic tubing upstream of the orifice. The orifice is an ASME standard orifice with orifice diameter 0.1m, and is placed upstream of the gypsum test section as shown in Figure 3.23. The orifice to pipe diameter ratio was kept at 0.5 to be consistent with the tests in the 2.5 cm diameter bore facility. A 0.92 m long hydrocal test section is used immediately downstream of the orifice, followed by a 1meter PVC tubing with the same inner diameter. Chilled water from a dedicated chiller is circulated through the heat exchangers in the main tank to maintain the water temperature at 20 ± 0.5 ℃ during the tests. An orifice in the down comer is used to measure the flow rate. The conductivity and temperature of the water in the main tank is recorded directly into a dedicated computer. The wear in the test section is obtained by measuring the wall thickness of a gypsum lined test section using ultrasonic measurements at different run time intervals. In this case, only one sample is cast and tested per Reynolds number for different run times. After a given

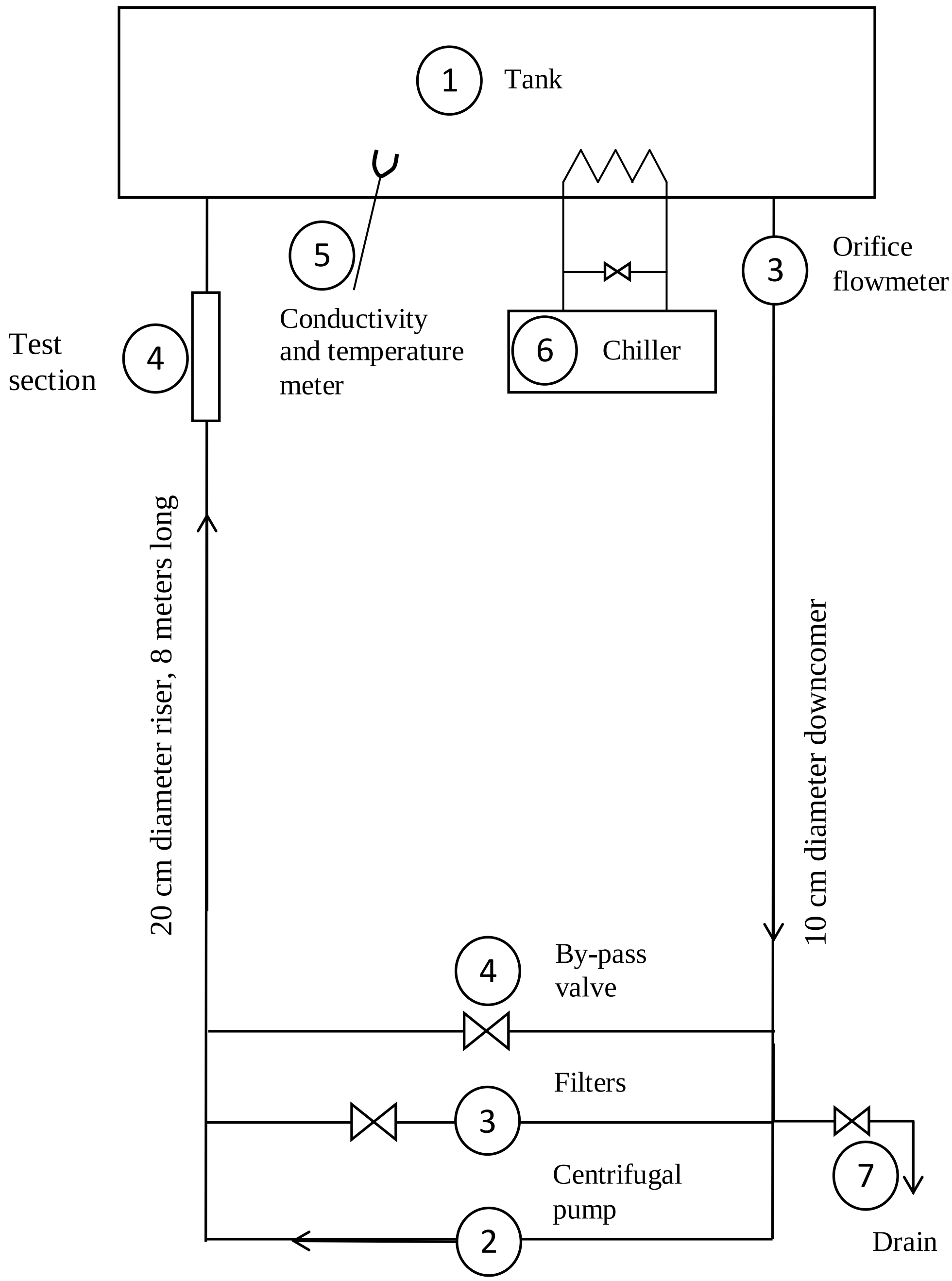

Figure 3.23 Schematic of the 20 cm diameter bore experimental test facility

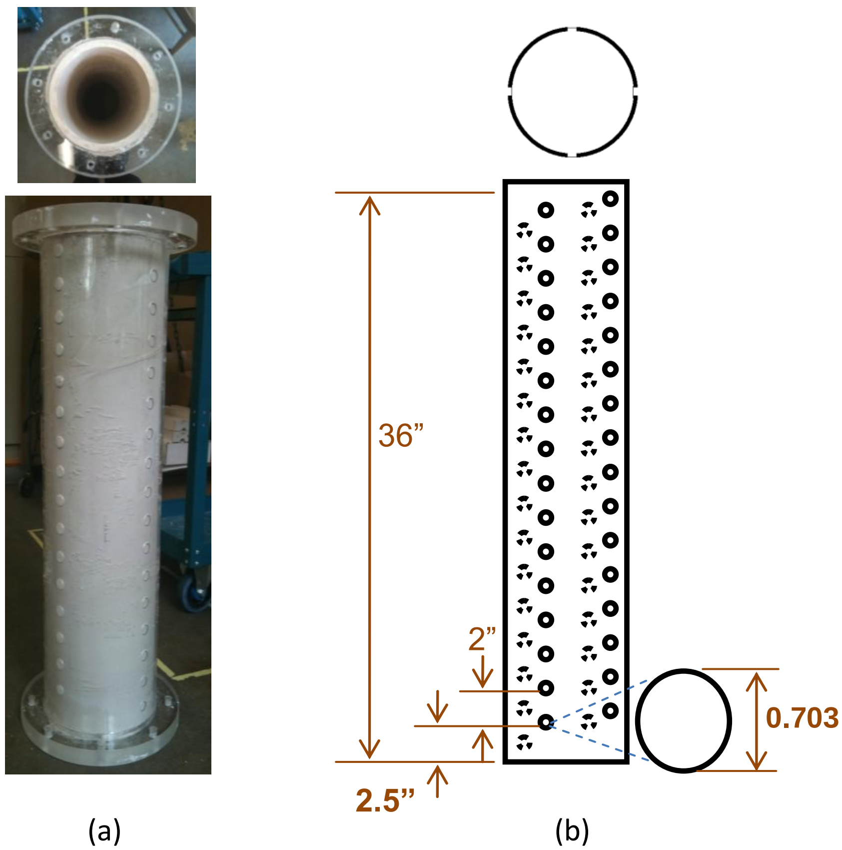

Figure 3.24 Picture and schematic of the 20 cm diameter test sample

run time, the ultrasonic measurements of the wall thickness at the designed locations are obtained. The local mass transfer rates are deduced from the variation of the wall thickness over time. At the end of the test, the section is cut into half, and laser scanned to capture the surface topology.

The 20 cm diameter test section is made of acrylic tubing with an inner gypsum liner that is nominally 1.5 cm thick. The gypsum is cast between two acrylic tubes that have 19.58 cm ID and 20 cm OD and 20.5cm ID and 20.92 OD respectively. The length of the test section in this instance is 92 cm, or approximately 4 diameters, which is sufficient to capture the location of maximum mass transfer. The inner tube has a lots along its axial length to allow it to be removed after casting. A customized fixture and three identical spacers are used to hold the two tubes concentrically with each other at each end of the two tubes. The strength of the ultrasonic signal decreases up to 95% at the interface between the acrylic tube and gypsum liner due to the presence of an air gap. In order to receive clear ultrasonic signals for the wall thickness measurement, through holes are machined on the outer acrylic tubing. There are four lines of through holes for the ultrasonic measurements located 90 °from each other. Along each line, the centers of the holes are spaced 5 cm away from one another as shown in Figure 3.24 (b), and each hole is 1.8 cm in diameter to accommodate the ultrasonic probe. The four lines are offset by 1.25 cm from one end of the tube to obtain a better spatial resolution along the axial direction, as shown in Figure 3.24 (b).

To prevent the liquid hydrocal mixture from leaking out of the mold during casting, packing tape is used to cover the holes from the inside surface of the outer tube, and to cover the outside surface of the seam of the inner tube. The two tubes are aligned concentrically in a fixture at the bottom for casting. The ratio of citric acid, deionized water and Hydrocal is 1:65:175, and is the same as it is for 2.5 cm bore sample. Since the capacity of the vacuum chamber is about 4 kg, a continuous casting method is implemented to cast the entire hydrocal sample. The fixture and inner tube is taken out after allowing the cast to dry for two hours. The tape at the outer tube holes is also

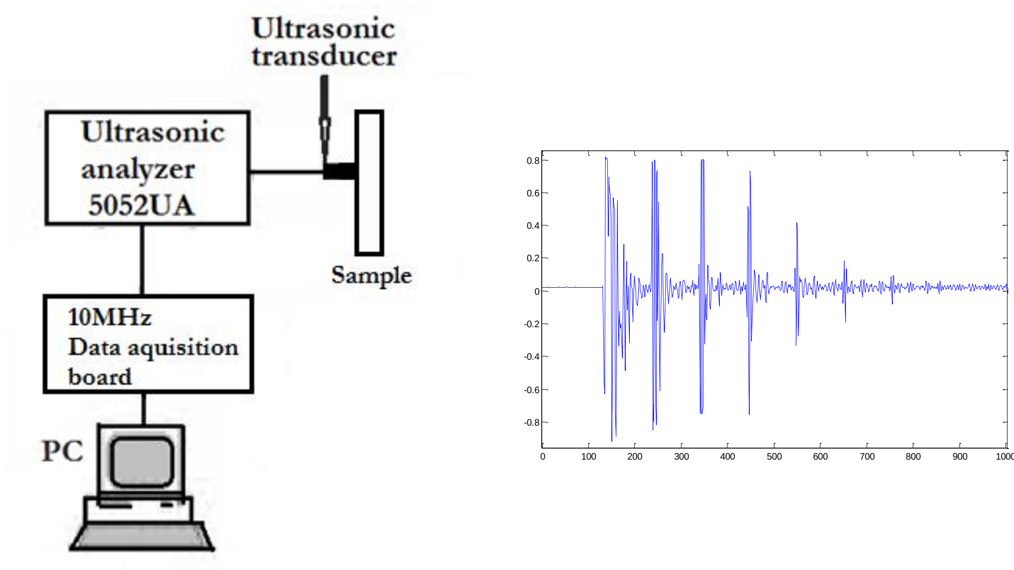

(a) (b)

Figure 3.25 Ultrasonic measurement setup and typical signal

removed before the ultrasonic measurements are taken. Typically, after 15 days of drying under room temperature, the weight of the sample stops changing. Thereafter the cast sample is ready for use as shown in Figure 3.24.

The mass transfer rate can be obtained from the ultrasonic measurements of the wall thickness at each measurement locations at the different run times. The wall thickness from the ultrasonic signal is calculated as

$$l = tV/2 \tag{3.24}$$

where t is the time for the ultrasonic wave to reflect off and travel back from the other face of the wall, and V is the speed of the ultrasonic wave travels in the material.

A Olympus® M1060-RM contact transducer, a 5052UA ultrasonic analyzer, and a dedicated computer with a built in 10 MHz sampling rate national instrument® data acquisition board were used to measure the wall thickness. The schematic diagram of the measurement set up is shown in Figure 3.25 (a). The ultrasonic analyzer generates electric pulses for the transducer at a peak frequency at 2.5 MHz. The natural frequency of the transducer is 2.25 MHz, which is the best match to the signal peak frequency of the signal analyzer to ensure accurate results. The ultrasonic transduce converts the electrical pulse signal from the analyzer to a wave signal that travels through the gypsum and then converts the reflected wave signal back to an electrical pulse, which is detected by the ultrasonic analyzer. The electrical analog signal is collected by the data acquisition board at a sampling frequency of 10MHz. The magnitude of the generated signals was set to be between -1 to 1 volt. The acquired ultrasonic signal is analyzed by a customized Matlab code. The detailed software code is provided in Appendix. A typical signal analyzed by Matlab is shown in Figure 3.25 (b).

The ultrasonic transducer works by measuring how long it takes for a sound pulse that has been generated by the transducer to travel through a test piece. The period of time for the ultrasonic wave to travel back and forth can be determined by

$$t = \frac{n}{f} \qquad 3.25$$

where f is the ultrasonic peak frequency (10MHz), and n is the count of the ultrasonic analyzer pulse between the beginning of the initial signal and the first echo. The measurement is made from one side of the test piece, where it measures the round trip transit time of a pulse that reflects off the far side of the test piece.

A threshold method is used to detect the reflected wave from the far surface of the object. The amplitude of the ultrasonic wave generated by the ultrasonic analyzer is 1 V. When the wave encounters a boundary between two dissimilar materials, part of the wave is reflected back from the boundary, and part of it transmitted across the boundary. The magnitude of the reflected wave depends on the material properties on both sides of the boundary. One important property is the characteristic impedance of the material. The characteristic impedance of a material is the product of mass density and wave speed given by

$$z = \mu c \qquad 3.26$$

where z is the impedance of the material, μ is mass density and c is wave speed in that material. The reflection wave strength is given by

$$\xi_r = \frac{z_1/z_2 - 1}{z_1/z_2 + 1}\,\xi_1 \qquad 3.27$$

where ξ_r is the magnitude of the reflected wave speed, z_1 is the impedance of the material where the wave is from, z_2 is the impedance of the material that the wave travels to, and ξ_1 is the magnitude of the initial wave. For metal/air boundaries commonly seen in ultrasonic flaw detection applications, nearly 100% of the wave is reflected back. The value of ξ_r is about the same as ξ_1. The ultrasonic transducer has a limited contact surface with the sample, so it could detect only part of the reflected wave in certain areas. The detected wave also depends on the boundary surface conditions including shape and smoothness. According to the law of reflection, the directions of the reflected wave depend on the incident angles. Generally, a rough interface surface reflects the wave in all directions. Therefore, the

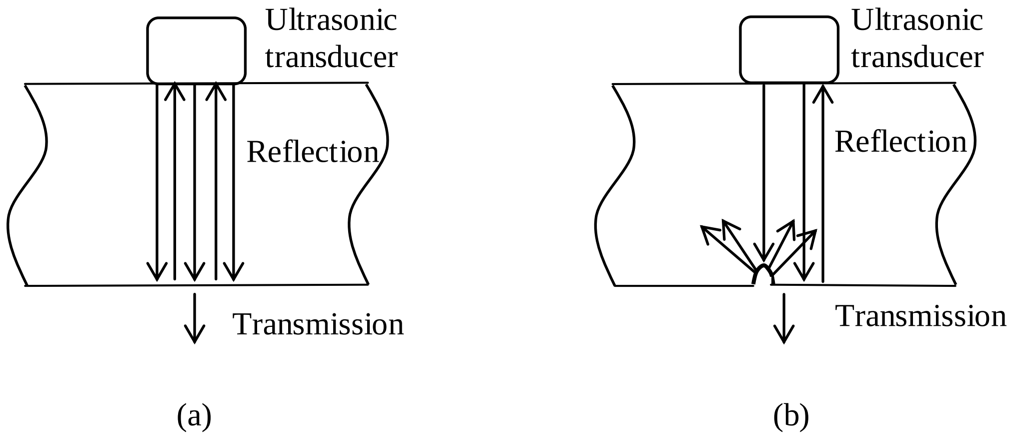

Figure 3.26 Schematic diagram of ultrasonic wave reflection and transmission

intensity of the ultrasonic wave detected by the ultrasonic transducer is less on rough interfaces. Similarly, the intensity of the wave detected is less if deep scallops are formed on the surface as shown in part (b) of Figure 3.26. For example, the first detectable echo received by the ultrasonic transduce could be reflected from the top of the scallops instead of the next parallel surface.

By analyzing thousands of wave reflections, a threshold amplitude of -0.1 V is used to identify a wave reflection. Generally, a -0.1 V threshold would not pick up the noise signals due to imperfection of the gypsum material, because the signal intensities from the imperfections are much smaller. Therefore, the signal noise is filtered out, and more than

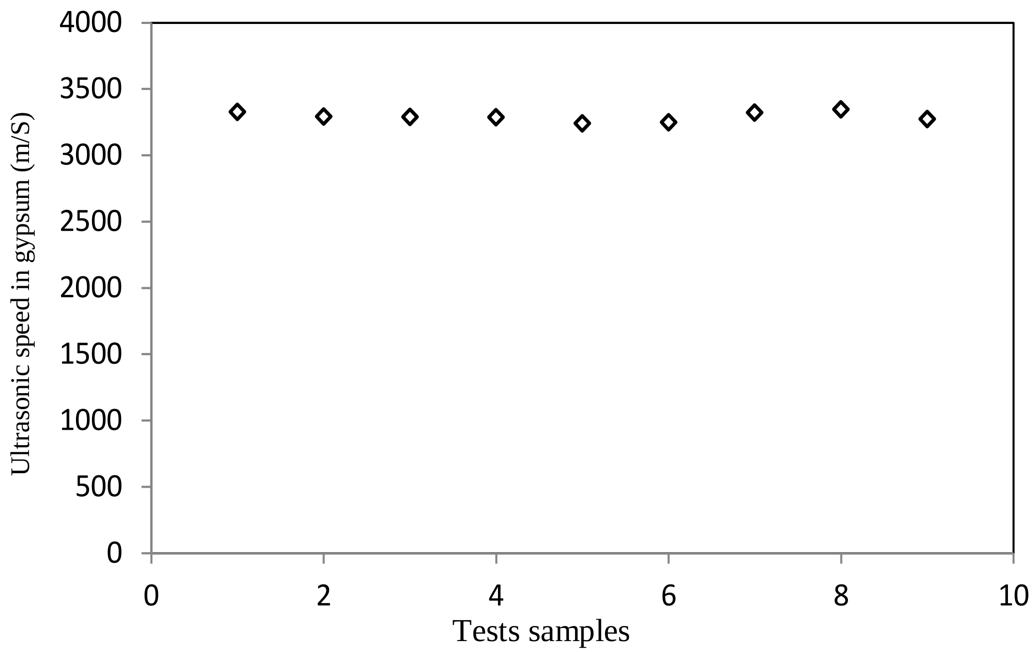

Figure 3.27 Ultrasonic speed in saturated gypsum measured with different test samples

95% of the reflections can be detected. After each experimental run, the ultrasonic signal and its echo are recorded for 1 second at every measurement location. The ultrasonic analyzer frequency is set to 2 KHz. Therefore, 2000 pulses and their echoes are used to analyze the wall thickness, and the averaged value from these is used as the local wall thickness.

Since the velocity of sound in the test material is essential, separate experiments were performed to determine this using gypsum blocks of known thickness. Three sample blocks of 11.9, 16.5 and 23.3 mm thick were cast to determine the speed of sound in water saturated gypsum. The casting procedure for these sample blocks were the same as that used for the test sections. Four different locations on each block with the same thickness were chosen to conduct the measurement. For a given sample thicknesses l, and the time t that the wave travels through the thickness, the speed of the ultrasonic wave can be calculated as v = l/t. The travel time measured by the ultrasonic wave will be explained in detail in the following sections. The average speed of ultrasonic sound obtained at 9 spots of these 3 sample blocks is 3270 m/s with a standard deviation of 1.1% as shown in Figure 3.27.

Ultrasonic wall thickness measurements were obtained for different run times in the 20 cm diameter bore loop. The impedance of water is much greater than it is of air, thus the reflection wave is much stronger at the gypsum and air interface than at gypsum and water interface. The water in the loop was drained below the test section before taking the ultrasonic measurements to increase the sensitivity of the ultrasonic wave signals detected by the ultrasonic transducer. Once the thickness measurements are made, water is refilled into the system to its original level, and the temperature of the system is brought back to 20 ± 0.5 ℃ before running the experiment for another period of time. In total, ultrasonic wall thickness measurements were taken for a total of 6 times during the test at 1, 2, 3.5, 4.5, 6.5, 9.6 and 13 hours. Locations that showed a sudden decrease of wall thickness compared with the previous experimental time indicated initiation of deep scallops at that location. These measurement locations were not considered to eliminate isolated deep scallops. The variation of the wall thickness with time is shown in Figure 3.25. At each measurement location, the mass transfer rate is calculated in a similar manner to that in the 2.5 cm diameter bore loop as shown.

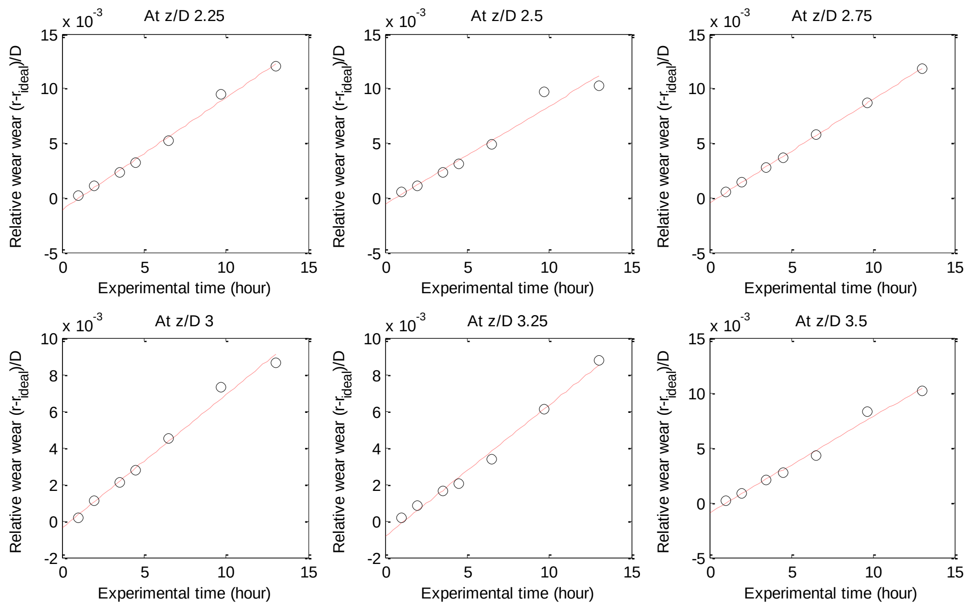

Figure 3.28 Variation of averaged mass transfer removal at different axial location with modified time at Re_o 180000 in 20 cm diameter bore loop

Wall thickness measured by the ultrasonics at each location was analyzed and recorded with experimental time. The local wear was calculated by taking the difference between the initial wall thickness and current thickness at that location. The slopes of the best fit straight lines of the local wear with time represent the local mass transfer coefficient. The variation of the gypsum concentration during the test is less than 8% of the gypsum solubility, therefore the difference in the mass transfer rate calculated by using experimental time or modified time is small. Thus, the experimental time was used in the mass transfer coefficient calculation for the 20 cm diameter test.

After running the test for 14 hours at Re_o 180000 in the 20 cm diameter bore facility, the test section was sectioned into half. The inner surface of the test sections were scanned by a Creaform® hand held scanner to characterize the worn surface morphology.

The contour plot of the 20 cm bore loop test is obtained by taking the difference between the local radius of the image and ideal radius, 10 cm, of the worn test section.

Chapter 4
RESULTS & DISCUSSION

The objective of the experiments was to determine the mass transfer rate downstream of an orifice and evaluate the effect of Reynolds number and surface roughness on the mass transfer rate. The wear contours, wear profiles and the results for the mass transfer rate from the 2.5 cm and 20 cm bore tests are presented and discussed in this chapter. The worn surface morphologies of the test sections are analyzed and compared with each other.

The wear contour plots for orifice Reynolds number 80000, 140000, and 200000 from the 2.5 cm diameter tests are shown in Figure 4.1, Figure 4.2 and Figure 4.3. UThe wear contours indicate a nearly axisymmetric wear, which is expected due to the axisymmetry of the flow. The maximum wear is seen to occur at 1.5 to 2.0 diameters downstream of the orifice. The contour lines are denser around this location, which indicates more significant change of wear levels in this region. The waviness of the contours indicates the worn surfaces are not perfectly smooth, and the small

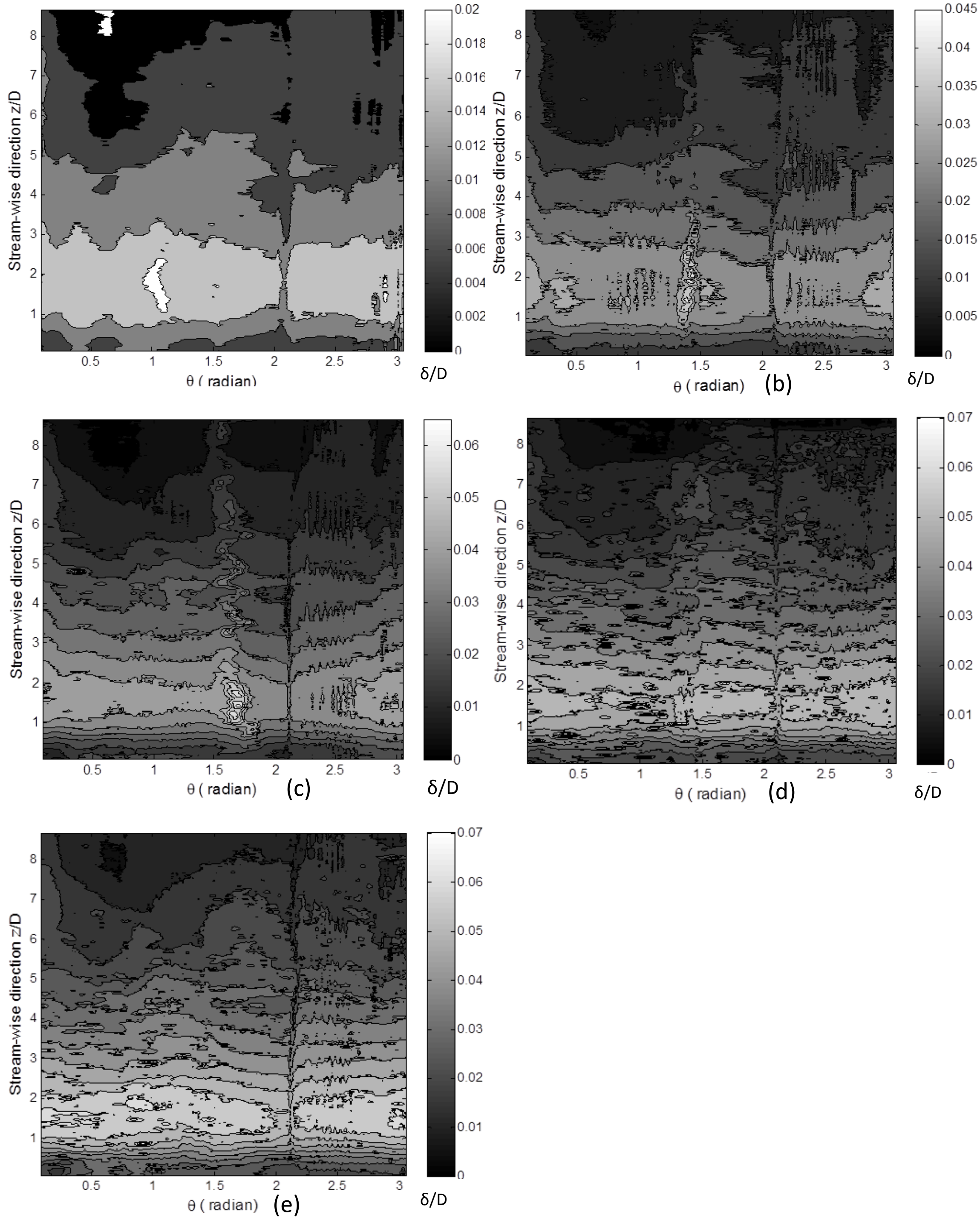

Figure 4.1 Relative wear contour plots at Re_o 80,000 in 2.5 cm bore loop at (a) 15 min (b) 30 min (c) 45 min (d) 60 min (d)75 min

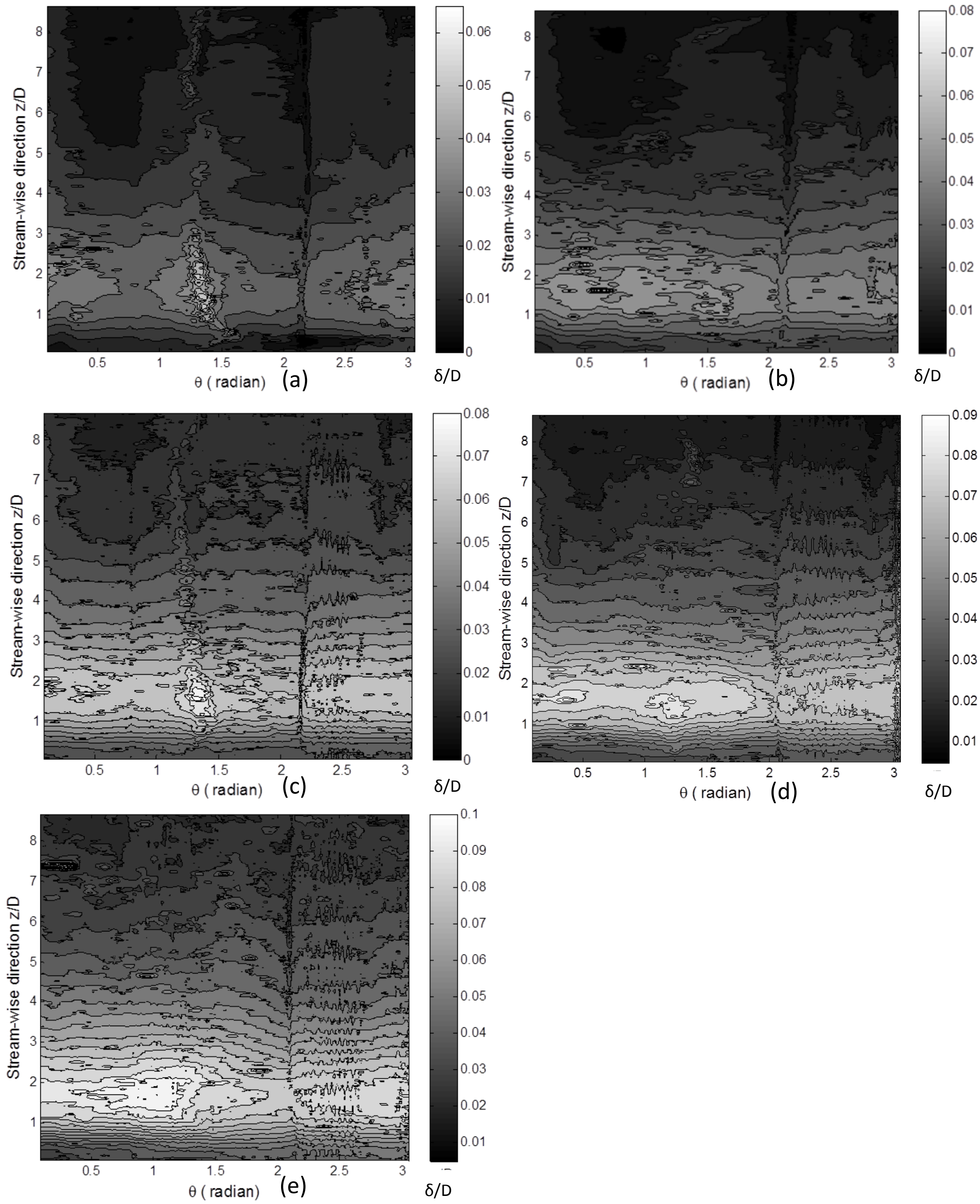

Figure 4.2 Relative wear contour plots at Re_o 140,000 in 2.5 cm bore loop at (a) 15 min (b) 25 min (c) 35 min (d) 45 min (d)60 min

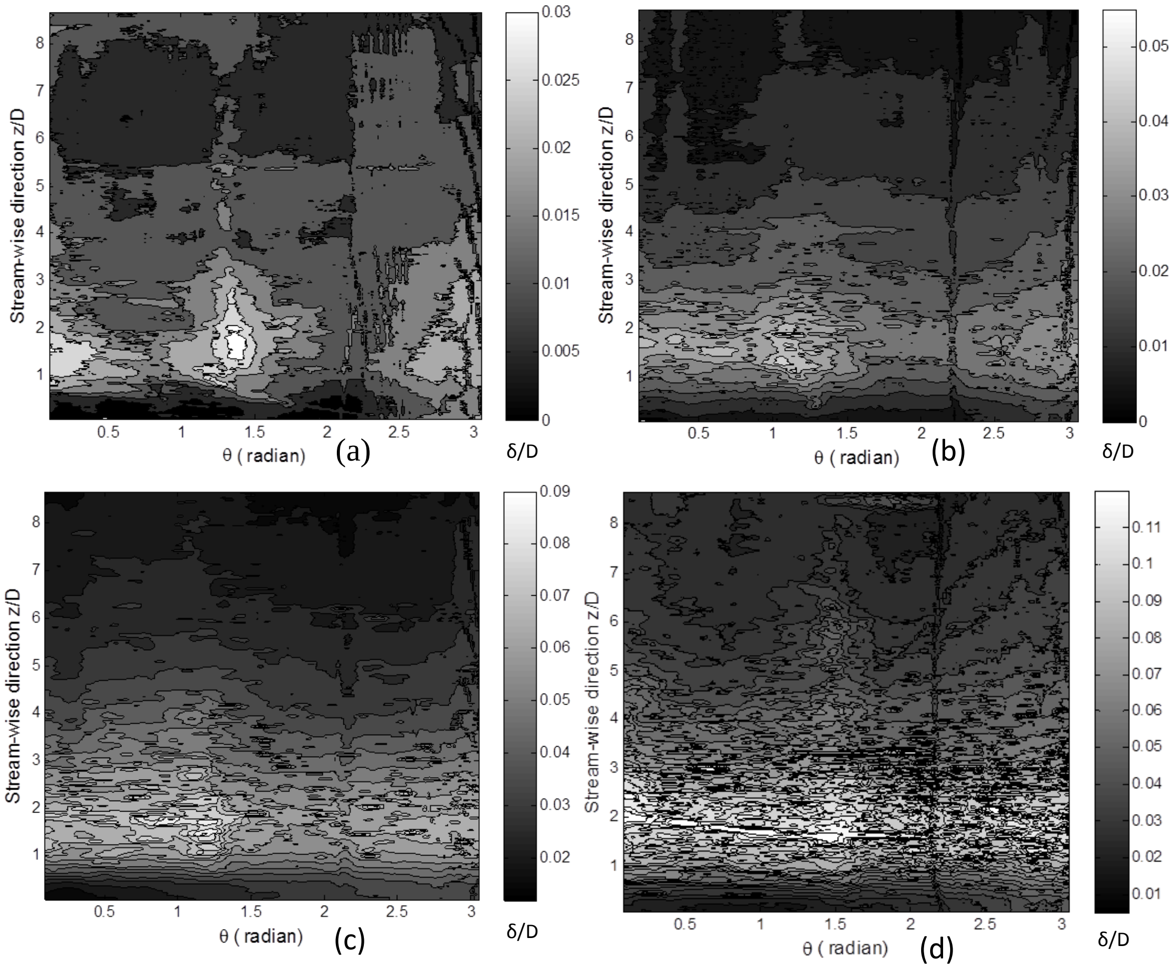

Figure 4.3 Relative wear contour plots at Re_o 200,000 in 2.5 cm bore loop at (a) 6 min (b) 10.5 min (c) 25 min (d) 35 min

circles indicate the presence of scallop. For each Reynolds number, the higher wear levels at longer experimental times indicate the progression of wear over the entire surface as expected. The levels of the contour plots at different Reynolds numbers indicate that, generally, the wear reaches a given level with less time at higher Reynolds numbers. There is a seam along the axial direction at $\theta \approx 2.1$ radians. This is due accuracy of the scanner at the overlapped region of the scanned images from different angles.

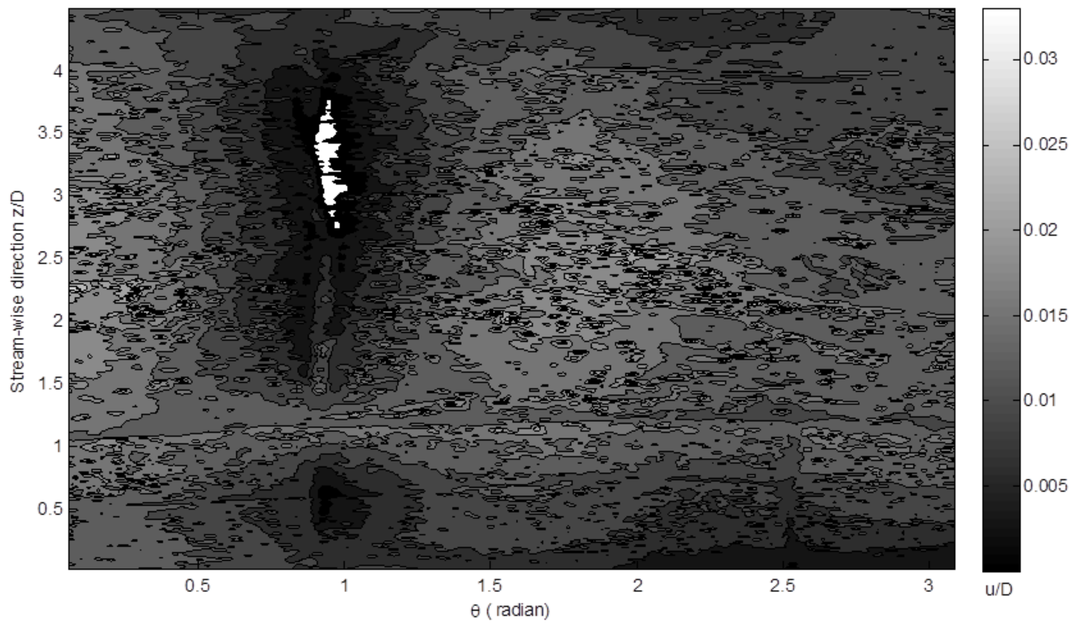

Figure 4.4 Relative wear contour plot at Re_o 180000 in 20 cm diameter bore facility after 14 hours

The wear contour plot of the 20 cm diameter test section at the end of the test corresponding to 14 hours is shown in Figure 4.4. The circles on the contour plot indicate the presence of scallops on the pipe surface. In this case, the scallops are formed over most of the surface. Denser circles are observed around 2 to 2.5 diameters downstream of the orifice. There is a lower wear region axially along $\theta \approx 1$, which is due to a slight ovalness of the inner core during casting at this location.

The circumferentially averaged wear profiles along the axial direction downstream of the orifice from the 2.5 cm diameter bore loop experiments are shown in Figure 3.15. The wear increases rapidly with distance downstream of the orifice, reaches a maximum value

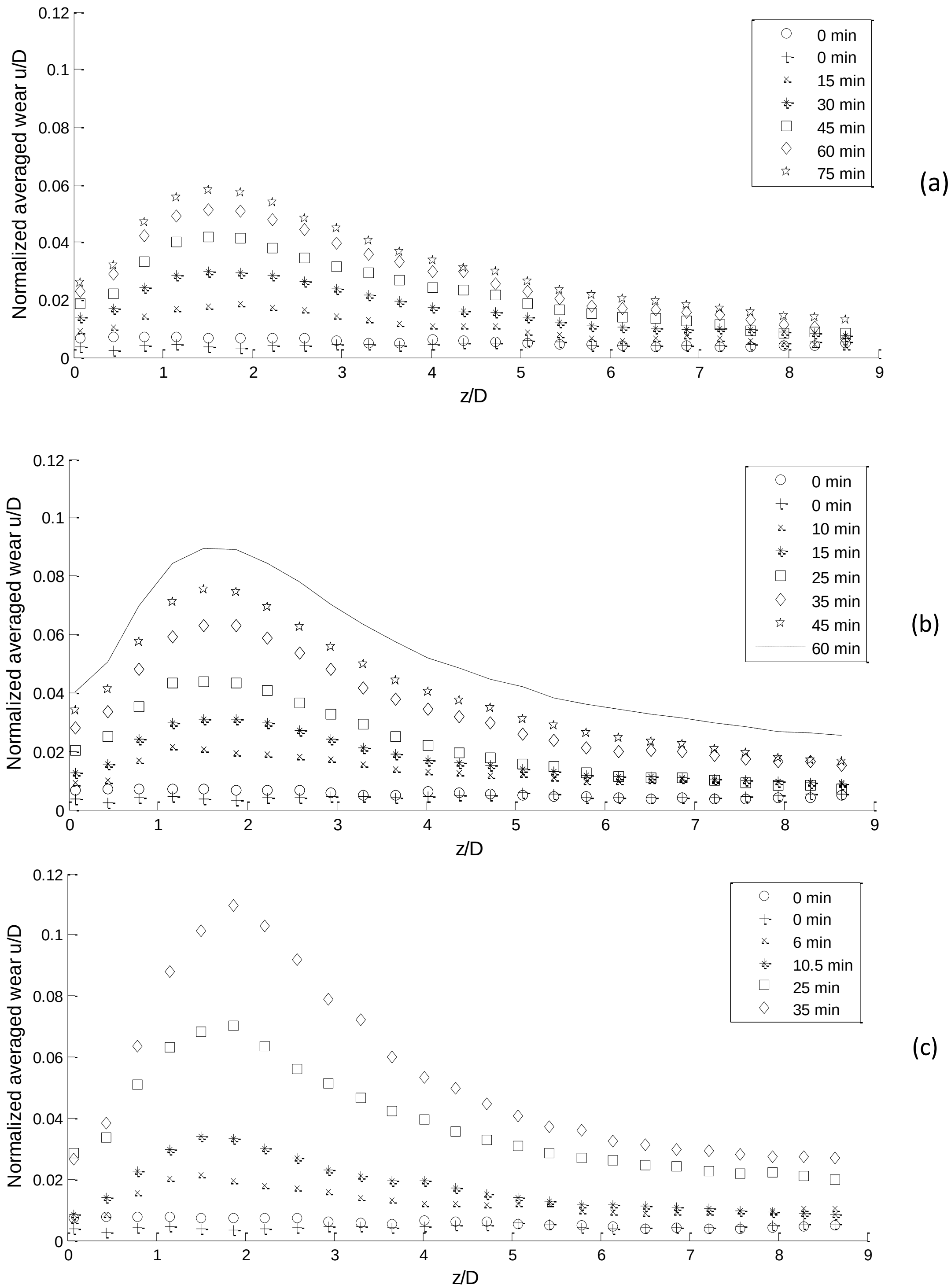

Figure 4.5 Axial distribution of circumferentially averaged wear profiles at Re_o (a) 80000 (b) 140000 and (c) 200000

and then decreases gradually with streamwise distance. The progression of the wear with time at each downstream location is clearly seen in each of these figures in Figure 4.5 Generally, the maximum wear location at each Reynolds number does not change with time. However, the location moves downstream with an increase in Reynolds numbers. The peak wear occurs at about 1.5 diameters downstream of the orifice at Re_o 80000, while it is at about 1.7 and 1.85 diameters downstream of the orifice at Re_o 140000 and Re_o 200000 respectively. The two unworn profiles are also plotted in these figures in Figure 4.5. The average deviation of the two unworn profiles is 0.003 pipe diameters, which is a magnitude lower than the maximum wear at Re_o 80000 for 15 min.

The wear profiles at the different times of the mass transfer tests performed in the 20 cm diameter bore facility at Re_o 180000 are shown in Figure 4.6. There is considerable more scatter in this data compared to that for the 2.5 cm bore data, since they are point measurements using the ultrasonic probe at specific locations compared to circumferentially averaged profiles using the laser scanned image over the entire surface. The data, however, clearly shows the progression of wear with time at all measurement locations, and the wear profiles between different run times are consistent. The wear is relatively low immediately downstream of the orifice, and reaches a maximum at about 1.8 diameters downstream of the orifice. The wear then decreases along the downstream direction as also seen in the data from the 2.5 diameter tests.

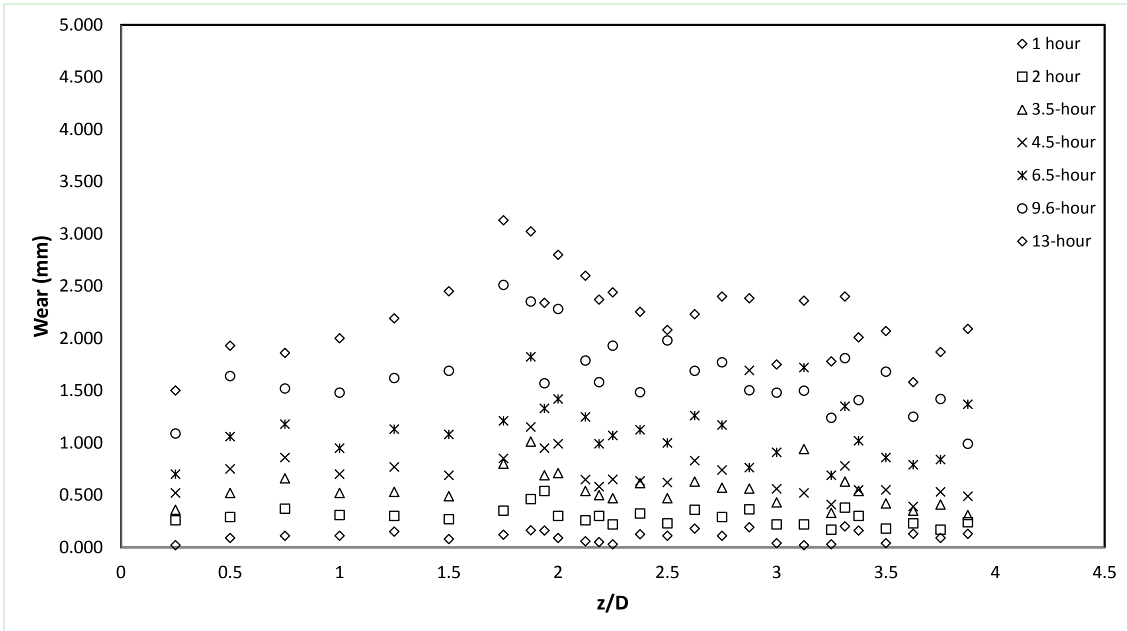

Figure 4.6 Axial distribution of wear at different times at Re_o 180000 in 20 cm diameter bore facility

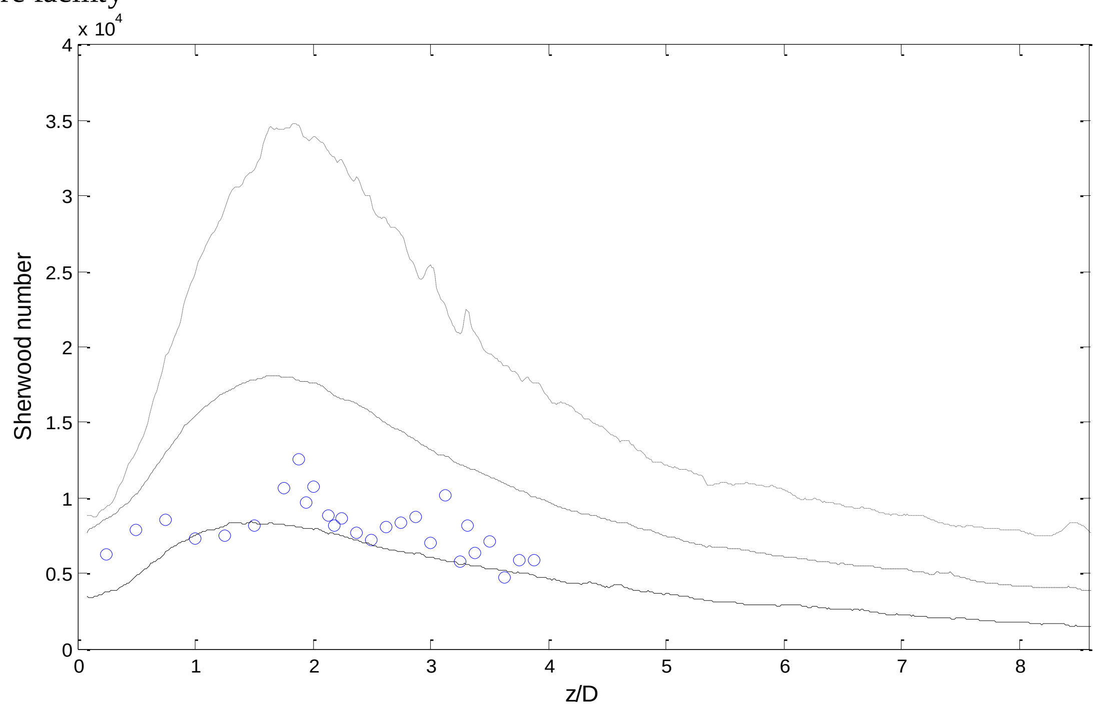

Figure 4.7 Averaged Sh profiles of the present experiments at —Re_o 80000, —-— Re_o 140000 and ---- Re_o 200000 in 2.5 cm diameter bore facility experimental data at ◦ Re_o 180000 in 20 cm diameter bore facility

The circumferentially averaged Sh profiles downstream of the orifice of the present experiments at the three Re_o in the 2.5 cm diameter bore loop, and the Sh profile at Re_o 180000 in the 20 cm diameter bore loop are shown in Figure 4.7. For the 2.5 cm diameter loop experiments, there is an increase in the mass transfer rate over the entire test section as the Reynolds numbers is increased. However, the mass transfer rate of the experiment in the 20 cm diameter bore loop at Re_o 180000 is significantly lower than it is in the 2.5 cm diameter bore loop at Re_o 200000 at corresponding axial z/D locations.

The Sherwood numbers increase rapidly immediately downstream of the orifice, reaches a maximum, and would slowly relax back to the fully developed pipe value. Poulson (9) suggested that the flow and mass transfer relaxes back to the fully developed flow at approximately 7 diameters downstream of the orifice (41). The higher Sherwood numbers immediately downstream of the orifice can be attributed to the recirculating zone upstream of the reattachment point, as also seen in the data of Tagg et al. (42) and Poulson(41). The shape of the present Sherwood number profiles is consistent with the results of other researchers as shown in Figure 4.8. In this figure, the Sherwood number profiles of the present experimental data at Re_o = 80000 in the 2.5 cm diameter bore facility, are compared with the experimental data of Tagg et al.(43) at Re_d of 13500, 25074 and 62686(42) and the predicted Sherwood number profiles by Coney's correlation(33) at Re_d of 62686 and 80000. The maximum Sherwood numbers predicted by the correlation of Coney is higher than the value of experimental data of Tagg et al. (43) at the same Reynolds number by about 16 % at the Reynolds number of 13500, 25074 and

62686(43). However, the predicted profile at Re_d = 800000 is lower than that of present tests.

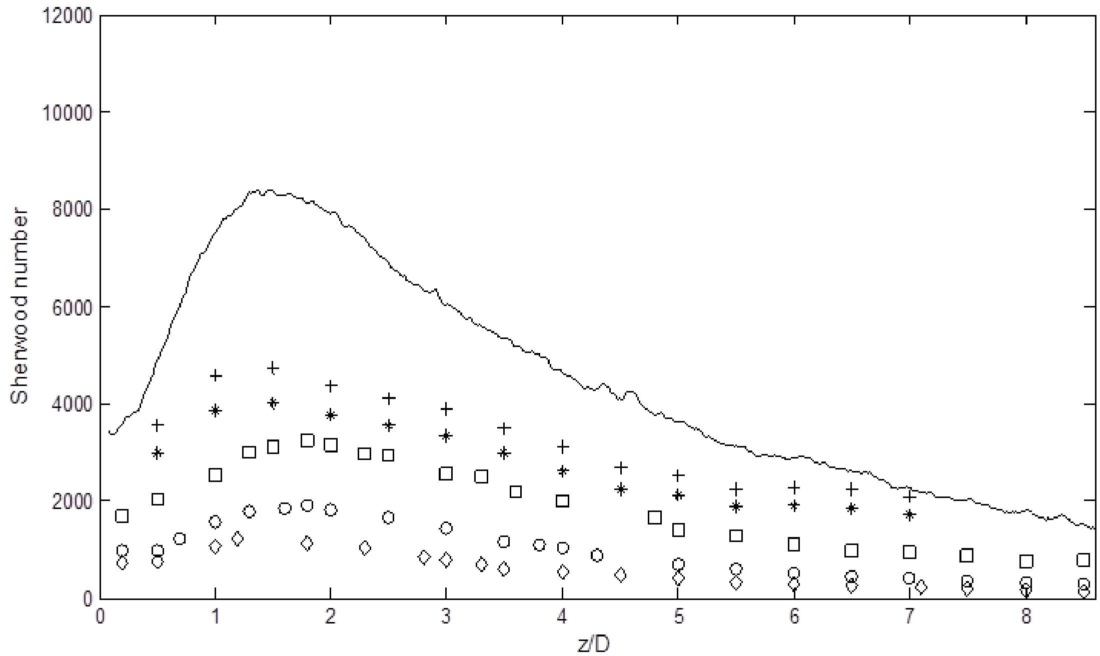

Figure 4.8 Comparison of averaged Sh profiles of the present experiments at Re_o 80000 in 2.5 cm diameter bore facility—, experimental data at Re_d of □ 62686 ○ 25074 and ◊ 13500 with d/D = ½ sudden expansion(42) , and Predicted Sh profile at Re_o of * 62686 and + 800000 by Coney's correlation(33)

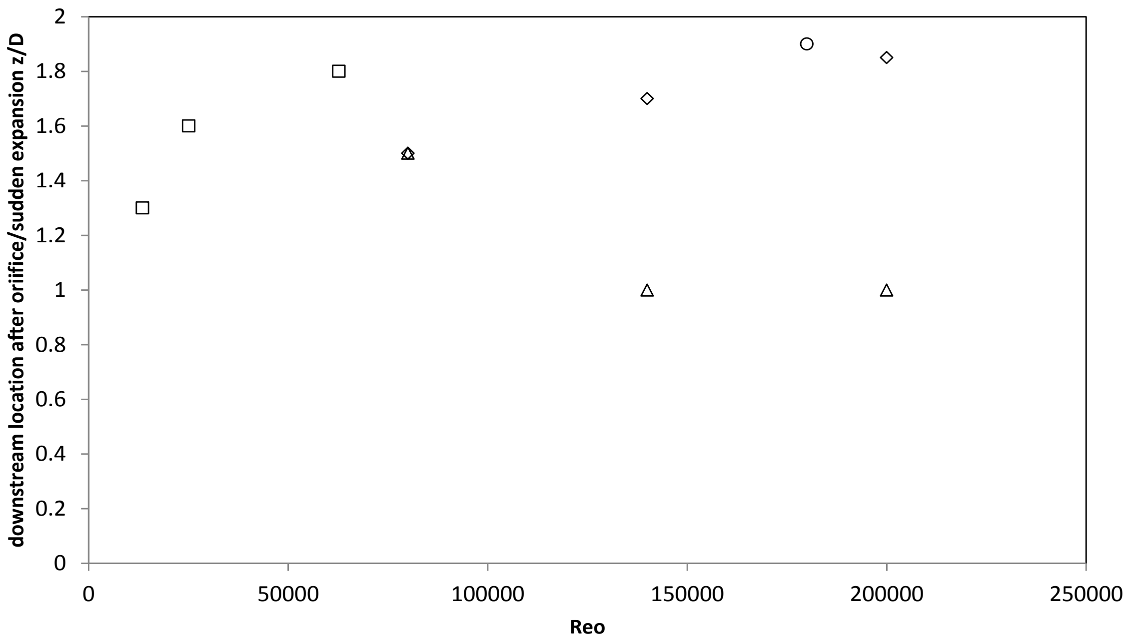

Figure 4.9 Axial location of the maximum mass transfer downstream of the orifice/sudden expansion from □ Tagg et al. data(42) ◊ experimental data in 2.5 cm diameter bore loop ○ experimental data in 20 cm diameter bore loop Δ Coney's correlation(33)

The maximum local mass-transfer coefficient of the present experiments occur at axial locations of 1.5, 1.7 and 1.85 diameters downstream of the orifice at Re_o of 80000, 140000 and 200000 respectively. Therefore, the data suggests that the peak Sherwood number location shifts downstream of the orifice as the Reynolds number increase. This phenomenon was also evident in the data of Tagg et al.(43) for mass transfer downstream of a sudden expansion as shown in Figure 4.8. The location of the maximum mass transfer rate moved downstream from about 1.2 diameters to 1.8 diameters downstream of the orifice as Re_d increased from 13500 to 62686. It is also evident in the experiments of Adam (44), that the reattachment length increases with Reynolds numbers.

The variation of the axial location of the maximum Sherwood number with Reynolds number from the present experiments in both facilities is shown in Figure 4.9

along with the data from Tagg et al. (43) and the correlation of Coney (33). The axial location of the maximum mass transfer shifts downstream with increase of Reynolds numbers, which is evident in both the present data and the data of Tagg et al.(43). The axial location of the maximum Sherwood number for the present experiment at Re_o of 180000 in the 20 cm diameter bore loop is at 1.9 diameters downstream of the orifice, which is slightly further downstream than the location at Re_o of 200000 in the 2.5 cm diameter bore loop. The locations of maximum mass transfer from Tagg et al.(43) at Re_d 25074 and 62686 are further downstream than the location of the present experiments at Re_o of 140000.

The axial location of the maximum Sherwood number predicted by the correlation of Coney exhibits a different trend, showing a decrease with an increase in Reynolds numbers. The correlation was developed and validated against the data of Krall & Sparrow(45), and Tagg et al.(42), which are only valid for either relatively high Reynolds numbers $10^4 \leq Re \leq 1.3x10^5$ but low Prandtl numbers $3 \leq Pr \leq 6$ (45), or relatively low Reynolds numbers $8x10^4 \leq Re \leq 2.2x10^5$ and high Sc =1450 (42). The data suggests that the correlation of Coney(33) is only valid in the narrow range of Reynolds number and Schmidt/Prandtl numbers from which it was developed. It has been suggested that the location of the maximum Sherwood number corresponds to the point of flow reattachment (8). A schematic diagram of the flow field downstream of an orifice is shown in Figure 4.10. The direction of the near-wall flow in the recirculation zone downstream of an orifice flow would be opposite to the main stream flow direction. This is evident in the scallop patterns observed in the present experiments. There are three types of scallop shapes observed in the present experiments. A picture of a typical worn surface of the test at Re_o=80000 for 25 minutes is shown in Figure 4.12 (a). In the region about 2 diameters downstream of the orifice, the shape of the scallops are round. In the region immediately downstream of the orifice, a tail-like shape was formed on the upstream side of some scallops. In the region beyond 3 pipe diameters downstream of the orifice, generally, the scallops formed were significantly smaller, while the 'tails' were longer and located downstream of the orifice. These enlarged scallop shapes are shown in Figure 4.12 (b) (c) and (d). The flow field downstream of an orifice could be divided into three regions based on the near wall flow directions: recirculation region, reattached region and redeveloping region. These are indicated by the direction of the 'tails' of the scallops pointed in the flow direction. The present data suggested the reattachment region coincide with the maximum Sherwood number region. The overlap between the location for Sh_{max} and the flow reattachment point for an abrupt enlargement geometry observed by Sparrow et al. (46) is shown in Table 4.1. z is the characteristic length of the enlargement step, u is the velocity upstream of the enlargement, ν is the kinematic viscosity of the fluid, x_r is the distance downstream of the enlargement for flow reattachment point, and x_{max} is the distance downstream of the enlargement for maximum heat/mass transfer. The difference between these two locations at the given test conditions are less than 9.2%.

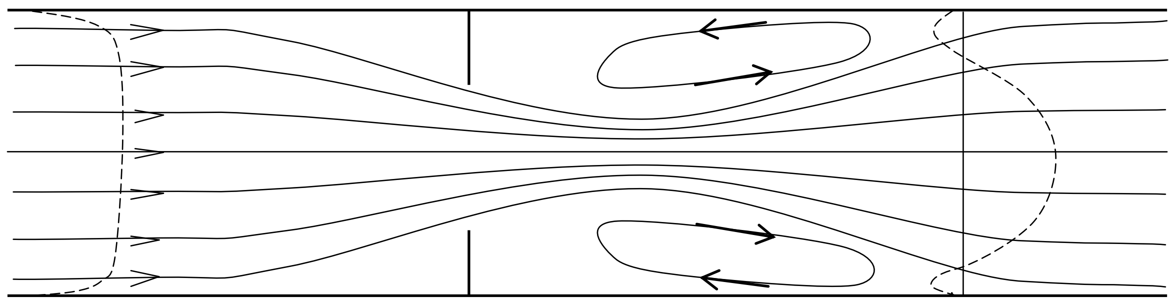

Figure 4.10 An idealized schematic diagram of fluid flow after orifice, showing turbulence velocity in the upstream and complex velocity field with reverse flow behind the expansion

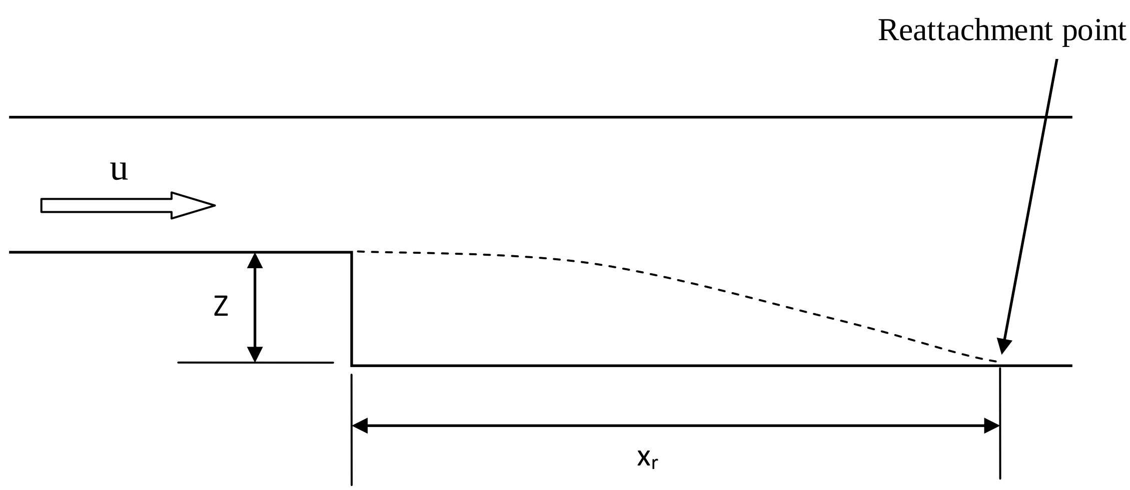

Figure 4.11 Schematic of the geometry of sudden enlargement

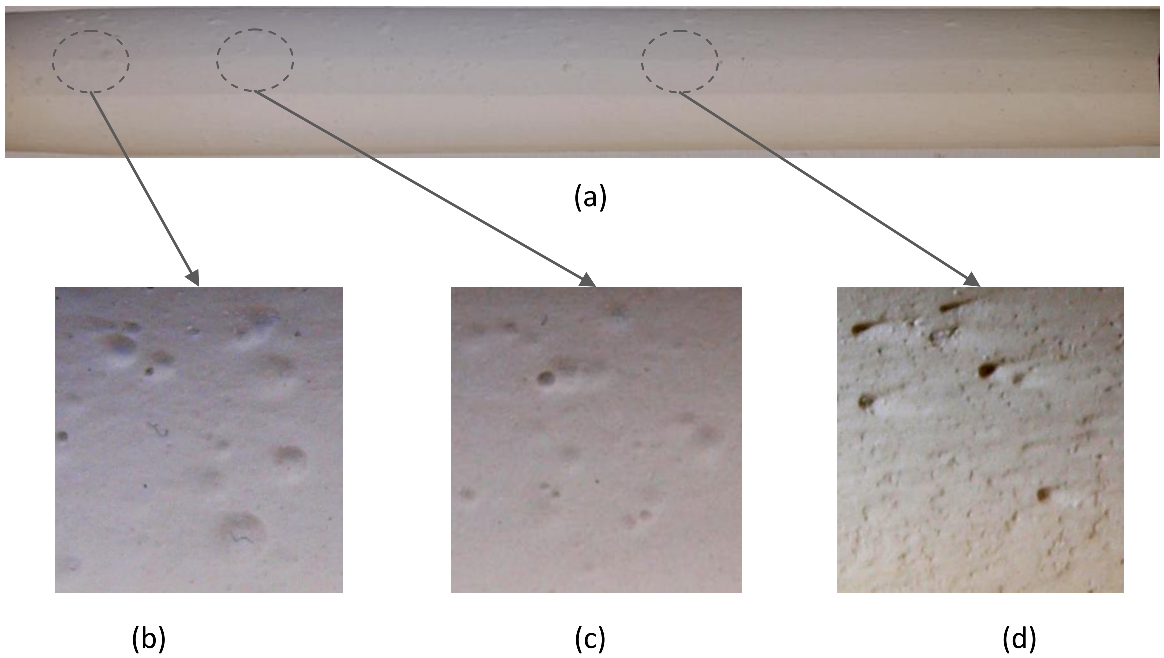

Figure 4.12 Different types of scallops observed on the worn surface at Re_o 80000

Table 4.1 Location of flow reattachment and maximum mass/heat transfer for a sudden enlargement

uz/ν	x_r/z	x_{max}/z
100	4.405	4.533
200	7.672	7.167
300	10.380	9.431

The maximum Sherwood numbers from the 2.5 cm and 20 cm diameter bore facility are plotted against other published experimental data in Figure 4.13. The present data are higher than the data of Krall and Sparrow(45), Wragg et al.(42) and Poulson(9), but lower than that of Rizk et al.(47). The experimental data from the 2.5 cm diameter facility indicates that the maximum mass transfer rate increases more rapidly with

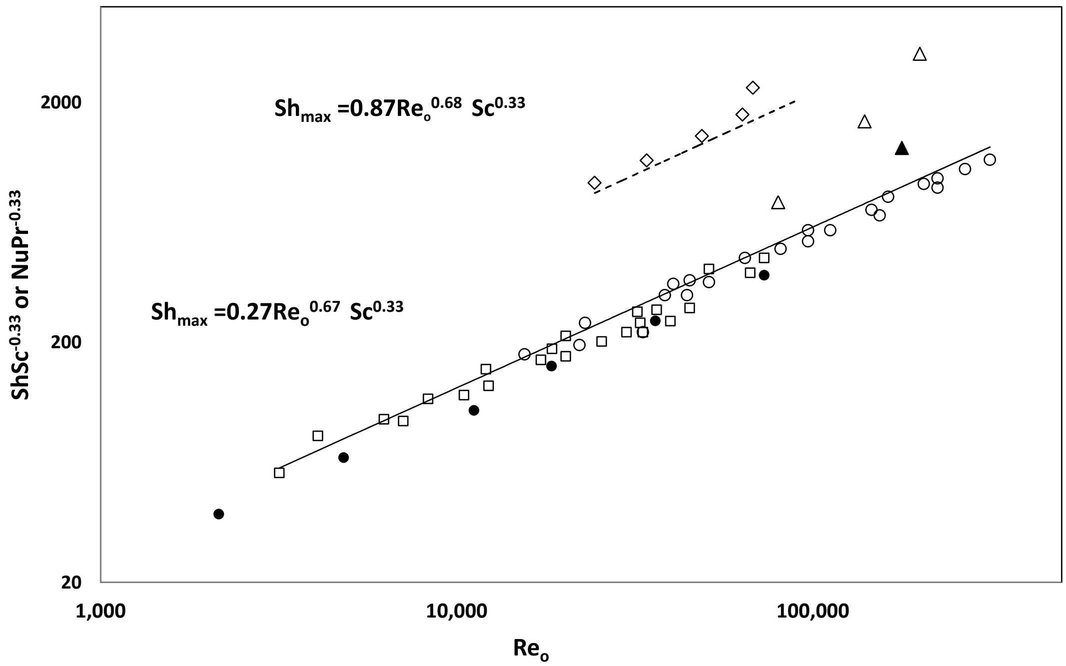

Figure 4.13 Maximum Sh for Δ 2.5cm bore experiments at Re_o 80,000, 140,000 and 200,000, ▲ 20 cm diameter bore at Re_o 180000 □ Wragg et al.(1979), ○ Krall and Sparrow(1966), ◊ Rizk et al.(1996) ● Poulson and Russell (1986)

Table 4.2 Comparison between predicted values for fully developed pipe and present values in 2.5 cm bore facility at z/D = 8 downstream of the orifice

Re_o	Present Sh	Smooth Sh	Rough Sh
80000	1648	1625	3351
140000	3886	2630	5215
200000	7664	3575	6912

Reynolds numbers. The maximum mass transfer rate obtained in the 20 cm diameter bore facility is much less than the value obtained in 2.5 cm diameter bore facility at Re_o = 200000. The data of Krall and Sparrow(45), Tagg et al.(42) were obtained using the LCDT method on smooth pipes. The data of Poulson(9) were obtained by a dissolving wall method at orifice Reynolds number in the range of 2151 to 73151, which are lower than that of the present tests. The test section of Poulson (9) did not develop pronounced scallops at the lower Reynolds numbers. Some shallow smooth craters developed at high Reynolds numbers after a prolonged exposure and in the maximum mass transfer region (41). There is only little or no roughness on the test section used by Poulson(9). In this case, the data agree with the other data for maximum mass transfer downstream of an orifice/sudden expansion on smooth wall fairly well.

Rizk et al. (47) also employed the LCDT method. However, a different electrode design was employed in the experiments. The cathode design included a 0.5mm nickel wire as a local cathode, and it was inserted into another 90mm OD cathode, which is explained in detail in Chapter 2. The mass transfer was much higher in their experiments and can be attributed to the roughness introduced at the joints between the tubing and outer cathodes, and between the outer cathodes and inner wire cathode. The maximum mass transfer rates observed by them are significantly higher than the others.

The present Sherwood numbers at z/D = 8 are shown in Table 4.2 along with the values for smooth and rough wall pipes from the correlation of Berger and Hau(17), and Zhao and Trass(48). It was suggested by Poulson(9) that it takes about 7 pipe diameters for the flow to relax back to a fully developed pipe mass transfer rate downstream of an orifice. The Berger and Hau correlations for a wall mass transfer in a smooth pipe(17) is given by

$$Sh_{pipe} = 0.0165Re^{0.86}Sc^{0.33} \quad 4.1$$

and the Sherwood number correlation for rough wall (48) is given

$$Sh_{rough\ pipe} = 0.03Re^{0.79}Sc^{0.45} \quad 4.2$$

The correlation for rough pipes was developed from experiment was performed with LCDT on premade rough wall with rough surface characteristics of 0.173 mm depth and 1.25 mm pitch (48). This correlation is valid for $500 \leq Sc \leq 5000$ and $Re \geq 60000$. The Sherwood number data from the 2.5 cm diameter bore facility at z/D=8 are close to the smooth wall value at Re_o of 80000, and is about 150% higher than smooth wall Sh and 25% lower than rough wall value at Re_o 140000. At Re_o = 200000, it is 11% higher than the rough wall value. Therefore, the data suggests that the surface roughness has a significant effect on the mass transfer rate, and also the mass transfer enhancement due to the developed roughness is higher at higher Reynolds numbers.

Roughness can enhance the mass transfer rate up to 3 to 4 on fully developed pipes(48). The ratio between the present maximum Sherwood number data and the predicted smooth wall mass transfer data by Krall and Sparrow`s correlation(4) downstream of an orifice are1.5, 2.2 and 3.3 at Reynolds number 80000, 140000 and 200000 respectively. The roughness effect on the maximum mass transfer rate in the pipe flow downstream of the orifice is evident in the present experiments. Both of the enhancement factors at the maximum mass transfer region and at the pipe flow region increase with Reynolds numbers. The surface roughness is examined in more detail to determine how it affects the mass roughness. Five scanned images of the worn test section are presented in Figure 4.14, which includes the unworn surface, and three test sections in the 2.5 cm bore loop, and the test section in the 20 cm bore loop at different Re_o. The entire scanned worn surfaces are shown, which include 8 diameters downstream from the orifice for the tests in 2.5 cm bore loop and 4 diameters downstream from the orifice for the tests in 20 cm bore loop. The flow direction is from left to right. A higher Reynolds number results in higher mass transfer rate, therefore for comparison, the test section are selected to have approximately the same non-dimensional wear of w_{max} /D = 0.03, where w is the circumferential wear at z/D = 8, and D is the pipe diameter.

At Re_o 80000, a shallow waviness is formed over the entire surface as shown in Figure 4.14(a), rather than typical scallops. No significant surface morphology difference is observed between 1.5 and 1.9 diameters downstream of the orifice, where the flow reattaches. At Re_o of 200000, Figure 4.14 (d), at about 2 diameters downstream of the orifice, there are a greater number of scallops that overlap with each other. Since the scallops are so compacted, no isolated round scallops could be identified. The roughness surface in this region looks like a washboard. The density of the scallops becomes less and the tails are directed either upstream or downstream away from the reattachment region. At Re_o of 140000, the surface roughness pattern shown in image (c) of Figure 4.14 seems a transition stage between (b) and (d). There are a few scallops observed in image (c) around 1.6 diameters downstream of the orifice. The scallop shapes shown in the scanned image (c) are mostly round, and are isolated from each other. The roughness is summarized in Table 4.1.

Enlarged photographs around the maximum mass transfer location from z/D = 1 to 2 of the worn sample surface are shown in Figure 4.15. The population and the size of the scallops increase noticeably from (a) to (b) as the Reynolds number is increased from 80000 to 140000. However, the majority of the scallops are isolated from each other.

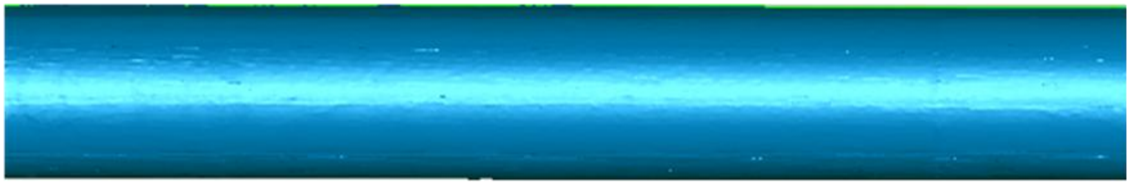

(a)

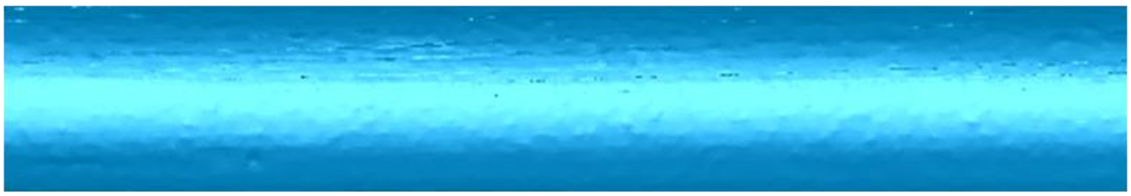

(b)

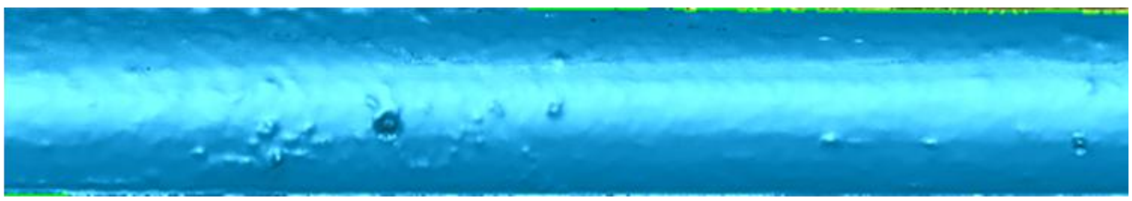

(c)

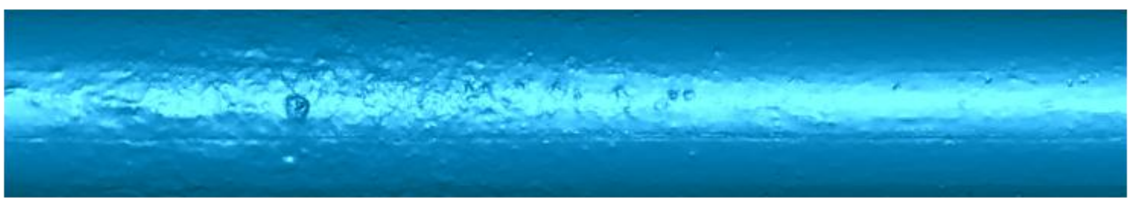

(d)

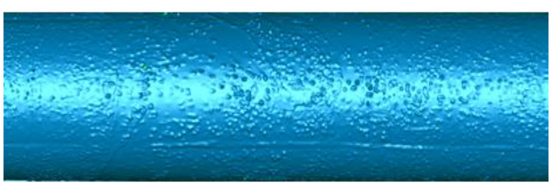

(e)

Figure 4.14 Scanned images of (a) unworn surface (b) surface at Re_o80000 in 2.5 cm pipe after 30 minutes, (c) surface at Re_o 140000 in 2.5 cm pipe after 15 minutes, and (d) surface at Re_o200000 in 2.5 cm pipe after 10 minutes (e) surface at Re_o 180000 Re_o in 2.5 cm pipe after 14 hours

Table 4.3 Description of surface roughness patterns downstream of an orifice

Test facility	Reo	time	Roughness shape	Roughness distribution
2.5 cm bore	80000	30 min	Shallow waviness	Shallow waviness observed over the entire surface
2.5 cm bore	140000	15 min	Round scallops, and shallow waviness	A few round scallops located around 1.8 diameters downstream of the orifice. Shallow waviness is developed else where
2.5 cm bore	200000	10 min	Washboard roughness caused by compact scallops, and shallow waviness	Washboard like roughness observed in the range of 1 to 3 diameters downstream of the orifice, shallow waviness is developed else where
20 cm bore	180000	14 hour	Round Scallops	Large population of scallops is developed over the entire surface however concentrated at about 1.9 diameters downstream of the orifice.

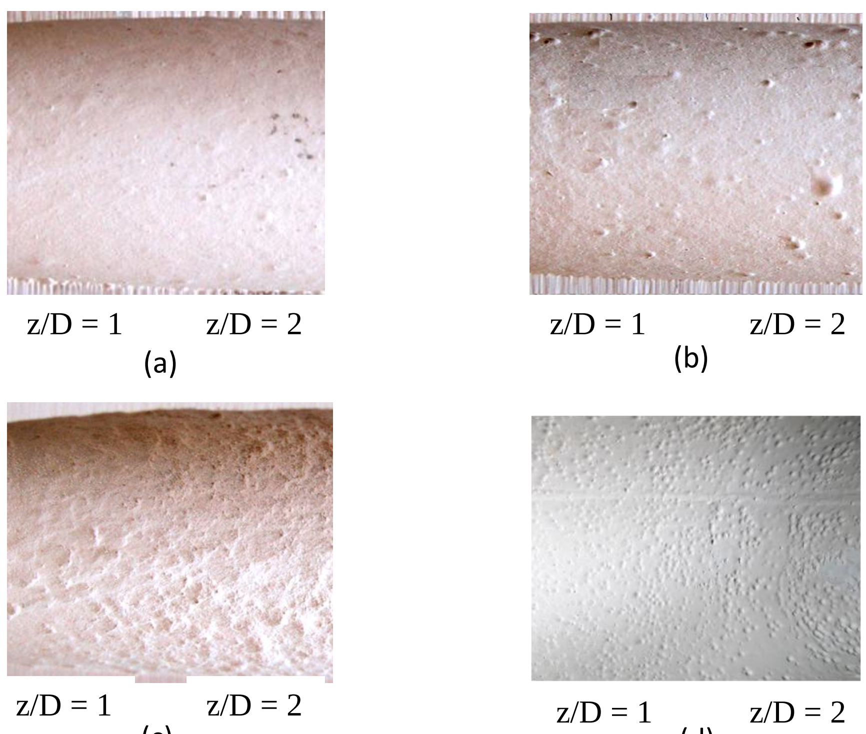

Figure 4.15 Photos of worn sample surface in 2.5 cm diameter facility at (a) Re_o80000 after 30 minutes, (b) at Re_o 140000 after 15 minutes, (c) at Re_o200000 10 minutes, and in 20 cm diameter facility at (d) Re_o 180000 after 14 hours

Image (c) shows that the scallops overlap with other and form washboard-like roughness. The maximum Sherwood number for the large bore tests is 14000, which is only about 40 % of the Sherwood number in the 2.5 cm diameter bore facility at similar Reynolds number.

The worn surface of the 20 cm test section after 14 hours (d) in Figure 4.15 shows larger scallop sizes, which seem to scale up with the pipe diameter. The average diameter of the scallops developed is in the order of 1.5 mm. However, the scallops are isolated from each other compared to the overlapped scallops shown in (c) for Re = 200000 in the 2.5 cm test section. Therefore, the present experiments suggest that the roughness patterns are critical factor of enhancing mass transfer. The roughness pattern of overlapped scallops has a much greater effect on mass transfer, with an enhancement factor of 3.3 from smooth wall than the effect of the isolated scallop pattern on mass transfer at similar Reynolds number, a factor of 1.3 from smooth wall.

CONCLUSIONS AND RECOMMENDATIONS

4.1. CONCLUSIONS

The effect of Reynolds number and surface roughness on the mass transfer downstream of an orifice was determined. Experiments were performed in a 2.5 cm diameter bore loop at orifice Reynolds number of 80000, 140000 and 200000, and in a 20 cm diameter bore loop at orifice Reynolds number 180000. A wall dissolving method was used with test sections cast of hydrocal and water as the working fluid. The test sections had an initially nominally smooth wall surface. In the 2.5 cm bore loop, multiple test samples were prepared and run for different times at each Reynolds number. At the end of each test time, the wear topology was obtained by laser scanning the worn surface. A non-destructive test was performed in the 20 cm bore loop. In this case, one test sample is prepared for each Reynolds number with an inner hydrocal lining, and ultrasonic measurements for the wall thickness were taken online during the test to determine the pipe wall thinning rates. The worn surface topology was determined at the end of the test by laser scanning.

The Sherwood number profiles downstream of the orifice are generally consistent at the different Reynolds numbers. The Sherwood number increases rapidly immediately after the orifice, reaches a maximum, and then and would slowly relax back to the fully developed pipe value. B. Poulson(41) suggested that the flow fully relaxes back to the fully developed pipe flow state around 7 diameters downstream of the orifice. The maximum mass transfer location occurs in the range 1.5 to 1.9 pipe diameters downstream of the orifice, and this location shifts downstream of the orifice as the Reynolds number is increased.

The enhancement of the maximum Sherwood number downstream of the orifice increases with Reynolds number in the 2.5 cm diameter bore facility compared with the smooth wall values. The maximum Sherwood number at Re_o = 180000 in the 20 cm bore loop is significantly smaller than that in the 2.5 cm diameter facility at Re_o200000. The maximum mass transfer values are greater than that predicted by the correlation of Krall and Sparrow(4), which are based on smooth wall mass/heat transfer measurements. The higher value of maximum mass transfer rate of the present measurement can be attributed to surface roughness. Different roughness patterns are developed at different Reynolds numbers and pipe diameter. At Re_o of 80000 in the 2.5 cm bore loop, only a small waviness was observed over the entire surface of the test sections, while at Re_o of 200000, a large population of scallops developed around the maximum mass transfer locations. The population of the scallops over the test sample surface and magnitude of the waviness are between the previous two cases at Re_o 140000. The enhancement factor of the maximum Sherwood number downstream of the orifice increased from 1.5 to 3.3 as the roughness pattern changed as described above for the different Reynolds numbers.

A large amount of scallops developed in the 20 cm bore test section over the entire surface at $Re_o = 180000$. The density of the scallops were higher concentrated around 1.9 diameters downstream of the orifice corresponding to the location of maximum mass transfer. However, the scallops are isolated from each other, and no washboard patterns were observed. For the 2.5 cm diameter test section at Re_o 200000, compact scallops developed around 1 to 3 diameters downstream of the orifice. The roughness enhancement factor for the compact scallop surface is 3.3, while it is 1.4 for the isolated scallop surface in the larger diameter section. The compact roughness pattern had a much more significant effect on mass transfer rate than the roughness patterns of isolated scallops.

4.2. RECOMMENDATIONS

The present data suggests that the surface roughness has a significant effect on the mass transfer rate downstream of an orifice. The shape, size and spacing are important for characterizing roughness (13). The naturally developed roughness due to the flow from a smooth surface depends on the Reynolds number and orifice to pipe diameter ratio. Due to the complexity of the surface roughness patterns, the characteristics of the roughness were not quantified in the present research. It would be very useful to quantify the roughness to better evaluate its effect on the mass transfer.

Tests were performed to determine the mass transfer rate at 3 different Reynolds numbers in the 2.5 cm diameter bore loop, and one Reynolds number in the 20 cm diameter bore loop. In order to determine the Reynolds number effect on mass transfer rate, additional data points at different Reynolds numbers are required. In addition, because of the dependence of the roughness on the mass transfer, additional experiments are needed to better understand how roughness evolves with different Reynolds numbers and its effect on mass transfer.

Thus, the recommendations for future work are:

1. To perform experiments at higher Reynolds numbers in both 2.5 and 20 cm diameter bore facility to better define the Reynolds number effect on mass transfer rate.
2. To quantify the evolving surface roughness, including the shape, size and spacing or density.
3. To determine how roughness downstream of an orifice evolves from a smooth surface at different flow conditions and different pipe diameters.
4. To determine quantitatively the effect of surface roughyness on the mass trasfer rate.

REFERENCES

1. *Flow-accelerated corrosion in fossil and combined Cycle/HRSG plants.* **Dooley, R. Barry.** 2008, PPCHEM, pp. 68-89.
2. *A correlation of maximum turbulent heat transfer coefficient in reattachment flow region.* **Nishiyama, Hideya.** 6, 1987, International journal of heat and mass transfer, Vol. 30, pp. 1193-1200.
3. *A review of experimental study of Turbulent heat transfer in separated flow.* **Togun, Hussein , Kaxi, S.N. and Badarudin, Ahmed.** 10, 2011, Australian jurnal of basic and applied sciences, Vol. 5, pp. 489-505.
4. *Turbulent heat transfer in separated, reattached, and redevelopment regions of a circular tube.* **Krall, K.M. and Sparrow, E.M.** 1966, Journal of heat transfer, pp. 131-136.
5. *Mass transfer investigation in turbulent flow downstream of sudden enlargement of a circular pipe for bery high Schimidt numbers.* **Runchal, A.K.** 1971, Internatiional journal of heat and mass transfer, pp. 781-792.
6. *Heat and mass transfer downstream of abrupt nozzle expansions in turbulent flow.* **Tagg, D. J., Patrick, M.A. and Wragg, A.A.** 1979, Trans IchemE, pp. 176-181.
7. *Mass trasnfer enhancement associated with sudden flow expansion.* **Rizk, T.Y., Thompson, G.E. and Dawson, J.L.** 1996, Corrosion Science, pp. 1801-1814.
8. *A correlation of maximum turbulent heat transfer coefficient in reattachment flow region.* **Ota, Terukazu and Nishiyama, Hideya.** 60, 1987, International journal of heat and mass transfer, Vol. 30, pp. 1193-1200.
9. *The use of a corrosion process to obtain mass transfer data.* **Poulson, Bryan and Robinson, Russel.** 1986, Corrosion Science, pp. 265-280.
10. *Flow accelerated corrosion and its control measures for the secondary circuit pipelines in Indian nuclear power plants.* **Kain, Vivekanand, et al.** 383, mumbai : Journal of Nuclear Materials, 2008.
11. *Complexities in prediction erosion corrosion.* **Poulson, Brayn.** 1999, Wear, pp. 497-504.
12. *Mass transfer at rough surfaces.* **Dawson, David A. and Trass, O.** 1972, Inernational Journal of mass transfer, Vol. 15, p. 1317.
13. *Electorchemical mass transfer measurement in rough surface pipe flow: geometrically similar v-Shaped grooves.* **zhao, W and Trass, O.** 1997, Internationsl journal of heat and mass transfer, pp. 2785-2797.
14. *Mass transfer at smooth and rough surfaces in a circular Couette Flow.* **Grifoll, J., Farriol, X. and Giralt, Francesc.** 12, 1986, International journal of heat and mass transfer, Vol. 29, pp. 1911-1918.
15. *Surface controlled dissolution rates of gypsum in aqueous solutions exhibit nonlineardissolution kinetics.* **ALEXANDER A. JESCHKE, KATRIN VOSBECK and WOLFGANG DREYBRODT.** 1, Bremen : Elsevier Science Ltd, 2001, Vol. 65.
16. **Frank, Incropera.** *Fundamentals of Heat and Mass Transfer.* New York : John Wiley and Sons, 1985.

17. *Mass transfer in turbulent pipe flow measuremed by the electrochemical method.* **Berger, F.P. and Hau, K.F F.L.** 1977, International Journal of heat and mass transfer, pp. 1185 - 1194.
18. *Electrochemical measurement in flowing solutions.* **Poulson, Bryan.** 4, 1983, Corrosion Science, Vol. 23, pp. 391-430.
19. **Butler, G and Ison, H. C. K.** *Corrosion and its prevention in waters.* New york : Reinhold publishing corporation, 1966.
20. **Raboian, R.** *Electrochemical Techniques for corrosion engineering.* Houston : National association of corrosion engineers, 1986. ISBN 0-915567-23-7.
21. **Pourbaix, Marcel.** *Lectures on electrochemical corrosion.* New york -London : Cebelcor, 1973.
22. *Mass transfer in straight pipes and 90 degree bends measured by the dissolution of plaster.* **Wilkin, S.J., Oates, H.S. and Coney, M.W.E.** 1983. TPRD.
23. **Szklarska-Smialowska, Z.** *Pitting corrosion of metals.* Houston : National Association of corrosion engneers, 1986. 0-915567-19-9.
24. **wilkin.** 1982.
25. *Experimental and theoretical studies of dissolution roughness.* **Blumberg, Paul N. and Curl, Rane L.** 4, Ann Arbor : J. Fluid Mechanical, 1974, Vol. 65.
26. *Bed forms due to mass transfer in turbulent flows: a kaileidoscope of phenomena.* **Allen, J.R.L.** 1971, Journal of fluid mechanics, pp. 49-63.
27. *Surface dissolution and the development of scallops.* **Villien, Benoit, Ying, zheng and Lister, Derek.** New : s.n., 2005, Chemistry Enginenring communication, pp. 125-136.
28. *The kinetics of dissolution of calcium sulfate dihydrate.* **Liu, Sung Tsuen and Nancollas, G.H.** 1971, Journal of Inorganic and nuclear chemistry, pp. 2311-2316.
29. *mass transfer (absorption) coefficients prediction from data on heat transfer and fluid friction.* **T. H. CHILTONA and A. P. COLBURN.** 11, Wilmington : Industrial and engineering chemistry, 1934, Vol. 26.
30. *A solution to the turbulent Graetz problem-III Fully developed and entry region heat transfer rates.* **R. H. N0TTER and C. A. SLEICHER.** Seattle : Chemical Engineering Science, 1972, Vol. 27.
31. **T.H. Chilton and A.P. Colburn.** s.l. : Ind. Engeering chem., 1934.
32. **White, Frank M.** *Viscous fluid flow.* New York : McGraw-Hill, 2006.
33. **Coney, M.** *CERL REport RD/L/N197/80.* 1980 November.
34. **Robert, W. Fox, Alan , T. McDonald and Philip, J. Pritchard.** *Introduction to Fluid Mechanics.* s.l. : Hachette Filipacchi Media U.S. Inc., 2004.
35. BS 1042. *British Standards INstitute 1042 ,Part 2.* London : s.n., 1964.
36. *Surface dissolution and the Development of Scallops.* **Villien, Benoit, Zheng, Ying and Lister, Derek.** 2005, Chemimcal Engineering communication, pp. 125-136.
37. **Roland GD.** *LPX-600 User's manual.* Hamamatutsu-shi, Shizuoka-ken, Japan : s.n., July 26, 2001.

38. *THE KINETICS OF DISSOLUTION OF CALCIUM SULPHATE DIHYDRATE IN WATER.* **Jorgen , Christoffersen and Margaret, Christenoffersen.** 35, 1976, Journal of crystal growth, pp. 79-88.
39. **Castrup, Howard.** *Uncertinty Analysis for risk management.* Anaheim, California : Measurement Science conference, 1995.
40. **Shine, Annette D.** *Fitting experimental data to straight lines(including error analysis).* s.l. : Chemical engineering, 2006.
41. *The use of a corrosion process to obtain mass trasnfer data.* **Poulson, B. and Robinson, R.** 1986, Corrosion Science, pp. 265-280.
42. *Heat and mass trasnfer downstream of abrupt nozzle expansions in turbulent flow.* **Tagg, D.J., Patrick, M.A. and Wragg, A.A.** 1979, Trans IchemE, pp. 176-181.
43. *Diffusion-controlled current distributions near cell entries and coners.* **A.A. Wragg, D.J. Tagg and M.A. Patrick.** Exeter : Shapman and Hall LTD., 1980, Journal of applied electrochemistry , Vol. 10. 43-47.
44. *Effects of the separating shear layer on the reattachment flow structure Part 2: Reattachment length and wall shear stress.* **Adam, E. W. and Johnston, J.P.** 1988, Experiments in Fluids, Vol. 6, pp. 493-499.
45. *Turlulent heat transfer in the separated reattached, and redevelopment regions of a circular tube.* **Krall, K.M. and Sparrow, E.M.** 1966, Journal of heat transfer, p. 131.
46. *Relation between the points of flow reattachment and maximum heat transfer for regions of flow separation.* **E.M. Sparrow, S.S. Kang and W. Chuck.** 7, Mineapolis : International journal of heat and mass transfer, 1986, Vol. 30. 1237-1246.
47. *mass transfer enhancement associated with sudden flow expansion.* **Rizk, T.Y., Thompson, G.E. and Dawson, J.L.** 1996, Sorrosion Science, pp. 1801-1814.
48. *Electrochemical mass trasfer measurements in rough surface pipe flow: geometrically similar V-Shaped grooves.* **Zhao, W. and Trass, O.** 1997, International Journal of heat and mass trasnfer, pp. 2785-2797.
49. *EROSION CORROSION AND SYNERGISTIC EFFECTS IN DISTURBED.* **Malka, Ramakrishna, Nešić, Srdjan and Gulino, Daniel A.** Athens : s.n., 2006. Corrosion NACExpo . p. 1.
50. *Mass transfer in straight pipes and 90 degree bends measured by the dissolution of plaster.* **Wilkin, S.J., Oates, H.S. and Coney, M.W.E.** 1983. Central electricity generating board.

APPENDIX A: MATLAB CODE

1. Code for alignment of each scanned image of 2.5 cm test sections to a common cylindrical coordinate and transfer the point clouds of the images into a mesh with the same dimensions with respect to the coordinates

```
%%%%%%%%%%%%%%%%%%%%%%%%%%%%%%%%%%%%%%%%%%%%%%%%%%%%%%%%%%%%%%%%%%%%%%
%%%%
%%%%%% function of this code:
%%%%%% 1) computing
%%%%%% a) convert the data points from cartesian to cylidrical
coordinates
%%%%%% b) regridding the point clouds
%%%%%% c) align the wear based on axial symmetry
%%%%%% 2) plotting
%%%%%% a) how the realignment was done based on unaxymmetry

%%%%%% Input:
%%%%%% 1) point clouds from geomegic

%%%%%% User input
%%%%%% a) Compute tha allignment
%%%%%%  1) How many experiments been conducted at this Re
%%%%%%  2) How many subdivision in angel direction
%%%%%%  3) Spacing between two adjacent grid in flow direction

%%%%%% Output:
%%%%%%  1)datapoints after realignment in cylindrical system
%%%%%%  2)Datapoints after realignment in Coordinate system

%%%%%% b) Plot the figures
%%%%%%  1) contour plots
%%%%%%  2) 3D wire frame
%%%%%%  3) 2D wire frame
```

```
%%%%%%  4) wear profiles at different cross sections
%%%%%%  5) Local Wear normalized by average radius
%%%%%%  6) Local Wear normalized by average wear

%%%%%% C) calculate  mass balance

%%%%%%%%%%%%%%%%%%%%%%%%%%%%%%%%%%%%%%%%%%%%%%%%%%%%%%%%%%%%%%%%%%%%%%
%%%%

close all,
clear all
clc

t0 = clock;
%% %%%%%%%%%%%%%%%%%%%%  code options
%%%%%%%%%%%%%%%%%%%%%%%%%%%%%%%%

opt = input(' 1 for computation; 2 for plotting ');

testOpt = 0;
%%%%%% 1 for NOT running the testting stem
%%%%%% 0 for running testting stem and saving them for further
comparison
%%%%%%      in Geomagic

plotOpt = 0;
%%%%%% 1 for ploting none dimension, 0 for mm

rIdeal = 0.5*25.4 ;
%%%%%% Assume the initial radius is 12.83 mm (0.5053") for figure 1
%% %%%%%% option of plots: none dimension or dimention (mm)
%%%%%% Note: unit in all the calculations are in metric system

if plotOpt == 1
      NDL = 1/0.0254; %%%%% factor for none dimensionalize the length
      NDA = 1;        %%%%% factor for none dimensionalize the length
else
      NDL = 1000;     %%%%% factor for converting m to mm
      NDA = 180/pi;   %%%%% factor for converting radian to degree
end

if opt == 1
      %% %%%%%% read in files
      rawData = importdata('worn.txt');
      %%%%%% rawData are in mm in cartisian coordinates

      datapoints = length(rawData);
      %%%%% the number of data points  in the original image

      %% %%%%% User Input, and user defined
      fprintf('How many angle subdivision are needed? \n');
```

```
noAng = input('Recommended Value: 150  ');

fprintf('The spacing between different cell in flow direction?
(mm) \n')
spacing = input('Recommended Value: 0.3  ');

%% %%%% predified variables by users for realignment

angelS = 5;     %%%%%%  in the 2nd iteration the grid starting
angel
angelE = 175;   %%%%%%  in the 2nd iteration the grid starting
angel

flowS = -2;     %%%%%% predefined flow starting point in the 2nd
iteration
flowE = -220;    %%%%%% predefined No. of columns in the 2nd
iteration

skippedLine = 20;
%%%%%best fit will skip the first skippedLine to avoid
significant flow
%%%%%caused unsymmetry

lines =25;
%%%%%using number of(lines) lines for the correction

nIter = 6;
%%%%% Maximumly, the code iterate N times

barSlope = 0.0002;  %%%%% iterate untill the slope is less than
this
barShift = 0.01;  %%%%% iterate untill the intersettion is less
than this

lineSlope = barSlope + 0.0001;
lineShift = barShift + 0.001;
%%%%%% initiate angleRot, and barshift Value to start iteration

%% %%%%%% Compute the gridding in angle direction

[allAngR, allRho, allZ] =
cart2pol(rawData(:,1),rawData(:,2),rawData(:,3));
%%%%%% transfer into cylindrical system
%%%%%% allAngR ==> Radians,  allRho ==> mm, and z ==> mm

allAngD = -allAngR * 180/pi;
%%%%%% convert the angle unit to degree, and convert into
positive
%%%%%% values

%%%%%% 1) angle part of the gridding
```

```
if(min(allAngD)>0)
      angleStart = ceil(min(allAngD))+2;
else
      angleStart = ceil(min(abs(allAngD)))+2;
end
%%%%%% define the angle of start

angleEnd = floor(max(allAngD))-2;
%%%%%% define the angle of start

lineAngR = linspace(angleStart, angleEnd, noAng)/180*pi;
%%%%%% difine the gridding along cross-flow direction

%% %%%%%% Compute the gridding in flow direction

samplelength = abs(max(rawData(:,3))-min(rawData(:,3)));
fprintf('The total length of the sample is %6.2f mm \n',...
      samplelength)

if max(allZ)>0
      flowStart = -spacing-2;
else
      flowStart = max(allZ)-spacing-2;
end
%%%%%% define where to start the gridding along flow direction

flowEnd = min(allZ)+spacing+1;
%%%%%% define where to finish the gridding along flow direction

noCol = ceil((abs(flowStart-flowEnd)/spacing));
%%%%%% calculate how many columns along flow direction
fprintf('There are %d rows in flow direction \n', noCol)

lineFlow = linspace(flowStart, flowEnd, noCol);
%%%%%% difine the gridding along flow direction

fprintf('Averagely, there are %4.1f points in each cell \n', ...
      datapoints/noCol/noAng)
%% %%%%%%% Complete meshing by combining the angel direction and
flow
%%%%%%  direction grid

[meshFlow meshAngR] = meshgrid(lineFlow, lineAngR);
%%%%%% lineFlow and gridCross are noCol * numOfAngle

meshRho = zeros(noAng,noCol);
%%%%%% initiate the radius value at each grid

%%% reshape allZ, angle theta, and wear amount matRds to m*n
matrix
zz = meshFlow(1,:);
```

```
%% %%%%%% Compute the value in each grid point

difAngle = (angleEnd - angleStart)/(noAng-1);
%%%%% calculate the spacing between two adjacent angles

for ir = 1:noCol
      for ia = 1:noAng
      Indth1 = find(allAngD>(angleStart+(ia-1)*difAngle));
      Indth2 = find(allAngD(Indth1)<=(angleStart+ia*difAngle));
      dumI1 = Indth1(Indth2);
      IndA1 = find(allZ(dumI1)<(flowStart-(ir-1)*spacing));
      IndA2 = find(allZ(dumI1(IndA1))>=(flowStart-ir*spacing));
      dumI2 = dumI1(IndA1(IndA2));
      meshRho(ia,ir) = mean(allRho(dumI2));
      end
end
%%%%%%% compute the cell value by taking the average of all the
points in
%%%%%%% that cell

%%  %%%%%%%%% Testing the gridding image
%%%%%%%%%%%%%%%%%%%%%%%%
%%%%%% convert the points back to Cart to be compared in
geomagic
%%%%%% before gridding
if testOpt ~= 1
      [testFGx testFGy testFGz] =
      pol2cart(meshAngR(:),meshRho(:),meshFlow(:));
end

testCartFG = [testFGx -testFGy testFGz];

dlmwrite('testCartFG.txt',testCartFG, 'delimiter', '\t')
%%%%% store the point clouds in cartisian coordinates

%% %%%%%%%%%%%%%%%% fill the holes of the image
%%%%%%%%%%%%%%%%%%%%
NotNumbers = isnan(meshRho);
%%%%%% find the empty cells ( isnan converts matrix into array
%%%%%% automaticly)
[NaNR NaNC] = find(NotNumbers);
%%%%%% get the index of the empty cells

threshRho = mean(allRho)/3;
%%%%%% the threshold for filling the empty cells
%%%%%% which is half of the average radius over the whole
surface

dumXInd = (1:noAng)';
      %%%%%% initiate a dummy index X for interpolation
```

```
for ic = 1:noCol
      indC = find(NaNC == ic);
      %%%%%% find the empty points in each column
      noEmp = length(indC);
      %%%%% calculate the number of empty points in that column
      emptyRs = NaNR(indC);
      %%%%%% locate where the empty points are in rows
      dumCol = meshRho(:, ic);
      meshRho(emptyRs,ic) = mean(dumCol(dumCol>threshRho));
      p = polyfit(dumXInd,meshRho(:,ic),3);
      meshRho(emptyRs,ic) = polyval(p,emptyRs);
end
%%  %%%%%%%%% Testing the gridding image
%%%%%%%%%%%%%%%%%%%%%%%%
%%%%%% convert the points back to Cart to be compared in
geomagic
%%%%%% before gridding
if testOpt ~= 1
      [testBGAFx testBGAFy testBGAFz] ...
                  =
                  pol2cart(meshAngR(:),meshRho(:),meshFlow(:));
end

testCartBGAF = [testBGAFx -testBGAFy testBGAFz];

dlmwrite('testCartBRAF.txt',testCartBGAF, 'delimiter', '\t')
%%%%% store the point clouds in cartisian coordinates

%%  %%%%%%%%%%%%%%%%%%%%%%% Realignment
%%%%%%%%%%%%%%%%%%%%%%%%%%%%%
%%%%%%%%%%%%%%%%%%%%%%%%%%%%%%%%%%%%%%%%%%%%%%%%%%%%%%%%%%%%%%%%%%%%%%%
%%%%% (noAng-lines)/2 as the first line to start
%%%%% the corresponding correction factor is
linesYStart = floor((noAng-lines)/2);
linesYEnd = linesYStart + lines -1;

%%%to find the shift in x directiona and y direction
counting = 0;
while (counting <= nIter)&&...
      ((abs(lineSlope)>barSlope)||(abs(lineShift)>barShift))
      counting = counting +1;

      %%%%%%%%%%%%%%%%%%% calculation of shifting in x
      %%%%%%%%%%%%%%%
      localShift = ones(1,noCol);
      for n = 1:noCol
      sum = 0;
      for m = 1:lines
            sum = sum + (meshRho(m,n) - meshRho(noAng-m+1,n))...
                  /cos(meshAngR(m,n));
            %%%%%%Dummy variable for LocalShift
      end
      localShift(1,n) = sum/2/lines;
```

```
%%%%% Averaged shift at each allZ location
end
shiftConsid = localShift(skippedLine+1:noCol);
zConsid = zz(skippedLine+1:noCol);
%%%%% take out the points at the beginning of the pipe
where
%%%%% the entrance effect and uneven wear is significant

%%% calculate the slope of the correction by 1st order fit
p = polyfit(zConsid, shiftConsid,1);
lineSlope = p(1,1);
lineShift = p(1,2);
fitVal = polyval(p,zz);

%%%%% Shift the points according to
cartX = meshRho.*cos(meshAngR)-meshFlow.*sin(lineSlope) -
lineShift;
cartY = -meshRho.*sin(meshAngR);
cartZ = meshFlow*(1 + abs(cos(lineSlope)*tan(lineSlope)));
%%%%% approximately cartZ = matZ
%%%%% transfer back to theta allZ and radius matrix form
meshAngR = -atan(cartY./cartX);
%%%%% angle theta should be always positive from 0 to pi/2
indices = find(meshAngR<0);

meshAngR(indices) = meshAngR(indices)+pi;    %%%%% update
angle
meshFlow = cartZ;                            %%%%% update
z coordinates
meshRho = sqrt(cartX.^2 + cartY.^2);         %%%%% update
radius

subplot(2,1,1)
plot(-meshFlow(1,:)/25.6,localShift,':r',-
meshFlow(1,:)/25.6,fitVal,'b')
title('Shift in X direction')
xlabel('Z/D down stream')
ylabel('Wear (mm)')

%%%%%%%%%%%%%%%%%%%%%%%%%%%% calculation of shifting in y
%%%%%%%%%%%%
localShift = ones(1,noCol);
for n = 1:noCol
sum = 0;
for m = 1:lines
      sum = sum + (meshRho(m,n) + meshRho(noAng-m+1,n));
end
aveWear = sum/2/lines;    %%%%% Average wear at each Z
location

sum = 0;
for m = linesYStart:linesYEnd
```

```
            sum = sum + (meshRho(m,n)-
            aveWear)/sin(meshAngR(m,n));
      end
      localShift(1,n) = sum/lines;
      end

      shiftConsid = localShift(skippedLine+1:noCol);
      %%%%%%if only part of the points need to be considered to
      %%%%%%avoid the part that has severe wear
      zConsid = meshFlow(1,skippedLine+1:noCol);

      %%% calculate the slope of the correction by 1st order fit
      p = polyfit(zConsid, shiftConsid,1);
      lineSlope = p(1,1);
      lineShift = p(1,2);
      fitVal = polyval(p,zz);

      cartX = meshRho.*cos(meshAngR);
      cartY = -(meshRho.*sin(meshAngR)-meshFlow.*sin(lineSlope)
      - lineShift);
      cartZ = meshFlow.*(1 +
      abs(cos(lineSlope).*tan(lineSlope)));
      %%%% approximately cartZ = matZ

      %%%%% transfer back to theta z and deviation matrix form
      meshAngR = -atan(cartY./cartX);
      %%%%% angle theta should be always positive from 0 to pi/2
      indices = find(meshAngR<0);

      meshAngR(indices) = meshAngR(indices)+pi;    %%%%% angle
      updated
      meshFlow = cartZ;                            %%%%%z
      location updated
      meshRho = sqrt(cartX.^2 + cartY.^2);         %%%%% radius
      updated

      subplot(2,1,2)
      plot(-meshFlow(1,:)/25.6,localShift,':r',-
      meshFlow(1,:)/25.6,fitVal,'b')
      title('Shift in Y direction')
      xlabel('Z/D down stream')
      ylabel('Wear (mm)')
end
fprintf('Alignment itered %d times \n',counting)

allAngR = meshAngR(:);
allRho = meshRho(:);
allZ = meshFlow(:);
%%%%%% transfer into cylindrical system
%%%%%% allAngR ==> Radians,  allRho ==> mm, and z ==> mm
```

```
%% %%%%%%%%%%%%%%%%%%%%%% regridding
%%%%%%%%%%%%%%%%%%%%%%%%%%%%%%%%

noAng = noAng-10;
%%%%% make the grid coarser to avoid empty values

%%%%%% Compute the gridding in angle direction

%%%%%% 1) angle part of the gridding
angleStart = angelS;
%%%%%% define the angle of start

angleEnd = angelE;
%%%%%% define the angle of start

lineAngD = linspace(angleStart, angleEnd, noAng);
%%%%%% difine the gridding along cross-flow direction

%% %%%%%% Compute the gridding in flow direction

flowStart = flowS;

spacing = spacing*1.1;

noCol = ceil(abs(flowS-flowE)/spacing)+1;

flowEnd = flowStart - spacing*(noCol - 1);

lineFlow = linspace(flowStart, flowEnd, noCol);
%%%%%% difine the gridding along flow direction

fprintf('For second gridding, there are %d angel divisions
\n',noAng)
fprintf('and there are %6.2f rows in flow direction \n', noCol)

%% %%%%%%% Complete meshing by combining the angel direction and
flow
%%%%%%  direction grid

[meshFlow meshAngD] = meshgrid(lineFlow, lineAngD);
%%%%%% lineFlow and gridCross are noCol * numOfAngle

allAngD = allAngR * 180/pi;
%%%%%% convert the angle unit to degree, and convert into
positive
%%%%%% values

meshRho = zeros(noAng,noCol);
%%%%%% initiate the meshRho for second gridding
```

```
%% %%%%%% Compute the value in each grid point

difAngle = (angleEnd - angleStart)/(noAng-1);
%%%%% calculate the spacing between two adjacent angles

for ir = 1:noCol
      for ia = 1:noAng
      Indth1 = find(allAngD>(angleStart+(ia-1)*difAngle));
      Indth2 = find(allAngD(Indth1)<=(angleStart+ia*difAngle));
      dumI1 = Indth1(Indth2);
      IndA1 = find(allZ(dumI1)<(flowStart-(ir-1)*spacing));
      IndA2 = find(allZ(dumI1(IndA1))>=(flowStart-ir*spacing));
      dumI2 = dumI1(IndA1(IndA2));
      meshRho(ia,ir) = mean(allRho(dumI2));
      end
end
%%%%%%% compute the cell value by taking the average of all the
points in
%%%%%%% that cell

meshAngR = meshAngD * pi/180;
%%%%%% convert degree into rediant

%%  %%%%%%%%% Testing the gridding image
%%%%%%%%%%%%%%%%%%%%%%%%
%%%%%% convert the points back to Cart to be compared in
geomagic After
%%%%%% Realignment
if testOpt ~= 1
      [testARx testARy
      testARz]=pol2cart(meshAngR(:),meshRho(:),meshFlow(:));
end

testCartAR = [testARx -testARy testARz];

dlmwrite('testCartAR.txt',testCartAR, 'delimiter', '\t')
%%%%% store the point clouds in cartisian coordinates

%% %%%%%%%%%%%%%%%% fill the holes of the image
%%%%%%%%%%%%%%%%%%%
NotNumbers = isnan(meshRho);
%%%%%% find the empty cells ( isnan converts matrix into array
%%%%%% automaticly)
[NaNR NaNC] = find(NotNumbers);
%%%%%% get the index of the empty cells

threshRho = mean(allRho)/3;
%%%%%% the threshold for filling the empty cells
%%%%%% which is half of the average radius over the whole
surface

dumXInd = (1:noAng)';
```

```
            %%%%%% initiate a dummy index X for interpolation

      for ic = 1:noCol
            indC = find(NaNC == ic);
            %%%%%% find the empty points in each column
            noEmp = length(indC);
            %%%%% calculate the number of empty points in that column
            emptyRs = NaNR(indC);
            %%%%%% locate where the empty points are in rows
            dumCol = meshRho(:, ic);
            meshRho(emptyRs,ic) = mean(dumCol(dumCol>threshRho));
            p = polyfit(dumXInd,meshRho(:,ic),3);
            meshRho(emptyRs,ic) = polyval(p,emptyRs);
      end

      %%  %%%%%%%%% Testing the gridding image
      %%%%%%%%%%%%%%%%%%%%%%%%
      %%%%%% convert the points back to Cart to be compared in
      geomagic After
      %%%%%% fill holes
      if testOpt ~= 1
            [testAFx testAFy testAFz] =
            pol2cart(meshAngR(:),meshRho(:),meshFlow(:));
      end

      testCartAF = [testAFx -testAFy testAFz];

      dlmwrite('testCartAF.txt',testCartAF, 'delimiter', '\t')
      %%%%% store the point clouds in cartisian coordinates

      %% %%%%%%%%% Save data to a file %%%%%%%%%%%%%%%%%%%%%%%%%%%%%%

      output = zeros(noAng,noCol,3);
      output(:,:,1) = meshAngR; %%%%%% angel components in polor
      coordinates
      output(:,:,2) = meshRho;  %%%%%% radius components in polor
      coordinates
      output(:,:,3) = meshFlow; %%%%%% z components in polor
      coordinates

      dlmwrite('output.txt',output, 'delimiter', '\t')
      %%%%% store the data with a column of angels, z locations and
      local
      %%%%% wears(mm)

      %% %%%%%%%%%%%%%% different plotting after realignment
      %%%%%%%%%%%%%%%%
%%%%%%%%%%%%%%%%%%%%%%%%%%%%%%%%%%%%%%%%%%%%%%%%%%%%%%%%%%%%%%%%%%%%%%%
%

else
      %% %%%%%% read in files to matrix 'output'
```

```
dumOutput = dlmread('output.txt', '\t');

%% user input
noLine = input('Number of Z locs for evaluation ? ');

%% %%%%%%  Global variables for plotting section  %%%%%%%%%%%

density = 1581;             %%%%% Gypsum density kg/m^3

skip = 20;                  %%%%% skiiping the first 20 lines

deviMax = 0.016;            %%%%% Scaling the axis for
%%%%% the deviation plot

Markers=['r','k','b','g','k','m','y','b','m','k',...
      'c','g','r','b','m','c','g','r','b','m',
      'k','c','g','r','b','m'];
%% %%%%%%%  calculate the size of the matrix
noAng = size(dumOutput,1);
noCol = size(dumOutput,2)/3;
%%%%%% noAng is the number of angels
%%%%%% noCol is the number of columns

output = reshape(dumOutput, noAng, noCol, 3);
%%%%%% make output a 3-D matrix
%%%%%% 1 layer is the mesh of angle coordinate in radiance
%%%%%% 2 layer is the mesh of radius coordinate in mm
%%%%%% 3 layer is the mesh of Z coordinate in mm

%% %%%%%%% calculate where to plot the lines
lineAngR = output(:,1,1);
%%%%%% get the line array of angels from the stored matrix

lineFlow = output(1,:,3);
%%%%%% get the line array of Z from the stored matrix

totLen = max(abs(lineFlow))-min(abs(lineFlow));
%%%%%% calculate the total length of the regrided sample

indices = floor(linspace(skip,(noCol-skip),noLine));
%%%%%% Z locations, where the evaluations are

gapPlot = abs(output(1,indices(2),3) - output(1,indices(1),3));
%%%%%% Gap(mm) betweet evaluated lines
fprintf('Distance between the lines is %3.3f mm \n',gapPlot)

%%
%%%%%%%%%%%%%%%%%%%%%%%%%%%%%%%%%%%%%%%%%%%%%%%%%%%%%%%%%%%%%%%%
%%%%
%%%%%%%%%%%%%%%% experiment validation contour Plots
%%%%%%%%%%%%%%%%%%
```

```
BWorColor = 2;
      %%%%%   plotting options of figure 1
      %%%%% 1 for black and white contour
      %%%%% 2 for color contour plot
      %%%%% 3 for meshing

figure(1)

if BWorColor == 1
[C, h] = contour(output(:,:,1),-output(:,:,3)/rIdeal/2,...
      ((output(:,:,2)-rIdeal))/(2*rIdeal),5,'k');
clabel(C, h, 'LabelSpacing', 400);

elseif BWorColor == 2
      colorLevel = 0:0.005:0.13;
      contourf(output(:,:,1),-output(:,:,3)/rIdeal/2,...
      ((output(:,:,2)-rIdeal))/(2*rIdeal), colorLevel)
      dumyUnit = colorbar;
      colormap(gray)
      xlabel(dumyUnit,'u/D')

else
      surf(lineAngR,lineFlow,(output(:,:,2)'-rIdeal)/(2*rIdeal))
      dumyUnit = colorbar;
      xlabel(dumyUnit,'u/D')
end

title('Contour plot of the relative wear (r-r_i_d_e_a_l)/D')
xlabel('\theta ( radian)', 'FontSize',12)
ylabel('Stream-wise direction z/D', 'FontSize',12)
set(gcf,'color','white')


%% %%%%%%%%%%%%%%%%%%%%%%%%%%%%%%%%%%%%%%%%%%%%%%%%%%%%%%%%%%
%%%%%%%%%%%%%%%%Show wire frame 3-D plot%%%%%%%%%%%%%%
figure(2)

for ip = 1:noLine
      [lineX lineY lineZ] =
      pol2cart(output(:,ip,1),output(:,ip,2),...
      output(:,ip,3));
      plot3(lineX/rIdeal,lineY/rIdeal,lineZ/rIdeal,Markers(ip))
      hold on
end
xlabel('X/D ')
ylabel('y/D ')
zlabel('Z/D')

set(gcf,'color','white')
title('Wire frame plot')
hold off
```

```
%%
%%%%%%%%%%%%%%%%%%%%%%%%%%%%%%%%%%%%%%%%%%%%%%%%%%%%%%%%%%%%%%%%
%%%
%%%%%%%%%%%%%%%%Show wire frame in 2-D
plot%%%%%%%%%%%%%%%%%%%%%%%%%%%
figure(3)

for ip = 1:noLine
      [lineX lineY] = pol2cart(output(:,ip,1),output(:,ip,2));
      plot(lineX/rIdeal/2,lineY/rIdeal/2,Markers(ip))
      hold on
end

axis([-0.65, 0.65, 0, 0.65])
title('Wear profile at different locations')
set(gcf,'color','white')
xlabel('x/D');
ylabel('y/D');
hold off

fprintf('Evaluated at %3.2f z/D downstream \n',-
lineFlow(indices)/rIdeal)

%%
%%%%%%%%%%%%%%%%%%%%%%%%%%%%%%%%%%%%%%%%%%%%%%%%%%%%%%%%%%%%%%%%
%%%
%%%%%%%%%% wear profiles at different cross sections
%%%%%%%%%%%%
figure(4)
for i = 1: noLine
      hold on
      wearLine = output(:,indices(i),2)/rIdeal;
      %%%%% wear at specified z/D normalized by the diameter
      plot(lineAngR,wearLine,Markers(i))
end

xlabel('\theta');
ylabel('Normalized wear((r-r_ideal)/D)');
title('Local wear at different z/D')
set(gcf,'color','white')
hold off


%%
%%%%%%%%%%%%%%%%%%%%%%%%%%%%%%%%%%%%%%%%%%%%%%%%%%%%%%%%%%%%%%%%
%%%%
%%%%%%%%%%%%%%%%%%Local Wear normalized by average
radius%%%%%%%%%%%%%%
figure(5)
for i = 1: noLine
      hold on
```

```
      wearMean = mean(output(:,indices(i),2));
      wearLine = (output(:,indices(i),2) -
      wearMean)/(wearMean*2)*100;
      %%%%% Local relative wear(in percentage)
      plot(output(:,1,1),wearLine,Markers(i))
end

ylabel('(r(local) - R(average))/D(average) (%)')
title('Local Wear normalized by average radius')
xlabel('\theta ( radian)')
set(gcf,'color','white')
hold off

%%
%%%%%%%%%%%%%%%%%%%%%%%%%%%%%%%%%%%%%%%%%%%%%%%%%%%%%%%%%%%%%%%%
%%%%
%%%%%%%%%%%%%%Local Wear normalized by average wear
%%%%%%%%%%%%%%%%%%
figure(6)
for i = 1: noLine
      hold on
      wearMean = mean(output(:,indices(i),2));
      wearLine = (output(:,indices(i),2) - wearMean)/(wearMean-
      rIdeal/2)*100;
      %%%%% Local relative wear(in percentage)

      plot(output(:,1,1),wearLine,Markers(i))
end

%%%%%%%%%%%%%plot the zero lines
count = length(wearLine);
weardummy = zeros(count,1);
plot(weardummy,wearLine,'k')

ylabel('(r(local) - R(average))/w(average) * 100%)')
title('Local Wear normalized by average wear')
xlabel('\theta ( radian)')
set(gcf,'color','white')
hold off

%%
%%%%%%%%%%%%%%%%%%%%%%%%%%%%%%%%%%%%%%%%%%%%%%%%%%%%%%%%%%%%%%%%
%%%%
%%%%%%%%%%%%%%% experiment validation by mass balance
%%%%%%%%%%%%%%%%%
celLen = abs(output(1,1,3) - output(1,2,3));        %%%%% Cell
length
cellAng = output(2,1,1)-output(1,1,1);              %%%%% cell
angle
cellV = celLen*cellAng/2*(sum(sum(output(:,:,2).^2 -
(rIdeal/2)^2)));
%%%%% cell volume(inch)
totalMR = cellV*1e-9 *density * 1000 ;
```

```
      %%%%%%% volume * density * 1000 = X gram
      fprintf('The total mass removed is %f gram \n', totalMR)

end
fprintf('It takes %3.2f sec to run this code \n', etime(clock, t0))
```

2. Sherwood number calculation of the tests in 2.5 cm diameter test facility

```
%%%% Calculate the wear rate based on different time steps
%%%% Calculations are based various bulk concentration

%%%% Part one : calculation
%%%% Input: 1)Data cloud points from Geomagic after realignment and
regriding
%%%%        2)Conductivity readings
%%%% Output: 1) time steps that experiments ran at
%%%%         2) Local accumulative mass removal

%%%%% Part two: Plots
%%%%%Input: 'DiffCoef.txt' the local diffusion coefficient
%%%%%Output 1) averaged wear profiles along flow direction
%%%%%       2-5) roughness plots
%%%%%       6-8) mass transfer rate calculation
%%%%%       9,10) sherwood number calculation
%%%%%%%%%%%%%%%%%%%%%%%%%%%%%%%%%%%%%%%%%%%%%%%%%%%%%%%%%%%%%%%%%%%%%%%%%%%
%%
clear all
% close all
clc

t0= clock;

%% %%%%%%% Property variables %%%%%%%%%%%%%%%%%%%%%%%%%%%%%%%%%%%%%%%%

%%%%%%%%Some constant been used for diffusion coefficient hm calculation
Cw = 2.4;           %%%%%The saturated concentration of gypsum is 2.4g/l
GypD = 1581;     %%%%%The density of gypsum is 1581 kg/m^3
rIdeal = 0.5*0.0254;  %%%%%Initial readius of the tested surface (m)
pOrder = 1;
    %%%%% using Xth order curve fit the mass transfer VS timeStep

%%%%%%%%%%%%%%%%%%%%%%%%%%%%%%%%%%%%%%%%%%%%%%%%%%%%%%%%%%%%%%%%%%%%%%%%%%%
%
opt = input(' 1 for computing , 2 for plotting  ');

if opt == 1
    %% %%%%%%% read files of point clouds after realignment
%%%%%%%%%%%%%%
    TM01 = dlmread('unworn01.txt','\t');
    TM02 = dlmread('unworn02.txt','\t');
    TM1 = dlmread('output10.txt','\t');
    TM2 = dlmread('output15.txt','\t');
    TM3 = dlmread('output25.txt','\t');
    TM4 = dlmread('output35.txt','\t');
    TM5 = dlmread('output45.txt','\t');
    TM6 = dlmread('output60.txt','\t');
```

```
    %% %%%%%% Global variables (different from case to case
%%%%%%%%%%%%%%

    %%%%% the time steps (in sec)
    time = [0 10 15 25 35 45 60]*60;

    condRead = [0,82 129.036,216.526,296.696,369.546,465.096];
    %%%%%% conductivity is from the conductivity meter measurement
    %%%%%% best curve fit all the points and then find the conductivity
at
    %%%%%% experiment times

    noUnworn = 2;
    %%%%%% the number of unworn cases

   %% %%%%%%%%  Enter the total length of the input file %%%%%%%
    CondOpt = 2;
    %%%%%% choose the order for polynomial fit

    calibration = 0.0011 ;
    %%%%%% (g/l)/(uS/cm) used to calculate the bulk concentration

    %% %%%%%%%%%%%%%% Calculate the dimensions  %%%%%%%%%%%%%%%
    timeStep = length(time);
    %%%%% calculate how many time steps

    noAng = size(TM01,1);
    noCol = size(TM01,2)/3;
    %%%%%% noAng is the number of angels and noCol is the number of
columns

    mm = noAng * noCol;
    %%%%%% mm is the total number of data points

    %% %%%%%%%%%%%%%%%  Calculate modified time  %%%%%%%%%%%%%%%%%%%%%%
    CbMatrix = condRead * calibration;
    %%%%%% Cb is instant bulk concentration

    CwMatrix = Cw*ones(1,length(CbMatrix));
    %%%%%% Initiate the matrix Cw

    Cw_Cb = CwMatrix - CbMatrix;
    %%%%% instant conductivities of each experiment time

    Cw_CbCoef = polyfit(time,Cw_Cb,CondOpt);
    %%%%% step1, fit 2nd order polynomial through Cw-Cb VS. time

    Cw_CbBestFit = polyval(Cw_CbCoef,time);

    Cw_CbInt = polyint(Cw_CbCoef);
```

```
    %%%%% step2, integrate the curve fit

    modifT = polyval(Cw_CbInt, time)/Cw_Cb(1,1);
    %%%%% modified time = (1/(initial Delta C)) * (integral(Delta C) over
time)

    %% %%%%% Redimensionalize all the matrices to match gridding
%%%%%%%%%%%

    %%%%% put all the unworn case into one matrix

    MRadius01 = reshape(TM01, noAng, noCol, 3);
    MRadius02 = reshape(TM02, noAng, noCol, 3);
        %%%%%% MRadius01, MRadius02 are the radius of the two unworn case

    MRadius1 = reshape(TM1, noAng, noCol, 3);
    MRadius2 = reshape(TM2, noAng, noCol, 3);
    MRadius3 = reshape(TM3, noAng, noCol, 3);
    MRadius4 = reshape(TM4, noAng, noCol, 3);
    MRadius5 = reshape(TM5, noAng, noCol, 3);
    MRadius6 = reshape(TM6, noAng, noCol, 3);
    %%%%%% total matrix includes angel matrix, wear matrix and
    %%%%%% the flow direction matrix

    oRadius01 = MRadius01(:,:,2)/1000;
    oRadius02 = MRadius02(:,:,2)/1000;
    oRadius1 = MRadius1(:,:,2)/1000;
    oRadius2 = MRadius2(:,:,2)/1000;
    oRadius3 = MRadius3(:,:,2)/1000;
    oRadius4 = MRadius4(:,:,2)/1000;
    oRadius5 = MRadius5(:,:,2)/1000;
    oRadius6 = MRadius6(:,:,2)/1000;
    %%%%% convert the wear from milimeters into meters

    oRadius0 = mean([oRadius01(:),oRadius02(:)],2);
    %%%%% convert the unworn cases into arrays, and averge those two
    %%%%% different cases

    oriLineRadius = [oRadius01(:),oRadius02(:),oRadius1(:),...
           oRadius2(:),oRadius3(:),oRadius4(:),oRadius5(:),oRadius6(:)];
    %%%%%% extract the all the original wear data and put them into lines
    %%%%%% there is one line for each unworn case

    lineRadius = [oRadius0,oRadius1(:),oRadius2(:),oRadius3(:),...
                oRadius4(:),oRadius5(:),oRadius6(:)];
    %%%%%% extract the wear data and put them into lines for computation
    %%%%%% unworn wear is averaged between different cases

    %% %%%%%% Calculate the local mass been removed from the local radius
    lineWear = oriLineRadius - rIdeal;

    %% %%%%%%%%%%%%%%%%%%%%%%%%%%%%%%%%%%%%%%%%%%%%%%%%%%%%%%%%%%%%
```

```
    %%%%%% transfer the deviation matrix from row vectors to column
vectors

    MRR = zeros(mm,timeStep-1);     %%%%% mass removal rate
    MTC = zeros(mm,timeStep-1);     %%%%% mass removal coefficient
    %%%%%Each mass transfer coefficient(MTC) is calculated based on the
adjacent
    %%%%%wear progression and averaged bulk concentration
    %%%%%Therefor at each location(number of mm) there will be (timeStep
-1)
    %%%%%MTC value

    %%%%%% Using
    coefMassTran = zeros(mm, pOrder+1);
    %%%%%%% Coefficients of the 4th order best fit curve of mass VS time

    coefMR = zeros(mm, pOrder);
    %%%%%%% derivative of the 4th order polynomial curve

    %%%%%% coefMR
    for i = 1:mm
        coefMassTran(i,:) = polyfit(modifT, lineRadius(i,:), pOrder);
        coefMR = polyder(coefMassTran(i,:));
        MRR(i,:) = polyval(coefMR, modifT(2:timeStep))*GypD;
        for ii=1:timeStep-1
            MTC(i,ii) = MRR(i,ii)/Cw;
        end
    end

    meshRadius = reshape(oriLineRadius,noAng,noCol,timeStep+noUnworn-1);
    %%%%%% Wear of each case in meter, including all the unworn cases

    meshMRem = reshape(lineWear,noAng,noCol,timeStep+noUnworn-1)*GypD;
    %%%%%kg/m^2  mass removal per area for each time step(from unworn)

    meshMRR = reshape(MRR,noAng,noCol,timeStep-1);

    meshMTC = reshape(MTC,noAng,noCol,timeStep-1);

    meshSh = meshMTC*2*rIdeal/6.49e-10;
    %%%%% Local sherwood number

    timeVariable = [time; modifT];
    %%%%% pass the time variable to next code

    coordinates = [MRadius01(:,:,1),MRadius01(:,:,3)/1000];
        %%%%%% it passes the noAng*noCol*2 matrix for mesh angels and
        %%%%%% columns

    %%  %%%%%% save the matrix into files %%%%%%%%%%%%
    dlmwrite('time.txt',    timeVariable,   'delimiter', '\t');
```

```
    dlmwrite('coord.txt',   coordinates,    'delimiter','\t');
    dlmwrite('LocRad.txt',  meshRadius,     'delimiter','\t');
    dlmwrite('LocMRem.txt', meshMRem,       'delimiter', '\t');
    dlmwrite('LocMRR.txt',  meshMRR,        'delimiter', '\t');
    dlmwrite('LocMTC.txt',  meshMTC,        'delimiter', '\t');
    dlmwrite('LocSh.txt',   meshSh,         'delimiter', '\t');

else
    %%  %%%%% read in calculated files

    time = dlmread('time.txt', '\t');
    %%%%% read time (hours)

    coord = dlmread('coord.txt', '\t');
    %%%%%% noAng*noCol*2 matrix for mesh angels and columns

    matRadius = dlmread('LocRad.txt', '\t');
    %%%%% 1) Local wear (meter) at different experiment time

    matMRem = dlmread('LocMRem.txt','\t');
    %%%%% 2) Local mass removal per area kg/m^2

    matMRR = dlmread('LocMRR.txt', '\t');
    %%%%% 3) Local mass removal rate per area kg/m^2/sec

    matMTC = dlmread('LocMTC.txt', '\t');
    %%%%% 4) Local mass transfer coefficient m/sec

    matSh = dlmread('LocSh.txt', '\t');
    %%%%% 5) Local Sherwood number

    %% %%%%% predefined Global variables
    plotsPC = 6;
    %%%%%% how many plots per case

    LineSkip = 25;
    %%%%% how many lines been skipped for plotting

    runAve = 25;  %%%%%% the number points for running average
    %%%%%% over cross-wise direction

    roughCell = 20;  %%%%%%% Number of roughness cell over flow direction
    %%%%% for option 1 in figure(4)

    roughnessOpt = 2;
    %%%%% Choose which figure to present roughness
    %%%%% 1 for histagram, and 2 for profiles  in figure (4)

    diam = 0.0254;  %%%%% diameter of the test section is 0.0254 meters

    Markers=['r','k','b','g','k','m','c','b','m','k',...
```

```
        'c','g','r','b','m','c','g','r','b','m',
'k','c','g','r','b','m'];
    lineType = {'ko','k+','kx','k*','ks','kd','kp','k-.','bo','b+',...
                            'bx','b*','b-.','bd','bs'};
    %%%%%% plotting lines specifications

    %% %%%%%% reshape the arrays into matrices  of noAng*noCol
    [noAng,noCol2] = size(coord);
    noCol = noCol2/2;
    %%%%%% noCol calculates the number of rows from noAng
    %%%%%% noAng calculates the number of angels from noAng

    coordinates = reshape(coord, noAng, noCol,2);

    timeStep = size(time,2);
    %%%%% calculate how many time steps

    meshZ = coordinates(:,:,2);
    %%%%% ZLocas restores the z coordinates as noAng by noCol matrix

    zLine = meshZ(1,:)* -1;
    %%%%% zLine restores the z coordinates as noCol arrey

    meshAngR = coordinates(:,:,1);
    %%%%% meshAngR restores the angel coordinates as a matrix

    matRadius = reshape(matRadius,noAng,noCol,[]);
    matMRem = reshape(matMRem,noAng,noCol,[]);
    matMRR = reshape(matMRR,noAng,noCol,timeStep-1);
    matMTC = reshape(matMTC,noAng,noCol,timeStep-1);
    matSh = reshape(matSh,noAng,noCol,timeStep-1);

    noUnworn = size(matRadius,3)-size(matMRR,3);
    %%%%% the number of unworn cases

    timeR = zeros(1,timeStep+noUnworn-1);
    timeUn(noUnworn:timeStep+noUnworn-1) = time(1,:);
     %%%%%% add zero(min) for unworn cases to time array (for plotting)
    timeMUn=zeros(1,timeStep+noUnworn-1);
    timeMUn(noUnworn:timeStep+noUnworn-1) = time(2,:);
     %%%%%% add 0min for unworn cases to modified time array (for
plotting)

    %% %%%%% User input
    fprintf('which case to plot for checking the roughness scaling? \n ')
    fprintf('Input an integer from 1 to %d ', timeStep+noUnworn-1)
    roughTime = input('');
    %%%%%% ask the user which experimental time to use for plotting

    %% %%%%%% calculate the experiment times
    timegap = ones(1, timeStep-1);
    timeAve = ones(1, timeStep-1);
```

```
    for i = 1:timeStep-1
        timegap(i) = (time(2,i+1) - time(2,i));
        %%%%% timegap is the time interval between two time steps (in
sec)

        timeAve(i) = (time(2,i)+time(2,i+1))/2;
        %%%%% the averaged time between every two near steps(sec), where
mass
        %%%%% transfer rates are evaluated
    end

    %%
%%%%%%%%%%%%%%%%%%%%%%%%%%%%%%%%%%%%%%%%%%%%%%%%%%%%%%%%%%%%%%%%%%%%
    %%%%%%%%%%%%%%%%%%%%%  Roughness(arithmetic average)
%%%%%%%%%%%%%%%
    %%%%% Calculate the surface ruoghness based on arithmetic average
    %%%%% Input: how many lines for average, 3 lines by default

    roughFlowSub = floor(noCol/roughCell);
    %%%%%%% for getting the noCol, 20 cells by default

    %% %%%%%%   Ideal surface    %%%%%%
    %%%%%% inplement unbiased running average method which is slightly
    %%%%%% different from the 'filter' function. so that construction a
new
    %%%%%% matrix in order to use 'filter' function by adding a few rows
of
    %%%%%% the Rho matrix in front of the old matrix

    meshIdeal = zeros(noAng,noCol,timeStep+noUnworn-1);
    %%%%%%% Create a matrix to store the ideal value
    %%%%%%% which is the average radius at that downstream location

    dumAn = noAng+runAve-1;
    %%%%%%% the number of rows of the constructed matrix

    dumRho = zeros(dumAn,noCol,timeStep+noUnworn-1);
    %%%%%%% construct a matrix for raw data of running average(unbiased)
    dumIdeal =zeros(dumAn,noCol,timeStep+noUnworn-1);
    %%%%%%% construct a matrix for idea data of running average

    adAn = (runAve-1)/2;
    %%%%%% the number of row is added at each end of the constructed
    %%%%%% matrix so that the built-in function 'filter' can be used to
    %%%%%% calculate the 'unbiased' moving average

    for it = 1:timeStep+noUnworn-1
        dumRho(1:adAn,:,it) = matRadius((noAng-adAn+1):noAng,:,it);
        %%%%%% attaech the last few rows in front of the new matrix

        dumRho((1+adAn):(dumAn-adAn),:,it) = matRadius(:,:,it);
        %%%%%% exept the first few rows, the rest of the old matrix
```

```
        dumRho((dumAn-adAn+1):dumAn,:,it) = matRadius(1:adAn,:,it);
        %%%%%% attaech the first few rows to the end of the new matrix
    end

    coeA = 1;
    coeB = ones(1,runAve)*1/runAve;

    for it= 1:timeStep+noUnworn-1
        for ir = 1:noCol
            dumIdeal(:,ir,it) = filter(coeB,coeA,dumRho(:,ir,it));
        end
        meshIdeal(:,:,it) = dumIdeal(runAve:dumAn,:,it);
        %%%%%% take the average of each section in each row
    end

    %%  %%%%% Calculate the cell deviation from the ideal surface
    for it = 1:timeStep+noUnworn-1
        matDev = matRadius - meshIdeal;
        %%%%%% store the local deviation from the ideal surface for
roughness
    end

    matCellRough = zeros(timeStep+noUnworn-1,roughCell);
    %%%%%% Initiate a matrix for restore Roughness in that cell

    for it = 1:timeStep+noUnworn-1
        for ic = 1:roughCell
            firstRow = roughFlowSub*(ic - 1) + 1;
            endRow = roughFlowSub*ic;
            matCellRough(it,ic) =
sqrt(mean(mean(matDev(:,firstRow:endRow,it).^2)));
            %%%%% Rq = (1/n * sum((y^2))^0.5
        end
    end

    %%%%% convert roughness into relative roughness by deviding the
    %%%%% Diamter(1 inch)

    %% %%%%%% Overall roughness of each case
    overRough = zeros(1,timeStep+noUnworn-1);
    %%%%%% initiate an arrey for store the overall roughness of each case

    for it = 1:timeStep+noUnworn-1
        overRough(it) = sqrt(mean(mean(matDev(:,:,it).^2)));
    end

    %% %%%%% peak roughness of each case
    peakRough = zeros(1,timeStep+noUnworn-1);
    %%%%%% initiate an arrey for store the overall roughness of each case

    %%%%%% Find the location where to examine the roughness
```

```
    dumzInd = find(meshZ(1,:)<= -1.95*diam);
    dumzInd2 = find(meshZ(1,dumzInd)>= -2.05*diam);
    %%%%%% so the locations are in between 1.95 ~ 2.05 L/D downstream

    numP = length(dumzInd2);
    midP = floor(numP/2);
    ZMidInd = dumzInd(dumzInd2(midP));
    %%%%%% pick a middle location among the above locations (L/D)

    for it = 1:timeStep+noUnworn-1
        peakRough(it) = sqrt(mean(matDev(:,ZMidInd,it).^2));
    end

    %%%%%%%%%%%%%%%%%%%%%%%%%%%%%%%%%%%%%%%%%%%%%%%%%%%%%%%%%%%%%%%%%%%
    %%%%%%%%%%% 1) averaged wear profiles of different time
    aveWear = mean(matRadius)- rIdeal;
    %%%%%%% take the average of the wear along cross flow direction

    figure(1)
    hold on

    plotInd = ceil(linspace(1,(noCol-2),25));
    %%%%%%% pick the locations where to plot the averaged wear

    for it = 1:timeStep+noUnworn-1

plot(zLine(1,plotInd)/diam,aveWear(1,plotInd,it)/diam,lineType{it})
    end

    %title('Averaged wear profiles')
    xlabel('z/D', 'FontSize', 12)
    ylabel('Normalized averaged wear u/D','FontSize', 12)
    set(gcf,'color','white')
    legend([ num2str(timeUn(1,1)/60),' min'],...
            [ num2str(timeUn(1,2)/60),' min'],...
            [ num2str(timeUn(1,3)/60),' min'],...
            [ num2str(timeUn(1,4)/60),' min'],...
            [ num2str(timeUn(1,5)/60),' min'],...
            [ num2str(timeUn(1,6)/60),' min'],...
            [ num2str(timeUn(1,7)/60),' min'],...
            [ num2str(timeUn(1,8)/60),' min'])

    hold off

    %% %%%%%%% figure(2) contour plot of the selected case
    figure(2)

    contour(meshAngR*180/pi, meshZ/diam, matDev(:,:,roughTime)/diam)
    dumyUnit = colorbar;
    xlabel(dumyUnit,'u/D')
    title(['Relative roughness contour plot at ',...
        num2str(timeUn(1,roughTime)/60),' min'])
```

```
    xlabel('Cross-section (Degree)')
    ylabel('Flow direction z/D')

    %% %%%%% figure 3, try to find how roughness scales after time at the
    %%%%%%%% peak wear locations
    figure(3)

    ylimit = max((matRadius(:,ZMidInd,roughTime)-rIdeal))/diam*1.2;
    %%%%%%% define the limit of the y axis for the following plots
    %%%%%%% so that subplot 1 and 2 have the same scale

    AnLocNon = meshAngR/2;
    %%%%% None dimentionalize angel location by converting them to
    %%%%% circumferencial length and devided by Diameter

   subplot(3,1,1)
    plot(AnLocNon(:,ZMidInd), (matRadius(:,ZMidInd,roughTime)-
rIdeal)/diam)
    axis([0,0.5*pi, -ylimit, ylimit])
    title(['Relative Wear at ', num2str(timeUn(1,roughTime)/60),...
                                    ' min at max location'])
    xlabel('Relative position along circumference l/D')
    ylabel('Nominal surface r_l_o_c_a_l/D')
    %%%%%% plot the initial wear at that experimental time

    subplot(3,1,2)
    plot(AnLocNon(:,ZMidInd), (meshIdeal(:,ZMidInd,roughTime)-
rIdeal)/diam)
    axis([0,0.5*pi, -ylimit, ylimit])
    xlabel('Relative position along circumference l/D')
    ylabel('Ideal surface r_a_v_e/D')
    %%%%%% plot the ideal surface at that experimental time

    subplot(3,1,3)
    plot(AnLocNon(:,ZMidInd), matDev(:,ZMidInd,roughTime)/diam)
    xlabel('Relative position along circumference l/D')
    ylabel('Relative deviation e/D')
    %%%%%% plot the roughness at that experimental time

     %% %%%%%%%% plot the deviation profiles along flow direction %%%%%%
    figure(4)

     flowLR = 25;
        %%%%%% the line choosen to show roughness in flow direction

    plot(zLine/rIdeal/2, matDev( flowLR, :, roughTime)/rIdeal/2)
    xlabel('Flow direction')
    ylabel('Relative deviation e/D')
    %% %%%%% plot either the histograms or profiles of all the cases
    figure(5)

    plotColumn = ceil(timeStep/2);
```

```
    %%%%%% the number of figures in a row

    if roughnessOpt == 1
        for it = 1:timeStep
            subplot(2,plotColumn,it)
            matDummy = matDev(:,:, it);
            hist(matDummy(:), 60)
            title(['deviation hist at ',num2str(time(1,it)/60),' min
(u/D)'])
            axis([-0.025,0.025, 0 40000])
        end
    elseif roughnessOpt == 2
        xplot = linspace(0,8.5,roughCell);
        %%%%%% creat an x axis for plotting the angle averaged rougness
        for it = 1:timeStep+noUnworn-1
            plot (xplot(1,:),matCellRough(it,:)/diam, Markers(it))
            hold on
        end
        legend([ num2str(timeUn(1,1)/60),' min'],...
            [ num2str(timeUn(1,2)/60),' min'],...
            [ num2str(timeUn(1,3)/60),' min'],...
            [ num2str(timeUn(1,4)/60),' min'],...
            [ num2str(timeUn(1,5)/60),' min'],...
            [ num2str(timeUn(1,6)/60),' min'],...
            [ num2str(timeUn(1,7)/60),' min'])
        xlabel('z/D')
        ylabel('Relative roughness (u/D)')
        title('Relative roughness profiles')
    end

    %% %%%%%% plot the overall roughness  and the peack roughness over
time
    figure(6)

    plot(timeUn(1,:)/60,overRough/diam, 'ko',...
                timeUn(1,:)/60,peakRough/diam,'r*')
    legend('Overall surface','Max wear location')
    xlabel('Experimental time (min)')
    ylabel('Realative roughness (u/D)')

    disp(['Overall roughness  ',num2str(overRough)] )
    disp(['Max roughness      ',num2str(peakRough)] )

    %%
%%%%%%%%%%%%%%%%%%%%%%%%%%%%%%%%%%%%%%%%%%%%%%%%%%%%%%%%%%%%%%%%%%
    %%%%%%%%%%%%%%%%%%%% 6) averaged profle along z/D
%%%%%%%%%%%%%%%%%%%

    aveMRem = mean(matMRem);
    %%%%% take the average of mass transfer rate  of every timestep at
each Z
    %%%%% location
```

```
    xdummy = linspace(0,max(time(2,:)), 50);
    %%%%% creat a x axis for plotting

    figure(7)
    figInd = 1;
    set(gcf,'color','white');
    for ZlocInd = LineSkip: floor(noCol/plotsPC):noCol

        lineAveMRem = aveMRem(1,ZlocInd,:);

        pc = polyfit(timeMUn(:),lineAveMRem(:),pOrder);
            %%%%%% the polynomial coefficients of the best fit line
        ydummy = polyval(pc, xdummy);

        subplot(2,3, figInd)
        plot(timeMUn(:)/60, lineAveMRem(:),'ko',xdummy/60,ydummy,'r:')

        title(['z/D = ',num2str(-1*meshZ(6,ZlocInd)/diam,'%3.1f\n')])
        xlabel('Modified time')
        ylabel('kg/(m^2)')
        figInd = figInd+1;
        axis([0, max(timeMUn(:))*1.1/60, 0, 5])
    end

    %%
%%%%%%%%%%%%%%%%%%%%%%%%%%%%%%%%%%%%%%%%%%%%%%%%%%%%%%%%%%%%%%%%%%%
    %%%%%%%%%%%%%%%%%%%%%% 7) Mass transfer rate plot
%%%%%%%%%%%%%%%%%%%%

    AveMRR = mean(matMRR);
    %%%%% take the average of mass transfer rate  of every timestep at
each Z
    %%%%% location

    figure(8)
    figInd = 1;
    set(gcf,'color','white');
    for ZlocInd = LineSkip: floor(noCol/plotsPC):noCol

        lineAveMTR =  AveMRR(1,ZlocInd,:);

        subplot(2,3, figInd)
        plot(timeAve/60, lineAveMTR(:)*3600,'ko')
        title(['z/D = ',num2str(-1*meshZ(6,ZlocInd)/diam,'%3.1f\n')])
        xlabel('Modified time (min)')
        ylabel('mass transfer rate (kg/(m^2*hr))')
        axis([0, max(time(1,:))/60, 0, 14])
        hold on
        figInd = figInd+1;
    end
```

```
    %%
%%%%%%%%%%%%%%%%%%%%%%%%%%%%%%%%%%%%%%%%%%%%%%%%%%%%%%%%%%%%%%%%%%%
    %%%%%%%%%%%%%%%%%%%%%% 8) Mass transfer coefficient
%%%%%%%%%%%%%%%%%%

    aveMTC = mean(matMTC);
    %%%%% take the average of mass transfer rate  of every timestep at
each Z
    %%%%% location

    figure(9)
    figInd = 1;
    set(gcf,'color','white');
    for ZlocInd = LineSkip: floor(noCol/plotsPC):noCol

        lineAveMTC =  aveMTC(1,ZlocInd,:);

        subplot(2,3, figInd)
        plot(timeAve/60, lineAveMTC(:)*3600*1000 ,'r*')
        title(['z/D = ',num2str(-1*meshZ(6,ZlocInd)/diam,'%3.1f\n')])
        xlabel('Modified time (min)')
        ylabel('mass transfer coefficient (mm/hr)')
        axis([0 max(time(1,:))/60 0 5000])
        hold off
        figInd = figInd+1;
    end

    %%
%%%%%%%%%%%%%%%%%%%%%%%%%%%%%%%%%%%%%%%%%%%%%%%%%%%%%%%%%%%%%%%%%%%
    %%%%%%%%%%%%%%%%%%%%%% 9) Local Sherwood number
%%%%%%%%%%%%%%%%%%%%
    AveSh = mean(matSh);
    %check4 = reshape(AveSh(:), mm/noAng,timeStep-1);
    %%%%% take the average of mass transfer rate  of every timestep at
each Z
    %%%%% location

    figure(10)

    set(gcf,'color','white');

    for it = 2:timeStep-1
        plot(zLine, AveSh(1,:,it) ,Markers(it+1))
        hold on
    end
    legend('8 min','17 min','28')
    title('Local Sherwood number')
    xlabel('L/D')
    ylabel('Local Sherwood number')
    hold off
```

```
    %% %%%%%%%%%%%%%%%%%%%%%%%%%%%%%%%%%%%%%%%%%%%%%%%%%%%%%%%%%%%%%%%
    %%%%%%%%%%%%%%%%%%%%%% 10) Averaged Sh over time   %%%%%%%%%%%%%%%%%%
    figure(11)
    set(gcf,'color','white');

    MAveSh = mean(AveSh,3);
    %%%%%%% Using moving average of the averaged sherwood number
    plot(zLine/diam, MAveSh, '-.k')

    xlabel('z/D', 'FontSize', 12)
    ylabel('Sherwood number', 'FontSize', 12)
    axis([0,8.6, 0, 40000])

    hold on

    %% %%%%%%%%%%%%%% Max Sh and pipe(min) Sh %%%%%%%%%%%%%%%%%%%%%%%%%%
    maxSh = max(MAveSh);
    shInd = find(MAveSh>(maxSh-1));
    maxShCell = mean(MAveSh(shInd(1)-5:shInd(1)+5));

    pipeSh = min(MAveSh);
    shInd = find(MAveSh<(pipeSh+1));
    pipeShCell = mean(MAveSh(shInd(1)-10:shInd(1)));

    fprintf('Max  Sh is %5.0f \n', maxShCell)
    fprintf('Pipe Sh is %5.0f \n', pipeShCell)


end

fprintf('It takes %3.2f sec to run this code \n', etime(clock, t0))
```

3. Wall thickness calculation of each individual spots by the ultrasonic measurements of the 20 cm diameter bore tests

Ada

```
%% function [Ch1 Ch2 time]=readbinary(fid)
clear all
clc, close all,


%% evaluate for each measurement
fid='G:\\FAC\\1scannedData\\bigLoop\\thirteenH\\thirteenH_7.tdms';
                            %%%%% File name to be read
ThreshHold = -0.1;          %%% counted as the beginning of the pulse
firstEcho = 93;             %%%%% threshold for the first echo
```

```
%%
numbit = 12;                %%% Number of bits for the given card (PCI-
6115 - 12bit)
datatype = 'int16';         %%% Data format set in DAQmx
vrange = 3;                 %%% Voltage range set in DAQmx
numsamp=10e6;                %%% number of samples to read
numch=1;                    %%% number of chanels

fin = fopen(fid, 'r');
[Inbuff,Count] = fread(fin,[1,(numsamp*numch)+59],datatype);
fclose(fin);
sig_V = ((Inbuff / 2^numbit )* vrange)'; % converts binary to volts
clear Inbuff fin Count ans
sig_V(1:59)=[];                     % First 59 Rows are header data and
can be ignored
for i=1:numch
    eval(['ch' num2str(i) ' = downsample(sig_V,numch,',num2str(i-
1),');'])
end
time=1e-7:1e-7:length(ch1)*1e-7;
time=time';
clear sig_V

subplot(2,1,1)
for i=1:numch
    eval(['subplot(' num2str(numch) '1' num2str(i) '),plot(time, ch'
num2str(i) ')']);
    xlabel('Time (s)');
    ylabel(['Signal of Chanel' num2str(i) ' (V)']);
    title(fid)
end


%%%%%%%%%%%%%%%%%%%%%%%%%%%%%%%%%%%%%%%%%%%%%%%%%%%%%%%%%%%
% Rxx = autom(ch1);
% plot(Rxx);
% grid;
% title('Autocorrelation function ultrasonic wave');
% xlabel('lags');
% ylabel('Autocorrelation');

%% %%%%%initiate parameters
    counts = 0;                     %%%%% count how many time intervals
    totalTime = 0;                  %%%%% adding the total time sound
travels
    PlasterV = 1675;                %%%%% Speed of Ultrasonic travels in
plaster
    newPulse = 2200;                %%%%% Threshhold for a new pulse
    newReflec = 50;                 %%%%% new reflection
    timeInc = 0;                    %%%%% Initiate time increament
between the
    %%%%% echoes
```

```
   % firstEcho = 213;              %%%%% threshold for the first echo
    secEcho = firstEcho*1.9 ;      %%%%% threshold for the second echo
    thirdEcho = firstEcho*2.8;     %%%%% threshold for the second echo
    wetSpeed = 1635*2;               %%%%% speed of ultrasonic in wet
Hydrocal
    %wetSpeed = 3492;               %%%%% speed of ultrasonic in dry
Hydrocal

    firstEcho2 = firstEcho+30;     %%%%% elimenate the noise of the wave
forms


    %% %%%%% if sampling only one channel
if numch == 1
    SigalCounted = find(ch1 < ThreshHold);
    rowd = length(SigalCounted) -1;      %%%%% one less number for diff
    echoCheck = zeros(rowd,1);

    %%%% Record where the first pulse starts
    difMatrix = diff(SigalCounted);
    %%%%%time difference between any adjacent signals that are >
    %%%%%threshold
    newPulsInd = find(difMatrix>newPulse);
    %%%%% If the time interval is > newPulse, it is considered as a new
    %%%%% pulse
    timeStart = SigalCounted(newPulsInd(1)+1);

    %%%%% time interval calculation
    for i=(newPulsInd(1)):rowd
        if difMatrix(i)>newReflec && difMatrix(i)<newPulse
            counts = counts + 1;
            %%%%%% counts how many echos
            timeInc = SigalCounted(i+1)-timeStart;
            echoCheck(counts) = timeInc;

        else if difMatrix(i) >= newPulse
                timeStart = SigalCounted(i+1);
                totalTime = timeInc + totalTime;
            end
        end
    end

    echoCheck = echoCheck(echoCheck>0);

    figure(2)

    hist(echoCheck, 350)
    %%%%% check the histgram of all the time intervals
    title('The histagram of the echo')

    oneEcho = mean(echoCheck(echoCheck<firstEcho));
    echoCheck =echoCheck(echoCheck>firstEcho2);
```

```
    twoEcho = mean(echoCheck(echoCheck<secEcho));
    echoCheck = echoCheck(echoCheck>secEcho);
    threeEcho = mean(echoCheck(echoCheck<thirdEcho));
    aveEcho = (oneEcho + twoEcho/2 + threeEcho/3)/3;
    EchoVector = [oneEcho, twoEcho/2, threeEcho/3];

    thickOne = oneEcho/2*wetSpeed/1E7*1000;
    thickTwo = twoEcho/4*wetSpeed/1E7*1000;
    thickness = (oneEcho/2 + twoEcho/4)/2 * wetSpeed / 1E7 * 1000;
    %%%%% wall thickness, by takeing the everage of
    xlabel(['The echos indicate ' num2str(thickOne) '  and ',...
        num2str(thickTwo), '  ', 'usec respectively' ...
        '  wall thickness is ' num2str(thickness), 'mm'])

    % figure(3)
    % index = (-(numsamp-1):numsamp-1)';
    % plotSignal = xcorr(ch1, 'biased');
    % plot(index, plotSignal/6E-3)
    % title('Autocorrelation of ultrasonic signals')
    % xlabel('lags')
    % grid;
    % ylabel('normalized autocorrelation')


    %% %%%%%If sampling two channels
elseif numch == 2
        chanIndex = (1:numch:numsamp)+1;
        ch2 = ch1(chanIndex);
        SigalCounted = find(ch2 < ThreshHold);
        rowd = length(SigalCounted) -1;      %%%%% one less number for
diff
        echoCheck = zeros(rowd,1);

        %%%% Record where the first pulse starts
        difMatrix = diff(SigalCounted);
        %%%%%time difference between any adjacent signals that are >
        %%%%%threshold
        newPulsInd = find(difMatrix>newPulse);
        %%%%% If the time interval is > newPulse, it is considered as a
new
        %%%%% pulse
        timeStart = SigalCounted(newPulsInd(1)+1);

        %%%%% time interval calculation
        for i=(newPulsInd(1)):rowd
            if difMatrix(i)>newReflec && difMatrix(i)<newPulse
                counts = counts + 1;
                %%%%%% counts how many echos
                timeInc = SigalCounted(i+1)-timeStart;
                echoCheck(counts) = timeInc;

            else if difMatrix(i) >= newPulse
```

```
                    timeStart = SigalCounted(i+1);
                    totalTime = timeInc + totalTime;
                end
            end
        end

        echoCheck = echoCheck(echoCheck>0);

        figure(2)

        hist(echoCheck, 350)
        %%%%% check the histgram of all the time intervals
        title('The histagram of the echo')

        oneEcho = mean(echoCheck(echoCheck<firstEcho));
        echoCheck =echoCheck(echoCheck>firstEcho2);
        twoEcho = mean(echoCheck(echoCheck<secEcho));
        echoCheck = echoCheck(echoCheck>secEcho);
        threeEcho = mean(echoCheck(echoCheck<thirdEcho));
        aveEcho = (oneEcho + twoEcho/2 + threeEcho/3)/3;
        EchoVector = [oneEcho, twoEcho/2, threeEcho/3];

        thickOne = oneEcho/2*wetSpeed/1E7*1000;
        thickTwo = twoEcho/4*wetSpeed/1E7*1000;
        thickness = (oneEcho/2 + twoEcho/4)/2 * wetSpeed / 1E7 * 1000;
        %%%%% wall thickness, by takeing the everage of
        xlabel(['The echos indicate' num2str(thickOne) '  ',...
            num2str(thickTwo), '  ','and  ' num2str(threeEcho/3), 'usec
respectively' ...
            '  wall thickness is ' num2str(thickness), 'mm'])
else
    fprintf('wrong channel specified')
end

disp(fid)
fprintf('first peak is %f \n',thickOne)
 fprintf('if it is second, %f',((oneEcho-12)/oneEcho*thickOne))
```

4. Sherwood number calculation of the tests in 2.5 cm diameter test facility

```
clear all,
close all,
clc,

%%%%%% Sherwood number calculation

matrixTime = [1, 2, 3.5,    4.5,    6.5,    9.67,   13];
%%%%%%% experiment time in hours
```

```
matrixLoc = [3.75   3.5 3.25    3   2.75    2.5 2.25    2   1.75    1.5
1.25   1   0.75    0.5 0.25...
    2.1875  1.9375  3.875   3.625   3.375   3.125   2.875   2.625   2.375
2.125   1.875   3.3125];
%%%%%%% measurement location

matrixWear = [0.090 0.170   0.41    0.530   0.84    1.42    1.87
    0.040   0.180   0.42    0.550   0.86    1.68    2.07
    0.030   0.170   0.33    0.410   0.69    1.24    1.78
    0.040   0.220   0.430   0.560   0.910   1.480   1.750
    0.110   0.290   0.57    0.740   1.17    1.77    2.4
    0.110   0.230   0.47    0.620   1   1.98    2.08
    0.030   0.220   0.47    0.650   1.07    1.93    2.44
    0.090   0.300   0.71    0.990   1.42    2.28    2.8
    0.120   0.350   0.8 0.850   1.21    2.51    3.13
    0.080   0.270   0.49    0.690   1.08    1.69    2.45
    0.150   0.300   0.53    0.770   1.13    1.62    2.19
    0.110   0.310   0.52    0.700   0.95    1.48    2
    0.110   0.370   0.66    0.860   1.18    1.52    1.86
    0.090   0.290   0.52    0.750   1.06    1.64    1.93
    0.020   0.260   0.36    0.520   0.7 1.09    1.5
    0.050   0.300   0.5    0.580    0.99    1.58    2.37
    0.160   0.540   0.69    0.950   1.33    1.57    2.34
    0.130   0.240   0.31    0.490   1.37    0.99    2.09
    0.130   0.230   0.35    0.390   0.79    1.25    1.58
    0.160   0.300   0.54    0.550   1.02    1.41    2.01
    0.020   0.220   0.94    0.52    1.72    1.50    2.36
    0.193   0.363   0.56    1.69    0.76    1.50    2.38
    0.180   0.360   0.63    0.83    1.26    1.69    2.23
    0.124   0.324   0.61    0.63    1.12    1.48    2.25
    0.058   0.258   0.54    0.65    1.25    1.79    2.60
    0.162   0.462   1.01    1.15    1.82    2.35    3.02
    0.200   0.380   0.63    0.780   1.35    1.81    2.4];

marCol=['r','k','b','g','k','m','c','b','m','k',...
        'c','g','r','b','m','c','g','r','b','m',
'k','c','g','r','b','m'];
    %%%%% define marker colors for plotting

marSty= ['+','o','*','s','h','x','.','^','*','x','.','^','d','*'];
    %%%%% define marker style for plotting

%% Coney's correlation (KS)
coneyX = [0.5   1   1.5 2   2.5 3   3.5 4   4.5 5   5.5 6   6.5 7];
coneyKSSh = [1.352061738    2.320709974 2.093980061 1.745460518
1.40667678  1.407466079 1.484915225 1.476464105 1.435586463 1.355986429
1.285893456 1.224630572 1.17503681  1.131277607];
ShPipe = 2568.3;
%%%%by berger's correlation

%% %%%%%%%%%%% user input for If plotting the coney's correlation
plotStart = input ('where do you wanna see the plot? (integer) ');
```

```
coneyOpt = input('1 for plotting Coney correlation, 0 for not ');

%% %%%%%%%%%%%%% global variables %%%%%%%%%%%%%%%%%%%

Cw = 2.4;           %%%%%% Hydrocal saturation value 2.4 kg/m^3
GypDens = 1581;     %%%%%The density of gypsum is 1581 kg/m^3
diffusivity = 6.49e-10; %%%%% diffusivity of hydrocal
diam = 0.0254*8;     %%%%% diameter of the pipe

nOrder = 1;
%%%%% the order of the curve fit

%% Evaluate the wear rate

timeStep = length(matrixTime);
%%%%% the number of experimental time

numLoc = length(matrixLoc);
%%%%% the number of experimental spots

[m, n] = size(matrixWear);
%%%%% m is the different locations
%%%%% n is different time steps

%%%%%validating the dimensions
if (m ~= numLoc || n ~= timeStep)
    disp('dimension does not match')
end

%% %%%%%%%   Sh number calculation 1     %%%%%%%%%%%%%
%%%%% step 1) Calculate instant mass transfer coefficient and average
them
%%%%% step 2) Calculate the sherwood number accordingly

curveCoef = ones( numLoc, nOrder+1);
%%%%% initiate a matrix to store the curve fit coeffcient

for i=1:numLoc
    curveCoef(i,:) = polyfit(matrixTime, matrixWear(i,:),nOrder);
end

massTransCurveDer = ones(numLoc, nOrder);
%%%% initiate the derivative of the mass removal curve

massTransCoe = ones(numLoc, timeStep);
%%%%% initiate the instant mass transfer coefficient h(T)

for i =1:numLoc
    massTransCurveDer(i,:) = polyder(curveCoef(i,:));
    massTransCoe(i,:) = polyval(massTransCurveDer(i,:),matrixTime);
```

```
end

meanMassTransCoe = mean(massTransCoe,2)*GypDens/Cw;
%%%%% mean mass transfer coefficient h (mm/hour)

meanSh = meanMassTransCoe*diam/diffusivity/1000/3600;
%%%%% mean Sherwood number


%% %%%%%%%%%%%%%%%%%  plot the wear rate  %%%%%%%%%%% %%%%%%%%%%%

plots = 6;          %%%%%% make 3 figures at one plot

if plots>3
    lines = 2;
else lines = 1;
end                 %%%%% how to orientate the plots

timeAxis = 0:0.25: max(matrixTime);
%%%%% creat time Axis for plotting

figure(1)
set(gcf,'color','white');
for i= 1: plots
    subplot(lines,ceil(plots/lines),plots-i+1)
    ii = i+plotStart-1;
    plot(timeAxis, polyval(curveCoef(ii,:),timeAxis)/(diam*1000),'r:',...
        matrixTime, matrixWear(ii,:)/(diam*1000),'ko')
    title(['At z/D ', num2str(matrixLoc(ii))])
    xlabel('Experimental time (hour)')
    ylabel('Relative wear wear (r-r_i_d_e_a_l)/D ')
end


    %% sort the locations for plotting
    sorting = [matrixLoc', meanSh];
    sorted = sortrows(sorting,1);

%% plot the sherwood number
figure(2)

set(gcf,'color','white');
plot(sorted(:,1),sorted(:,2),'o')
title('Sh plot of Re0 200,000')
axis([0 9 0 40000])
hold on

if coneyOpt == 1
    plot(coneyX, coneyKSSh*ShPipe,'k')
end
```

```
figure(3)

set(gcf,'color','white');
smoothSh = sorted;
smoothSh(:,2) = smooth(sorted(:,2),7);
plot(smoothSh(:,1), smoothSh(:,2),'r',sorted(:,1),sorted(:,2),'ro')
title('Sh plot of Reo 200000')
xlabel('Downstream location L/D')
ylabel('Sherwood number')
axis([0 4 0 13600])
hold on

if coneyOpt == 1
    plot(coneyX, coneyKSSh*ShPipe)
end


%% %%%%%%%%Sh number calculation 2 %%%%%%%%%%%%%%%
%%%%%%%% step 1: calculate Sh for each time step
%%%%%%%% Step 2: Average them

matrixWearAbs = zeros(numLoc,timeStep-1);
    %%%%%% initialized a matrix for store the absolute wear after time 0
    %%%%%% (wear at a specific time minus the unworn
for it = 1:(timeStep-1)
    matrixWearAbs(:,it) = matrixWear(:,(it+1))-matrixWear(:,1);
end

matrixWearRate = zeros(numLoc,timeStep-1);
    %%%%%% initialized a matrix for store the wear rate
    %%%%%% from unworn to thatspecific time
for il = 1:numLoc
    matrixWearRate(il,:) = matrixWearAbs(il,:)./matrixTime(2:timeStep);
end
    %%%%%% matrixWearRate stores the wear rate mm/hour

matrixMTC = matrixWearRate*GypDens/Cw;
    %%%%%% matrixWearRate stores the mass transfer coefficient(h) mm/hour

matrixSh = matrixMTC*diam/diffusivity/1000/3600;
    %%%%%% matrixWearRate stores the local Sh

matrixShMean = mean(matrixSh,2);
    %%%%%% matrixWearRate stores the mean Sh

%%%%%%%%%%%plotting %%%%%%%%%%%%%%%%%
figure(4)
%matLegend = zeros(timeStep);
    %%%%%% initialize an arrey to store a serious of strings for legend

for it = 1:timeStep-1
    plot(matrixLoc', matrixSh(:,it),[marCol(it) marSty(it)])
```

```
    %matLegend(it) = ['Sh at', num2str(matrixTime(it)),'hr'];
    hold on
end

%% sort the locations for plotting
    sorting = [matrixLoc', matrixShMean];
    sorted = sortrows(sorting,1);

plot(sorted(:,1), sorted(:,2))
%legend(matLegend)


%% %%%%%% plot the Smoothed Sh for 8" as comparison of 1" Sh %%%%%%%%%%%%

figure(11)

set(gcf,'color','white');
plot(sorted(:,1),sorted(:,2),'o')
title('Comparison of Sh profiles ')
axis([0 9 0 40000])
hold on

if coneyOpt == 1
    hsize = plot(coneyX, coneyKSSh*ShPipe,'ks');
    set(hsize,'markerSize',4)
end
```